Florida Water Resources Research Center
Annual Technical Report
FY 2006

Introduction

The mission of the Florida Water Resources Research Center at the University of Florida is to facilitate communication and collaboration between Florida's Universities and the state agencies that are responsible for managing Florida's water resources. A primary component of this collaborative effort is the development of graduate training opportunities in critical areas of water resources that are targeted to meet Florida's short- and long-term needs.

Under the direction of Dr. Kirk Hatfield, the Florida Water Resources Research Center is working to maximize the amount of graduate student funding available to the state of Florida under the provisions of section 104 of the Water Resources Research Act of 1984. Over the past year total funding through the Center was $1,157,652, including agreements with four of Florida's universities (Florida Atlantic University, Florida State University, University of South Florida, and the University of Florida) and four state agencies (South Florida Water Management District, Southwest Florida Water Management District, St. Johns River Water Management District, and the Florida Geological Survey) and has supported the research of 13 Ph.D. students and 3 Masters students focusing on water resources issues.

During FY 2006, along with providing support to graduate students within the state of Florida, the Center also facilitated development of research at both the state and national level and produced 23 peer reviewed publications some of which received international recognition (Best Technology Paper published in ES&T, 2006). The Center is also a state repository for water resource related publications. Final project reports for Center funded research efforts are available free of charge and can be requested through the WRRC website (WRRC Website.

Research Program

During FY 2006 the Water Resources Research Center supported eight 104B research projects and one 104G project. The supported research projects considered a wide range of water resource related issues while maintaining focus on topics specific to Florida. These topics include investigation of the geochemical processes that control the mobilization of arsenic during aquifer storage recovery (ASR), comparing widely used procedures by which radar- and gauge-derived rainfall are optimally combined for water management and regulatory decisions, investigating the measurement of evapotranspiration, recharge, and runoff in shallow water table environments characteristic of the Gulf of Mexico coastal plain, studying the measurement of erosion around and flow through hydraulic structures and culverts, and developing software for quantifying the impacts of saltwater up-coning and well field pumping.

Space-based monitoring of wetland surface flow

Basic Information

Title:	Space-based monitoring of wetland surface flow
Project Number:	2004FL76G
Start Date:	9/1/2004
End Date:	8/31/2007
Funding Source:	104G
Congressional District:	18
Research Category:	Not Applicable
Focus Category:	Wetlands, Surface Water, Hydrology
Descriptors:	
Principal Investigators:	Shimon Wdowinski

Publication

1. Bieler B., R. Garcia-Martine, S. Wdowinski and F. Miralles- Wilhelm, Modeling Water Flow in the Water Conservation Area 1 Using Interferometric Synthetic Aperture Radar (InSAR) Observations, Greater Everglades Ecosystem Restoration (GEER) Conference, Abstract Volume, p. 15, 2006.
2. Kim S., S. Wdowinski, J. Wang, T. Dixon and F. Amelung, Comparison of Water Level Changes in the Everglades as Calculated with the TIME Model and with Interferometric SAR Measurements, Greater Everglades Ecosystem Restoration (GEER) Conference, Abstract Volume, p. 118, 2006.
3. Kim S., S. Wdowinski, T. Dixon and F. Amelung, SAR Interferometric Coherence Analysis of Wetlands in South Florida, Greater Everglades Ecosystem Restoration (GEER) Conference, Abstract Volume, p. 119, 2006.
4. Wdowinski S., S. Kim, T. Dixon, F. Amelung, and R. Sonenshein, High Spatial-Resolution Space-Based Monitoring of Surface Water Level Changes in the Greater Everglades, Greater Everglades Ecosystem Restoration (GEER) Conference, Abstract Volume, p. 242, 2006.

Project Progress

Space-based monitoring of wetland surface flow

PI: Dr. Shimon Wdowinski

Division of Marine Geology and Geophysics, Rosenstiel School of Marine and Atmospheric Science, University of Miami

During the past six months, we have obtained progress in the following four categories:

1. Data acquisition

We continue acquiring C-band SAR data, mainly over the Everglades wetlands, but also over other wetlands. Our main source of data for Everglades is RADARSAT-1, which has a repeat orbit of 24 days. Using our Alaska SAR Facility (ASF) data project, we set 6 Data Acquisition Requests (DAR) that automatically acquire every repeat orbit. As a result, we get 6 new acquisitions within every 24 days, half using fine beam (7 m pixel resolution) and the other half with standard beam (15 m resolution). Due to a new agreement between ASF and CSTARS (University of Miami), since October we downlink the new acquisitions at CSTARS at no cost! So, we are getting high quality data at no cost and in real time.

We started new data acquisition projects in other wetlands, mostly in North and Central America, including Louisiana coast, Yucatan (Mexico), and the Bahamas. We also started a collaborative project with a French team to monitor wetlands in Mauritania (Africa). Our group acquires RADARSAT-1 data and the French team conducts ground measurements and develops hydrological model for the wetlands.

2. Data processing and results

We have continued processing both archive and current data. We recently received archived RADARSAT-1 data of both the Everglades and the Louisiana coast for the time period of 1996-2003. These data has been processed in order to constrain detailed flow model of both areas. We also continued processing current data that is downlinked at CSTARS. After a long effort we managed to automate the data processing procedures, resulting in an automated interferogram production every data acquired over the Everglades. Data acquired over other wetlands are partially processed automatically, but also requires human intervision.

3. Flow models

Water level is a key parameter in wetlands ecosystems, affecting flow and spatial extent of wetlands. As part of the Everglades restoration effort, the TIME model (Tides and Inflows in the Marshes of the Everglades) was developed by US Geological Survey and University of Miami, enabling us to investigate interacting effects of freshwater

inflows and coastal driving forces in and along the mangrove ecotone of the Everglades National Park. The TIME model solves for the spatial and temporal distribution of main hydrological parameters in both surface- and ground-water, including water levels, flows, and salinity, and is constrained by field measurements at its boundaries. The model has been calibrated for the 1996-2002 time period, because reliable field observations are available for that time period.

Twelve InSAR-measured water level change maps are produced using ERS-1/2 and JERS-1 SAR images during 1996-1997. In addition 2-D water level maps at the satellite acquisition times are derived from the TIME model simulation and used to synthesize water level change maps similar to those obtained from satellite radar observations. We compare InSAR measurement with the synthetic water level change map from the TIME model and field data. Our initial findings show that InSAR measurement indicates similar patterns to those obtained using modeled water level, but there are also some differences. Investigation of coincidence and discrepancy between the two mapping methods will provide new scientific insight, especially regarding the role of spatial variation of water level. Eventually, the InSAR analysis can be used to calibrate, verify and refine the existing numerical model as well as a powerful tool to determine water level changes in wetlands with remote sensing.

We also continued our modeling efforts of Water Conservation Area 1 (WCA-1), as part of the MS thesis of B.M. Bieler, at the University of Miami. Using the space-based data we obtained time series of water level changes in the entire area 1. These maps of water level changes show very interesting patterns. Preliminary modeling results show very good fit to some of the observations, but not all. The model needs further improvements, which will be conducted in the next few months.

Additional project details and long-term objectives are discussed in the following section.

Space-based monitoring of wetland surface flow

Statement of critical regional or State water problem.

Coastal wetlands provide critical habitat for a wide variety of plant and animal species, including the larval stages of many ocean fish. Globally, most such regions are under severe environmental stress, mainly from urban development, pollution, and rising sea level. However, there is increasing recognition of the importance of these habitats, and mitigation and restoration activities have begun in a few regions. A key element of wetlands restoration involves monitoring and modeling its hydrologic system, in order to understand the underlying flow dynamics, assess potential restoration strategies, mitigate effects of past construction, and predict the effects of future changes to infrastructure such as new dams or levies, or their removal.

The Everglades region in south Florida is a unique ecological environment. This gently sloping terrain drains Lake Okeechobee in central Florida southward into the Gulf of Mexico. The combination of abundant water and sub-tropical climate promotes a wide diversity of flora and fauna. Anthropogenic changes in the past 50 years, mainly for water supply, agricultural development and flood control purposes, have disrupted natural water flow and severely impacted the regional ecosystem. Currently, Everglades flow is controlled by a series of hydraulic control structures to prevent flooding and regulate flow rates, but which also suppress natural water level fluctuations, essential for supporting the fragile wetland ecosystem. This controlled Everglades environment provides a large-scale laboratory for monitoring and modeling wetland surface flow. Enhanced modeling capabilities and understanding of the Everglades hydrological system are essential for the Everglades restoration project, which is the largest and most expensive (multi-billion dollar) wetland restoration project yet attempted.

The Everglades are currently monitored by a network of stage (water level), meteorological, hydrogeologic, and water quality control stations, providing daily average estimates of water level, rainfall and other key hydrologic parameters. Due to the limited number of stations (station spacing ~ 10 km) and their distribution, mainly along existing structures, the current data can constrain regional scale models, such as the 2 x 2 $mile^2$ SFWMM, but lack the spatial density for more detailed models.

Statement of results or benefits.

The proposed research will provide high resolution (~300 x 300 m^2) regional scale observations, more than an order of magnitude higher than the existing ground network, of wetland water levels and their changes. The new observations will be used as (1) a monitoring tool for water resources managements, and (2) constraints for high spatial resolution of wetland surface flow. The new measurement are important for managing and restoring wetlands damaged by human activity, because many species are threatened by wetlands degradation depend on restoration of hydroperiod (water level as a function of time). Flow management to achieve this depends on accurate flow models and accurate, spatially dense elevation measurements, currently lacking. Our test area, the Florida Everglades, is the focus of the largest wetlands restoration project yet attempted.

Nature, scope, and objectives of the project, including a timeline of activities.

Nature – The proposed research promote the usage of space-based regional-scale high spatial resolution observations for monitoring and understanding wetland surface flow.

Scope – The proposed work contains three components: InSAR analysis of wetlands, hydrological analysis, and numerical modeling. In the first component we will us SAR data of the Everglades (both C-band and L-band) and other wetlands (Louisiana, Chesapeake Bay) to detect water level changes between SAR data acquisitions. The second component – hydrologic analysis – will allow us to understand and utilize the high spatial resolution InSAR observation, by evaluating the observation with respect to terrestrial-based (e.g., stage data) and field observations. In the third component we will use the high spatial resolution observations to constrain surface flow models. This part of the project will be conducted by the USGS, which already developed a flow model for the southern Everglades.

Objectives – Our proposed research will provide new space-based observations, which will be used to understand in details the complexity of wetland surface flow. Furthermore using the new observations as constraints in 3-D flow models, we will be able to evaluate the tempo-spatial distribution of key hydrologic parameters that govern shallow surface flow in the Everglades and other wetlands.

Timeline - During the first phase of the project, until the new Japanese L-band SAR satellite (ALOS PALSAR) will be launched in December 2004, we will use mostly archived SAR data (L-band JERS-1, and C-band ERS-1/2), but also current C-band data (ENVISAT and RADARSAT-1), for further developing the technique and for generating high resolution historic observations (1992-1998) for constraining flow models. After the ALOS satellite will launched and calibrated, we will focus the research on current L-band InSAR observations for monitoring purposes, as well as for providing better model constraints.

Methods, procedures, and facilities.

The proposed work contains three components: InSAR analysis of wetlands, hydrological analysis, and numerical modeling. The first two components will be conducted at the University of Miami and the third one by the USGS.

InSAR analysis of wetlands

This component of the proposed project includes additional InSAR data processing of the Everglades and other wetlands. We plan to process additional L-band JERS data of southern Florida, which were acquired during the JERS mission during 1992-1998. The data are available at the Japanese Space Agency (NASDA, which recently changed its name to JAXA). We also plan to process C-band ERS and EVISAT data collected by the European Space Agency (ESA). In order to obtain the C-band data, we submitted a data proposal to ESA, which was approved last August. Although so far only L-band data were successfully used to detect wetland water level changes, we plan

to test the C-band data and compare between the two data types. We also plan to purchase and process L-band data from other wetlands, such as the Louisiana Coast and the Chesapeake Bay.

Hydrological analysis of interferograms – interpretation of the observations

The new spaced-based observations (interferograms) describe with high spatial resolution (~30 x 30 m^2) lateral phase changes between two acquisitions. Because each phase cycle (2 pi) corresponds to 12 cm of displacement in the radar line-of-sight, which translates into 15.1 cm of vertical displacement, we were able to translate the observed phase changes into maps of water level changes occurring between two acquisitions. Producing such water level change maps is only one step in understanding the corresponding hydrological system, because the observations are relative both in time and in space. The relative aspect in the time domain is derived from the fact that the measurements describe water level changes from one unknown situation to another unknown situation. In the preliminary study described below, we spent almost a year to understand the hydrological significance of the InSAR measurements. Fortunately, we found that during one of the SAR data acquisitions (1994/12/19) water level conditions in the three water conservation areas (1, 2A, and 2B) were almost flat. As a result, we were able to calculate the dynamic water level topography occurring during the two other acquisitions (1994/6/26 and 1994/8/9). The relative aspect in the space domain arises from the nature of the InSAR observations, which measures relative changes continuously and not across levies or other structures. We resolved this issue by using stage data for validation and calibration of the InSAR technique. In summary, the translation of the interferograms into hydrological meaning observations requires a good knowledge of the wetland environment, which we acquired by field trips, and good integration between the high spatial resolution space-based observations with high temporal resolution stage data.

As part of the proposed research, we plan to continue our hydrological analysis of already processed observations (interferograms) to other regions in the Everglades, beyond the three water conservation areas, analyzed in the preliminary study presented below. The hydrological analysis will involve field trips to the study areas, including airboat trips to less accessible locations. The field trip will enable us to relate space-based phenomena to local structure, as we did in our preliminary study. The hydrological analysis component will also include integration of stage, gate and meteorological data with our observations. The stage and gate data collection will be conducted as a summer job of an undergraduate student. Field work and the integration of the space- and terrestrial-based observations will be conducted by a post-doc under the PI's supervision.

Numerical Modeling

After obtaining Hydrological understanding of surface flow in the Everglades and other wetlands, we will use the high spatial resolution observations to constrain surface flow models. This part of the project will be conducted by the USGS, which developed a 500 x 500 m^2 resolution grid for studying surface flow in the southern section of the Everglades. The space-based observations will allow us to (i) evaluate spatial and

temporal variation of the flow transmissivity, (ii) relate transmissivity variations to vegetation, and (iii) estimate spatial and temporal evapo-transpiration rates.

Facilities at the University of Miami

The Geodesy Lab at the University of Miami (UMGL), located at the Rosenstiel School of Marine and Atmospheric Sciences (RSMAS) on Virginia Key, maintains a network of 7 Unix workstations: one SGI Octane, one Sun Ultra 60, 3 Sun Ultrasparc 10's and 2 rack-mounted Sun "pizza boxes"(Sunfire V-100). The system includes a CD ROM reader, a CD writer for data archiving, an 8 mm tape drive, 100 Gbytes of hard disc storage, and color and black&white laser printers. All computer equipment except the printer is powered by a UPS (Uninterruptible Power Supply) to allow us to span power interruptions and protect data on hard disc against voltage spikes associated with electrical storms, a frequent problem in south Florida. The Sun workstations are equipped with the GIPSY software (release version 2.5) for high precision GPS data analysis, provided by the Jet Propulsion Lab. Two Linux boxes are equipped with the "roi-pac" software from JPL for processing raw SAR data and generating interferometric and other advanced image products. The SGI is equipped with EarthView SAR processing software from Atlantic Scientific and VEXCEL software with similar features. The computer facilities are adequate for all the data analysis and modeling described in this proposal.

The Geodesy Lab performs daily analysis of more than 900 globally distributed GPS stations, for studies of crustal deformation, volcano monitoring, coastal stability, plate motion and plate rigidity, as well as analysis of SAR images for crustal deformation. Selected results are available our web site: http://www.geodesy.miami.edu

CSTARS - http://cstars.rsmas.miami.edu/

UMGL is connected by 2Gb/s fiber optic to CSTARS (Center for Southeastern Advanced Remote Sensing) located at UM's Richmond campus, the center for much of the university's space-related activities. CSTARS includes 2 11.3 m diameter X-band antennas for downlinking data from a variety of earth-orbiting satellites. This facility includes a 64Tbyte tape cartridge archive for raw satellite data, and numerous computers for data analysis, with more than 2 Tbyte of hard disc storage.

Related research.

A recent study by *Wdowinski et al.* [2004] describes new space-based hydrologic observations of South Florida, revealing spatially detailed, quantitative images of water levels in the Everglades. Their observations capture dynamic water level topography, providing the first three-dimensional regional-scale picture of wetland sheet flow, showing localized radial sheet flow in addition to a well defined southward unidirectional sheet flow. In this preliminary work, they used a 1-D linear diffusive flow formulation to simulate the unidirectional flow and to determine its corresponding hydrological parameters (vegetative friction coefficient). This proposal expands upon the initial study of *Wdowisnki et al.* [2004]. The main points of this work and its relationship to this work are described below.

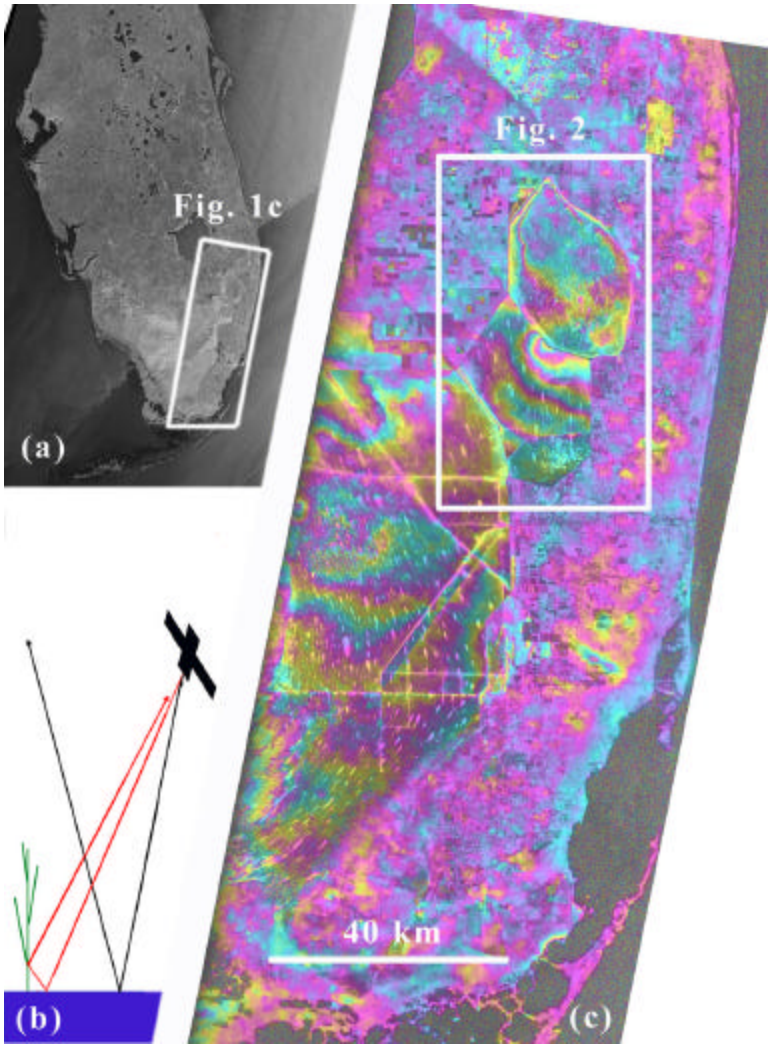

Figure 1: (a) RADARSAT-1 ScanSAR image of Florida showing location of study area (RADARSAT data © Canadian Space Agency / Agence spatiale canadienne 2002. Processed by CSTARS and distributed by RADARSAT International). (b) Cartoon illustrating the double-bounce radar signal return in vegetated aquatic environments. The red ray bounces twice and returns to the satellite, whereas the black ray bounces once and scattered away. (c) JERS L-band interferogram of the eastern south Florida area showing phase differences occurring during 44 days (1994/6/26-1994/8/9). Each color cycle represents 15.1 cm of elevation change (See color scale in Figure 2).

InSAR Data

InSAR combines SAR images of the same area acquired at different times from roughly the same location in space. By comparing the phase of individual pixels, cm-level changes of the Earth's surface can be detected. Most InSAR studies use C-band data (5.6 cm wavelength) to detect crustal deformation induced by earthquakes, magmatic activity, or water-table fluctuations [e.g., Massonnet et al., 1994]. L-band SAR data (24 cm wavelength), which penetrates through vegetation, were also used to study

crustal deformation in vegetated terrain [e.g., Murakami et al., 1996]. A different use of L-band data was developed by *Alsdorf et al.* [2000; 2001a; 2001b] to detect water-level variation in the Amazon wetland environment. They showed that interferometric processing of L-band SAR data (wavelength 24 cm) acquired at different times is suitable to detect water level variations in wetlands with emergent vegetation (measurement accuracy 3-6 cm). The radar pulse is backscattered twice ("double-bounce" [*Richards et al.*, 1987] – Figure 1b), from the water surface and vegetation (Figure 1b). A change in water level between the two acquisitions results in a change in travel distance for the radar signal (range change), which is recorded as a phase change in the interferogram.

The data consists of three SAR passes over South Florida acquired by the JERS satellite in 1994 (1994/6/24, 1994/8/9, and 1994/12/19), at the beginning, middle, and end of the local wet season (June-November). We calculated 3 interferograms, spanning 44 days (June-August), 132 days (August-December), and 176 days (June-December) covering the rural Everglades and urban Miami-Fort Lauderdale (Figure 1a).

The June-August interferogram shows very high interferometric coherence, in both rural and urban areas, and allows the following observations: (i) Significant elevation changes occur in the controlled-flow regions (within the white box in the upper half of Figure 1b). (ii) Discontinuities occur across man-made structures (canals, levees, and roads), and (iii) Elevation changes in Miami-Ft. Lauderdale metropolitan area are small. The two other interferograms, spanning longer periods, have lower coherence. *Wdowinski et al.* [2004] applied a spatial filter, improving the interferogram quality with some degradation in horizontal resolution (100x100 to 300x300 m^2), still significantly better than any available terrestrial monitoring technique.

InSAR detected water level changes

The most significant elevation changes occur in the northern section of the interferogram, across man-made structures, known as Water Conservation Areas (WCA) 1, 2A, and 2B. Figure 2 shows both the L-band backscatter amplitude and interferograms for the three time spans. The amplitude (brightness) variations (Figure 2a) represent the radar scatter, which depends on the surface dielectric properties and surface orientation with respect to the satellite. The small, elongated white areas are vegetated tree islands aligned along the long-term regional flow direction. The large white areas in areas 2A and 2B are dense vegetated areas. The pattern of water level change is unidirectional in the eastern section of area 2A and radial in the western part. In the northern section of area 2B the water level change is characterized by 3 radial ("bulls eye") patterns (b and c). The interferometric phase (Figure 2b, 2c and 2d) show water level changes in area 2A; the change direction and amount vary. The change in Figure 2b indicates water level decrease towards the NE by about 60 cm (4 cycles), in Figure 2c a NE decrease of about 105 cm (7 cycles), and in Figure 2d an increase by 45 cm (3 cycles with opposite color scheme), which agrees with the difference between (2b) and (2c).

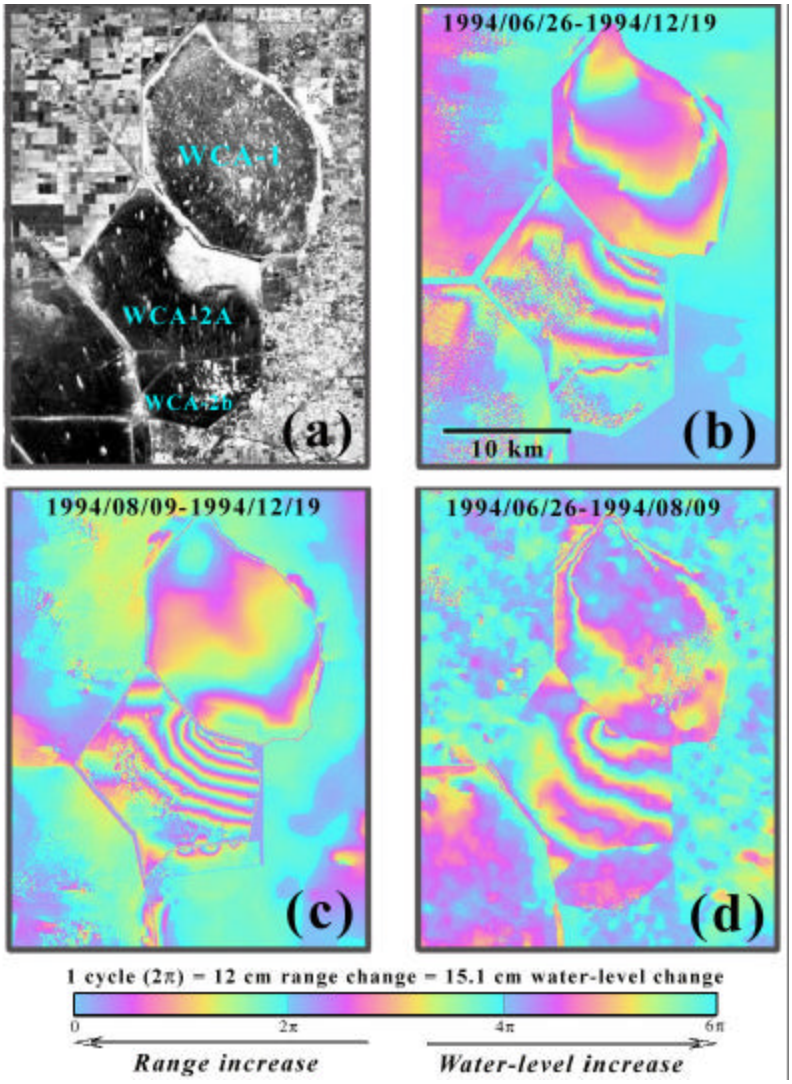

Figure 2: L-band backscatter amplitude and interferograms of the Water Conservation Areas (WCA) 1, 2A, and 2B (location in Figure 1c). (a) Amplitude (brightness) variations represent radar backscatter, which depends on the surface dielectric properties and surface orientation with respect to the satellite. The small elongated white areas in the WCAs are vegetated tree islands (*10*), aligned along regional flow direction. Large white areas in 2A and 2B are dense vegetated areas. (b) 176-day (June-December) interferogram, (c) 132-day (August-December) interferogam, and (d) 44-day (June-August) interferogram. The interferograms show the largest water level changes occurred in area 2A (up to 1 m – 7 cycles in (c)) and smaller scale ones in areas 1 and 2B. (ii) The pattern of water level change is unidirectional in the eastern section of area 2A and radial in the western part. In the northern section of area 2B the water level change is characterized by 3 bulls-eye radial patterns (b and c).

Figure 3 shows the June-December water level changes in areas 1, 2A, 2B and their surroundings. Because InSAR measures relative changes within each area, but not between the areas, we assigned in each area the lowest change level to zero. The most significant water level changes occur in the eastern section of area 2A, where the level changes can be described by a series of NWN-ESE almost parallel contours.

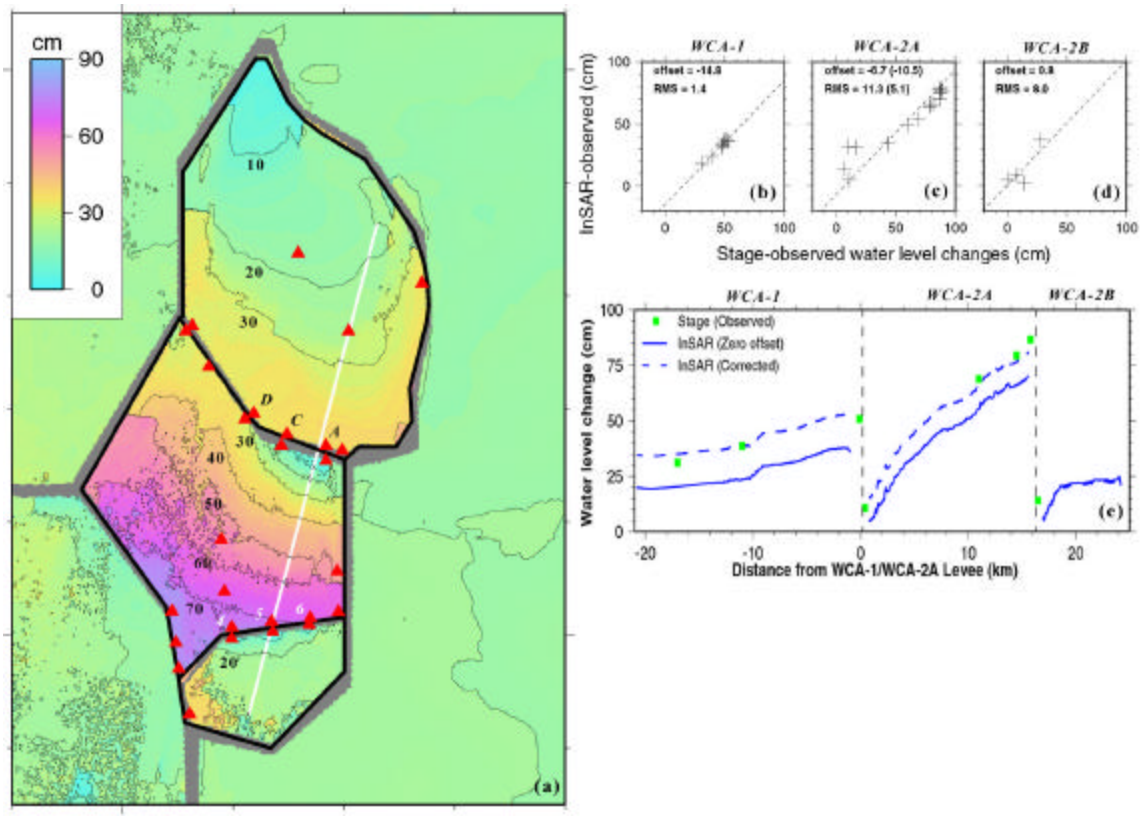

Figure 3: (a) InSAR-based water level change map for the June-December time interval of areas 1, 2A and 2B. Red triangles mark the location of stage stations and the white line marks the water level profile location. The characters (A, C and D) and (digits 4, 5 and 6) mark gate locations, presented in Table 1. (b, c, and d) Comparison between the zero-offset InSAR and the stage data calculated separately for each area. (e) Comparison between InSAR and stage water level changes along the profile. Stage data observed in the center of areas 1 and 2A are projected onto the profile. The vertical dashed lines mark the location of levees separating between the conservation areas. The corrected InSAR curve (dashed line) is calculated from a least-squares adjustment.

Table 1: Flow observation (CFS – cubic feet per second) collected by the SFWMD during the JERS data acquisition at the gates feeding and draining area 1A. (Data source: DBHYDRO - http://www.sfwmd.gov/org/ema/dbhydro/index.html). The symbol indicates the gate location in Figure 3a.

Station	Levee	Symbol	1994/06/26	1994/08/09	1994/12/19
S10D	1-2A	D	0	1170	0
S10C	1-2A	C	489	1447	88
S10A	1-2A	A	510	1485	0
S144	2A-2B	4	90	83	0
S145	2A-2B	5	117	95	0
S146	2A-2B	6	82	53	0

In order to validate and calibrate our InSAR technique, we compared the InSAR observations with stage data (red triangles in Figure 3a) collected by the South Florida Water Management District (SFWMD). The stage data consist of daily average level above the NGVD29 datum. We use these data to calculate water level differences

between the two acquisition dates. Comparison between the InSAR and stage data shows excellent agreement for each of the three water conservation areas (Figure 3b, 3c and 3d). It also allows us to compute and correct the datum offset between stage and InSAR data, which were set arbitrarily to zero value at the lowest level in each area (Figure 3e).

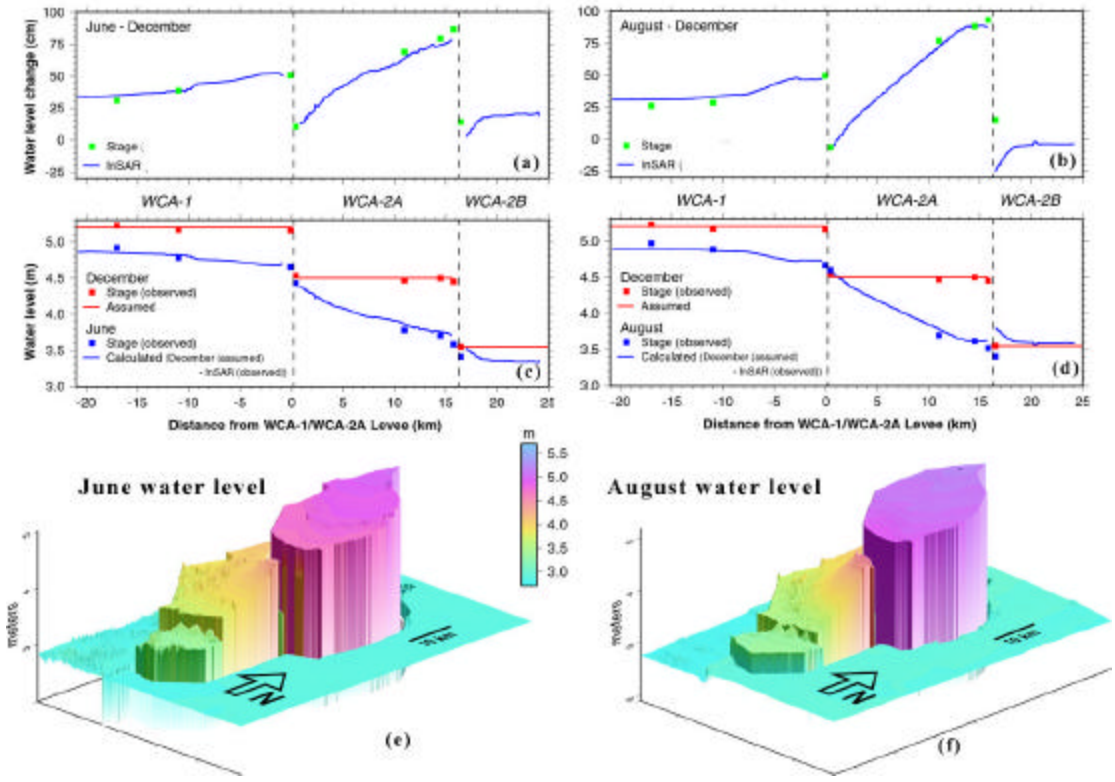

Figure 4: (a) Water level changes along the profile in Figure 3c, showing corrected InSAR curve and stage data for June-December time interval. Vertical dashed lines mark location of levees separating the WCAs. (b) Water level changes for the August-December time interval. (c) June and December water levels along the profile. Based on the December stage data (red squares) and gate information (Table 1), we assume flat water level in each area (red lines). The June water level (blue line) is obtained by subtracting the corrected InSAR curve from the assumed flat December level.(d) August and December water levels following the same procedure as in (c). (e) Three-dimensional illustration of the June water levels, calculated by subtracting the corrected InSAR data from the assumed flat December levels, for the entire studied area. (f) Three-dimensional illustration of the August water levels.

From water level change to absolute water level

The new space-based observations provide, with very high spatial resolution, water level changes in the Everglades occurring over 44, 136 and 176 day time intervals (Figures 3, 4a and 4b). Because these time intervals are long compared to the duration of natural and anthropogenic water level changes in the Everglades (days to several weeks), the observed water level changes represents the differences between two states and not a continuous process. Figures 4c and 4d present stage elevations during the three observation periods. The December InSAR observation occurred during a period of

negligible water flow across the conservation areas (Table 1), resulting in almost flat water levels in the three areas (red lines in Figures 4c and 4d).

Hydrologic Model

Wdowinski et al. [2004] used a diffusion flow model to explain the observed dynamically supported water topography and derive quantitative estimates of transmissivity and Manning's friction parameter. Their model follows the *Akan and Yen's* [1981] diffusion flow formulations, which are derived from conservation of mass and momentum principles, neglecting inertial terms. The model is appropriate to low-Reynolds hydrologic flows, where the flow is predominantly laminar. It follows the same formulation as the SFWMM [*Lal*, 1998, 2000] which has been used extensively to model surface flow in South Florida. For overland flow, the water level (H) can be describe in terms of its derivatives in time (dH/dt) and space (dH/dx), water transmissivity (or diffusivity) (D), and sink terms representing rainfall, evapotranspiration, and infiltration [Lal, 1998, 2000]. The transmissivity (diffusivity) represents a Fickian form for the relation between volumetric flow rate and surface water elevation gradient and is a function of flow frictional characteristics. For instance, if Manning's friction relationship is applied, then $D = h^{5/3} / (\boldsymbol{n}\ |dH/dx|^{1/2})$, where $\boldsymbol{n}$ is Manning's dimensionless friction coefficient, a measure of the resistance to flow [*Lal*, 1998, 2000].

In order to calculate dynamically supported water levels, we need to specify initial and boundary conditions, which are poorly constrained. Rather then modelling water levels in all three water conservation areas and accounting for complex gate operation history, we focus on the process that governs dynamically supported water level topography and model the region where this phenomenon is most pronounced - the eastern section of area 2A (Figure 3a). In this region the hydrologic flow lines are orthogonal to InSAR water level contours, indicating a southward flow during June and August 1994. The unidirectional flow in this region allows a simple one-dimensional analytical solution. As a first approximation, we: (1) assume a spatially uniform transmissivity (D); and (2) neglect sink terms, deriving the familiar one-dimensional diffusion equation:

$$\frac{dH}{dt} = D\frac{d^2H}{dx^2} \qquad (1)$$

The boundary conditions are derived from the stage and gate operation time series. We apply an instantaneous gate opening model, which assumes (1) a flat water level in area 2A prior to the opening of the gates (supported by the stage data), (2) area 2A is infinitely long, and (3) water level in area 1 remains constant (supported by stage data). The above assumptions allow us to determine initial and boundary conditions and to solve equation (1) analytically [*Carslaw and Jaeger*, 1959] using a three term series expansion. We use a best-fit adjustment to estimate the polynomial coefficients and calculate two flow parameters: the initial water elevation difference across the gate (H_0) and the flow characteristic length $(Dt)^{1/2}$.

Figure 5 and Table 2 show that the InSAR data constrain the model parameters to ~5% uncertainty. However, the full coupling of time and transmissivity as a single parameter - the diffusion characteristic length $(Dt)^{1/2}$ - does not allow us to uniquely determine the transmissivity coefficient (D). Nevertheless, we use the gate operation

history to estimate the time since opening, as 16±2 days for June and 8±2 days for August, in order to estimate transmissivity.

Wdowinski et al. [2004] also calculated the corresponding Manning friction factor *n* for diffusive flow. Reported values of *n* for sheet flow through vegetation are in the range $0.10 < n < 1.0$ [*Overton and Meadows*, 1976; *Akan and Yen*, 1993; *Nepf*, 1999; *Lal*, 2000; *Lee et al.*, 1999; *Wu et al.*, 1999; *Kouwen and Irrig*, 1992]. We find our InSAR based determined *n* to be in the same range. For the June period, *n* is somewhat higher (0.7-1.0) compared to the August period (0.3-0.7). The difference represents the influence of vegetation on flow, with higher friction at lower water levels (June) compared to higher water levels (August). This decrease of resistance to flow with increasing water depths has been reported in the literature [*Lee et al.*, 1999; *Wu et al.*, 1999; *Kouwen and Irrig*, 1992]. The obtained range of friction values of the flow transmissivity for vegetated flow is, as expected, higher than that of unvegetated earthen beds, in the range of 0.01-0.04 [*Akan and Yen*, 1993]. A higher Manning friction coefficient implies a lower flow transmissivity and vice versa. This finding is also consistent with estimated decreases of 1-2 orders of magnitude in scalar transport dispersion between unvegetated and vegetated surface flows [*Nepf*, 1999].

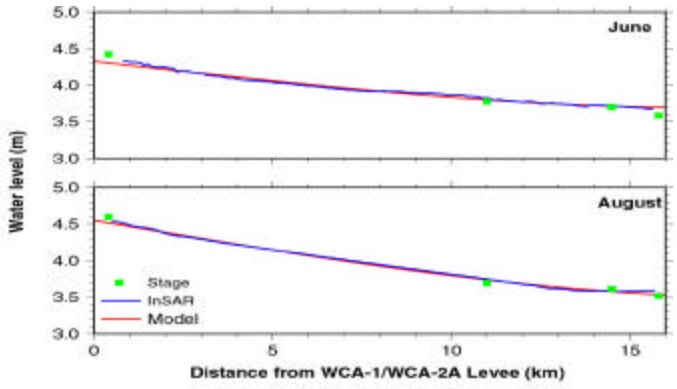

Figure 5: Comparison between observed stage, InSAR, and best-fit modeled water levels in June and August 1994 across area 2A (along the N-S profile shown in Figure 3). Model parameters are described in Table 2.

Table 2: Summary of Hydrologic Modeling (see in Figure 5).

Parameter	Description	June 1994	August 1994
H_0 (m)	Elevation difference	0.85±0.04	1.41±0.05
Dt (m^2)	Characteristic length	$73.2\pm3.3 \times 10^6$	$91.9\pm 3.8 \times 10^6$
D (m^2/s)	Transmissivity	52±11	133±46
$\boldsymbol{n}$ [1]	Manning's coefficient	0.7 – 1.0	0.3-0.7

[1]: $\boldsymbol{n}$ is estimated using reference values of $h=1$ m and $-dH/dx=7\ 10^{-2}$ m/km.

Training potential.

The proposed research will support the training of one graduate student and one undergraduate student. The graduate student is Dawn James, who is a USGS employee and is in the process of applying to UM for her Ph.D. program. She is hydrologist by

training and is interested to learn and apply InSAR technique and observations to hydrological problems. Her research focus will be on the usage of InSAR-measured surface elevation changes and aquifer-system deformation in southern Florida. Although her thesis research has a different focus than our proposed research to NIWR, she will greatly benefit from the data, resources and personnel working on a related problem.

An undergraduate student will work for the project during two summers. He will be trained in remote sensing, InSAR data processing and hydrology, as well as enriching his computer skills. The planned undergraduate training will prepare him/her to any good graduate programs in Earth Science and/or to a real job.

Statement of Government Involvement.

The co-PI Roy Sonenshein (USGS) will be responsible to transfer and use the space-based water-level observations for constraining the USGS's TIME (Tides and Inflows in the Mangroves of the Everglade - http://time.er.usgs.gov/) flow model of the Everglades. The high-spatial resolution InSAR measurements (300 x 300 m2) are excellent observations for constraining the 500 x 500 m2 spatial resolution of the TIME model.

Information Transfer Plan.

The project's disseminating information plan includes the following three components:

1. Local (southern Florida) – We plan to present the project results at local academic, research, environmental, and water managements organizations. So far, we presented our preliminary study results and received very positive feedback at following local institutes: University of Miami, Florida International University, Everglades National Park and the Loxahatchee Wildlife refuge. We plan to further inform these institutes about our results, as well as contacting other local organizations, such as the South Florida Water Management District, the local office of the Army Core of Engineers, the Miami and other regional offices of the USGS. We also plan to present the project results at the up coming GEER (Greater Everglades Ecosystem Restoration) Conferences. By presenting our results locally we hope to promote the usage of the space-based measurements as a monitoring tool, as well as important constraints for detailed surface flow models of the Everglades.
2. National – We plan to present the project results at least two national meetings, e.g., AGU, the NASA Surface Water Working Group (SWWG), etc. When we'll achieve significant results for the Louisiana Coast and Chesapeake Bay wetlands, we'll contact local organization in these areas, in order to expose them to the project and its results.
3. International – As part of project's information transfer plan, we also plan to attend the upcoming JAXA's (Japan Aerospace Exploration Agency) ALOS meeting (9 month after the launch of the ALOS satellite, which is scheduled for 12/04) to report on our progress and further promote the usage of SAR data for hydrological applications. If possible, we will also attend other international meetings with SAR/InSAR focus.

Literature Citations/References

Akan, A.O. and B.C. Yen, J. Hyd. Div. ASCE, **107**, 719, 1981.

Alsdorf DE, Melack JM, Dunne T, Mertes LAK, Hess LL, Smith LC, Interferometric radar measurements of water level changes on the Amazon flood plain, Nature, 404 (6774): 174-177 MAR 9 2000.

Alsdorf D, Birkett C, Dunne T, Melack J, Hess L, Water level changes in a large Amazon lake measured with spaceborne radar interferometry and altimetry, GEOPHYSICAL RESEARCH LETTERS, 28 (14): 2671-2674 JUL 15 2001a

Alsdorf DE, Smith LC, Melack JM, Amazon floodplain water level changes measured with interferometric SIR-C radar, IEEE TRANSACTIONS ON GEOSCIENCE AND REMOTE SENSING, 39 (2): 423-431 FEB 2001b.

Amelung, F., D. L. Galloway, J. W. Bell, H. A. Zebker, and R. J. Laczniak, Geol., **27**, 483, 1999.

Amelung, F., S. Jónsson, et al. (2000). "Widespread uplift and 'trapdoor' faulting on Galápagos volcanoes observed with radar interferometry." Nature 407(26 October): 993 - 996.

Bawden G. W., W. Thatcher, R. S. Stein, K. W. Hudnut, and G. Peltzer, Nature, **412**, 812, 2001

Bhallamudi, S.M., S. Panday and P.S. Huyakorn, Sub-timing in fluid flow and transport simulations, *Adv. Wat. Resour*. 26, 477-489, 2003.

Burgmann, R., P. A. Rosen, and E. J. Fielding, Ann. Rev. Earth Planet. Sci., **28**, 169, 2000.

Carslaw H. S., and J. C. Jaeger, *Conduction of heat in solids* (second edition), Oxford University Press, New York, 1959.

Kouwen N., and J. Irrig. Drain. E.-ASCE **118**, 733, 1992.

Lal, W.A.M, J. Hydraul. Eng., **124**, 342 1998; Water Resources Res., **36**, 1237, 2000.

Lee, J.K, V. Carter, and N.B. Rybicki, Proceedings of the Third International Symposium on Ecohydraulics, July 1999.

Massonnet, D., M. Rossi, C. Carmona, F. Adragna, G. Peltzer, K. Feigl, and T. Rabaute, The displacement field of the Landers earthquake mapped by radar interferometry, *Nature*, *364*, 138-142, 1993.

Massonnet, D., K. Feigl, M. Rossi, F. Adragna, Radar interferometric mapping of deformation in the year after the Landers earthquake. *Nature, 369,* 227-230, 1994.

Massonnet, D., and K. L. Feigl, Discriminating geophysical phenomena in satellite radar interferograms, *Geophys. Res. Lett., in press,* 1995a.

Massonnet, D., P. Briole, et al. (1995). "Deflation of Mount Etna monitored by spaceborne radar interferometry." Nature 375: 567-570.

Massonnet, D. and K. L. Feigl, Rev. Geophys., **36**, 441, 1998.

Mumby, P.J., Edwards, A.J., 2002, Mapping marine environments with IKONOS imagery: enhanced spatial resolution can deliver greater thematic accuracy, Remote Sensing of Environment, 82, 248-257.

Murakami, M., M. Tobita, et al. (1996). "Coseismic crustal deformations of the 1994 Northridge, California earthquake detected by interferometric analysis of SAR images acquired by the JERS-1 satellite." J. Geophys. Res. 101: 8605-8614.

Overton, D.E., and M.E. Meadows, *Stormwater Modeling* (Academic Press, New York, 1976).

Maidment D.R., *Handbook of Hydrology*, McGraw-Hill, New York, 1993.

McLaughlin, D.B. and L.R. Townley, A reassessment of the groundwater inverse problem, *Water Resour. Res*., 32(5), 1131-1161, 1996.

Nepf H. M., Water Resour. Res. **35**, 479, 1999.

Richards, L. A., P. W. Woodgate, and A. K. Skidmore., Inter. J. Remote Sensing, **8**, 1093, 1987.

Storm, B. and A. Rafsgaard, Distributed physically-based modeling of the entire land phase of the hydrologic cycle, Kluwer Academic Publishers, 1996.

Wdowinski, S., F. Amelung, F. Miralles-Wilhelm, T. Dixon, and R. Carande, Space-based measurements of sheet-flow characteristics in the Everglades wetland, Florida, Submitted to Geophys. Res. Lett., 2004.

Wu F.-C., H. W. Shen, and Y.-J. Chou, J. Hydraul. Eng.-ASCE, **125**, 934, 1999.

Yeh, G. T., 1999. Computational Subsurface Hydrology Fluid Flows. Kluwer Academic Publishers

Zebker, H. and J. Villasenor, Decorrelation in interferometric radar echoes, *IEEE Trans. Geosci. Rem. Sensing, 30*, 950-959, 1992.

Zebker, H., P. Rosen, R. Goldstein, A. Gabriel, and C. Werner, On the derivation of coseismic displacement fields using differential radar interferometry: the Landers earthquake, *J. Geophys. Res.*, 99, 19617-19634, 1994a.

Zebker, H.A., T.G. Farr, R.P. Salazar, and T. Dixon, Mapping the world's topography using radar interferometry: the TOPSAT mission, *Proc. Inst. Electrical Electonic Eng., 82.*, 1774-1786**,** 1994b.

Zebker, H.A., C. Werner, P.A. Rosen, S. Hensley, Accuracy of topographic maps derived from ERS-1 interferometric radar, *IEEE Trans. Geosci. Rem. Sens., 32*, 823-836, 1994c.

Zebker H. A., P. A. Rosen, and S. Hensley, J. Geophy. Res., **102**, 7547, 1997.

A comparison of FSU/NWS and OneRain precipitation data and their insertion into the WAM hydrologic model

Basic Information

Title:	A comparison of FSU/NWS and OneRain precipitation data and their insertion into the WAM hydrologic model
Project Number:	2006FL140B
Start Date:	3/1/2006
End Date:	2/28/2008
Funding Source:	104B
Congressional District:	2
Research Category:	Climate and Hydrologic Processes
Focus Category:	Climatological Processes, Hydrology, None
Descriptors:	
Principal Investigators:	Henry Fuelberg

Publication

1. Fuelberg, H.E., S.M. Martinaitis, J.L. Sullivan, Jr., and C.S. Pathak, 2007: An intercomparison of precipitation values from the OneRain Corp. algorithm and the National Weather Service Procedures. World Environmental and Water Resources Congress, Tampa, May 2007, in press.
2. Fuelberg, H.E., D.D VanCleve, Jr., and T.S. Wu 2007: An intercomparison of mean areal precipitation from gauges and a multisensor procedure, World Environmental and Water Resources Congress, Tampa, May 2007, in press.
3. D.D. VanCleve, and H.E. Fuelberg, 2007: An intercomparison between mean areal precipitation from gauges and a multisensor procedure, 21st Conf. on Hydrology, Amer. Meteor. Soc., San Antonio, January 2007, in press.
4. Martinaitis, S.M., H.E. Fuelberg, J.L. Sullivan, Jr., and C. Pathak, 2007: An intercomparison of precipitation values from the OneRain Corp. algorithm and the National Weather Service procedure. 21st Conf. on Hydrology, Amer. Meteor. Soc., San Antonio, January 2007, in press.

Progress Report

"A Comparison of FSU/NWS and OneRain Precipitation
Data and Their Insertion Into the WAM Hydrologic Model"

Submitted by

Henry E. Fuelberg
Florida State University

This project compares precipitation values from two procedures (National Weather Service (NWS) and the OneRain Corp. (OR)) that combine radar- and gauge-derived precipitation estimates into a single high resolution dataset over areas of the South Florida Water Management District. The NWS scheme is used operationally by the NWS to issue flood watches and warnings. The OR scheme is used by various private and government agencies to monitor potential flood situations and as data for making decisions about water quality regulations. This project intercompares the two procedures, noting their strengths and weaknesses, and using the two procedures as input to the WAM hydrologic model. The project research constitutes the M.S. thesis research for Mr. Steve Martinaitis.

The statistical intercomparison of precipitation from the two procedures is well underway. Initial results have been obtained for calendar years 2004 and 2005. A detailed study of rainfall differences during Hurricane Wilma also is well underway. The OR data are on a 2×2 km Cartesian grid at 15 min intervals, while the NWS hourly data are on a 4×4 km grid that is oriented approximately northeast-southwest. The OR data were summed to hourly values and placed onto the coarser NWS grid using procedures within GIS. Results show that this transformation was achieved with a very high degree of accuracy—differences between original and transformed data were < 1%. Our various kinds of intercomparisons are based on these data sets now on a common grid. Standard statistical products have been computed to quantify spatial and area-wide differences over days, months, and years. This is being done for individual basins within the SFWMD as well as for their entire area of jurisdiction.

Insertion of the two data types into the WAM Hydrologic Model is just beginning. The source code has been obtained from its inventors (SWET Corp. of Gainesville, FL), and the graduate student has been trained by SWET personnel. Some modifications currently are being made to the WAM model so it can accept the high resolution radar-derived data. These modifications will insure that differences in streamflow will be due to differences in the input rainfall data, and not to other factors.

We have made excellent progress so far. The results to date have been presented at seminars at the South Florida Water Management District in West Palm Beach and at the Florida Department of Environmental Protection in Tallahassee. The results will be presented as two accepted papers at the 2007 World Environmental and Water Resources Congress and two

papers at the 21st Conference on Hydrology (sponsored by the American Meteorological Society). As soon as the research is completed, results will be submitted to a refereed journal for publication. The results may be split into two manuscripts An additional one year of funding will be required for the graduate student to complete all of the tasks of the project.

Additional project details and long-term objectives are discussed in the following sections.

A Comparison of FSU/NWS and OneRain Precipitation Data and Their Insertion Into the WAM Hydrologic Model—Phase II

Key Words--Radar-derived Precipitation, Hydrologic Modeling

1. Statement of the Florida Water Problem

Two widely used procedures by which radar- and gauge-derived rainfall can be optimally combined are those by the OneRain Corporation and the National Weather Service (NWS). The several Florida Water Management Districts use rainfall data from the OneRain algorithm. Conversely, Florida State University (FSU) has employed the National Weather Service scheme to create an historical precipitation database for the Florida Department of Environmental Protection (FDEP). Although the methodologies to produce each dataset as well as the spatial and temporal resolution of each differ, each is being used by their respective agencies to make water management and regulatory decisions. Thus, it is important to know how rainfall values from the two schemes compare to each other. This research statistically compares results from the two schemes, develops procedures so that both versions of data can be inserted into the WAM hydrologic model, and performs WAM model runs over various watersheds within the South Florida Water Management District (SFWMD) using both datasets.

2. Statement of Benefits

The Florida Water Management Districts and the FDEP will base important decisions on their respective rainfall datasets. Thus, there is the possibility that the two groups will reach different conclusions—each of which is supported by their own data. This research will quantify differences between the two rainfall datasets to determine how similar/dissimilar they are. The research also will expand our understanding of how high resolution rainfall data can be best used effectively in hydrologic modeling.

3. Nature, Scope, and Objectives of the Research

a. Florida State University's High Resolution Historical Database

The FSU precipitation database was prepared for the FDEP using software developed by the NWS for real time use at their regional River Forecast Centers (RFCs) and local forecast offices. Called the RFC-wide Multi-sensor Precipitation Estimator (denoted MPE), the procedure blends radar-derived hourly digital precipitation data at 4 km resolution with hourly gage data. Details of MPE are provided by Fulton et al. (1998), Seo et al. (1999), and Marzen et al. (2005).

Radar Input—The continental United States is scanned continuously by approximately 125 Doppler (NEXRAD) radars operated by the NWS. Each radar produces an hourly estimate of rainfall on a 4 x 4 km grid. Since most grid points within the U.S. are viewed by more than one radar, MPE each hour determines the radar providing the best coverage of each individual 4

km grid point. Although radars provide excellent spatial resolution of rainfall, there are various limitations, many of which are described in Baeck and Smith (1998) and similar publications. These limitations include improper beam filling and the overshooting of low cloud tops at farther ranges, hail contamination, radar mis-calibration, and the unknown relation between radar reflectivity and rainfall (Z-R relations) for a particular storm. Because of these limitations, the MPE procedure also incorporates rain gauge data into its algorithm.

Gauge Input—FSU obtained hourly rain gauge data from each of the State's Water Management Districts and from gauges whose data are archived by the National Climatic Data Center. These gauge data were rigorously quality controlled—a very time consuming but very necessary task. The MPE scheme objectively analyzes the hourly gauge data onto the 4 x 4 km grid employed for the radar data.

Blending the Radar and Gage Estimates--Using pairs of rain gauges and raw radar precipitation estimates, the MPE software calculates bias correction factors each hour for every radar to improve the remotely sensed precipitation values. When the hourly radar-derived precipitation values are multiplied by this correction, radar wide biases due to factors such as radar mis-calibration are removed. Then as a second step, the bias corrected radar-derived precipitation data are merged with the hourly rain gage observations using optimal interpolation. There are a number of "adaptable parameters" within the MPE software that allow users to optimize the procedure for the specific area for which calculations are made.

An example of the final MPE product for the Black Creek Basin of the St. Johns River is given in Fig. 1. The figure shows the summation of hourly values for February 2001.

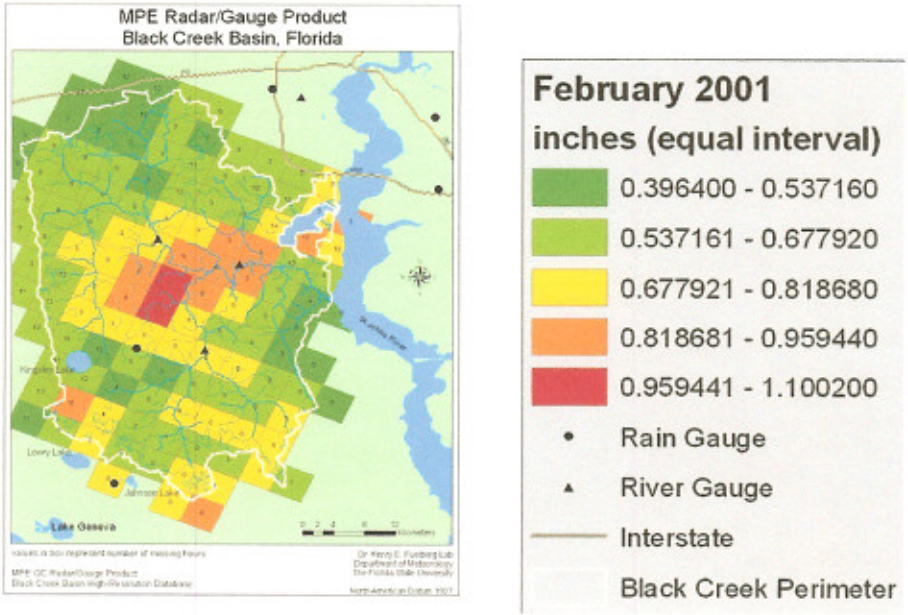

Fig. 1. The Black Creek Basin with superimposed total rainfall (inches) for February 2001. Note that only two rain gauges lie within the Basin.

Recent studies and validations that have utilized radar schemes to estimate precipitation include Smith et al. (1996), Steiner et al. (1999), Klazura et al. (1999), Wang et al. (2000), and Marzen and Fuelberg (2005). These studies have noted the improvements provided by optimally combining radar and gauge information.

b. The OneRain Precipitation Algorithm

The Florida Water Management Districts have contracted with the OneRain Corporation to provide real time and historical precipitation data. The historical database consists of years 2002-2005 (4 years). The OneRain product is on a 2×2 km grid at 15 min. intervals. Although the procedure that OneRain uses is proprietary, the cursory description below is believed to be correct based on information at their web site (http://onerain.com) and in Nelson et al. (2003).

Radar input for the algorithm is the composite radar reflectivity maps produced by the Weather Services International (WSI) Corporation based on data from the national network of WSR-88D radars operated by the NWS and other federal agencies. The Level III radar data from each site (Fulton et al. 1998) are collected by WSI and used to produce a national mosaic of radar-derived precipitation at 15 min. intervals on a 2×2 km grid. When one or more radars overlap a grid point, the greatest rainfall value is used. Rainfall estimates are based on the lowest available antenna angle at each radar. The web site states, "WSI's rainfall estimation procedure uses a dynamic weather condition-based algorithm to convert reflectivity values to rainfall estimates The WSI procedure uses a variety of weather parameters to sense what type of weather condition exists, then chooses the most appropriate conversion from reflectivity to rainfall rate."

Rain gauge-derived precipitation also is input to the OneRain algorithm. FSU assumes that data from most or all of the Florida Water Management Districts are employed. We do not know whether NWS or other gauge data are input. FSU also does not know the nature of the quality control that is used on the gauge data. The gauge data are used to calibrate the radar-derived dataset. The OneRain site states that if there is an insufficient number of gauges with 15-min data, "daily and hourly data were disaggregated to 15 min time steps using the normalized radar data at each gauge location as the distribution function. Calibrations were performed to adjust the radar estimates to match the rain gauge estimates, on average, at the monthly level."

Rainfall values from the OneRain and FSU/NWS procedures have never been compared by any group. Thus, this research will demonstrate the characteristics of these data within Florida.

c. Objectives

Available information about the OneRain and FSU/NWS precipitation algorithms clearly indicates that different methodologies and input data are used. The resolutions of the final products also differ, i.e., 2×2 vs. 4×4 km grid, and 15 min. vs. hourly intervals. This suggests that values from the two algorithms also differ. The objectives of this research are to 1) quantify the amount of that difference and 2) develop procedures to insert both types of rainfall data into

the WAM hydrologic model, and make separate runs using each type of data for selected watersheds within the SFWMD.

d. Estimated Timeline—Task 1 (described below) will be completed by the end of the initial one year period (Spring 2007). Tasks 2 and 3 (described below) will be completed by the end of the second year of funding.

4. Methods and Procedures

Task 1—FSU will quantify differences between the FSU/NWS historical dataset and the OneRain dataset using standard statistical procedures (scatter diagrams, mean differences, standard deviation of differences, etc.). This will be done for the four year period of record 2002-2005 when both datasets are available. This step is virtually complete, and a summary of results is provided in the following major section

Task 2—FSU will develop procedures so that both the OneRain and FSU datasets can be input to the Watershed Assessment Model (WAM) hydrologic model such that optimal results are obtained. WAM is a GIS-based model developed by Soil and Water Engineering Technology, Inc. (SWET) of Gainesville, FL. It is described in detail in a number of publications by SWET personnel. WAM simulates the hydrology of a watershed using various imbedded models. Although WAM has been coded to accept the FSU 4×4 km MPE rainfall, initial streamflow results for the Black Creek Basin were mixed (SWET report to FDEP, 2003). These findings are counter to most of the literature which indicates superior results from radar-derived precipitation. This suggests that WAM must be modified to properly utilize the high resolution data. That is one of the goals of the current proposed effort.

Successful use of either OneRain or FSU/NWS data requires more than just changing format input statements from accepting rain gauge data to accepting the gridded gauge plus radar combination. For example, a number of run off and percolation schemes have been developed for use in hydrologic models. GLEAMS is designed for daily precipitation input and works best in well drained soil. The EAAMod scheme can use any interval of rainfall data (hourly, daily, etc.) and was designed for regions with a high water table. A number of other models are described in the literature, and the SWET team currently is preparing alternative schemes for use in WAM. With the assistance of SWET personnel, several schemes will be tested within WAM to determine their impacts on runoff and percolation. Based on the results, FSU and SWET will select the most appropriate equation to use for each dataset, and develop coefficients for use with the various spatial and temporal scales of the rainfall data. Thus, the goal is to optimize WAM for using high resolution rainfall data.

It should be noted that the FDEP currently is supporting the Task 2 efforts for FSU/NWS input. One FSU student has received WAM training by SWET personnel, and SWET has been collaborating with us. The funds requested here will support similar efforts for OneRain data.

Task 3--This task will perform WAM-based hydrologic modeling using data from both the FSU/NWS and OneRain procedures.

a. Several basins will be selected for study. These basins will be of special interest to the Water Management Districts and to FDEP. SWET either already will have configured WAM for these basins or will currently be configuring them. FSU is not expected to perform the detailed model configuration for a basin.

b. FSU will make WAM runs over the selected basins over various periods of time and for various rainfall scenarios. These scenarios will include widespread heavy or light precipitation as well as scattered convective rain, different seasons, different basin sizes, etc. One set of runs will utilize the OneRain dataset. A second set of runs will utilize the FSU/NWS dataset and hopefully will be sponsored by FDEP.

c. The various computed streamflows, together with observed streamflows, will be compared using hydrographs and various statistical tools. As a result, we will understand the role of differences in the OneRain and FSU/NWS datasets in producing differences in streamflow.

5. Accomplishments from Last Year

The statistical intercomparison of precipitation from the two algorithms is almost complete. Results have been obtained for calendar years 2004 and 2005. A detailed study of rainfall differences during Hurricanes Wilma and Katrina also is nearly complete. The OneRain data on a 2×2 km Cartesian grid at 15 min intervals were summed to hourly values and placed onto the coarser hourly, 4×4 km NWS grid using procedures within GIS. This transformation was achieved with a very high degree of accuracy—differences between original and transformed data were < 1%. Our various inter-comparisons are based on these data sets now on a common grid. Standard statistical products have been computed to quantify spatial and area-wide differences over days, months, and years. As an example, Figure 2 shows spatial fields of the OneRain and NWS/FSU annual rainfall totals for 2004. The right panel of Fig. 2 shows that OneRain annual rainfall is greater than the FSU amounts over much of the area. Figure 3 shows scatter diagram comparing the two versions of rainfall for two individual months during 2004. Statistics also are being compiled for individual basins within the SFWMD. Table 1 compares mean areal precipitation for the Tamiami East Watershed.

Insertion of the two data types into the WAM Hydrologic Model is just beginning. The source code has been obtained from its inventors (SWET Corp. of Gainesville, FL), and a graduate student has been trained by SWET personnel. Some modifications currently are being made to the WAM model so it can accept the high resolution radar-derived data. These modifications will insure that differences in streamflow will be due to differences in the input rainfall data, and not to other factors.

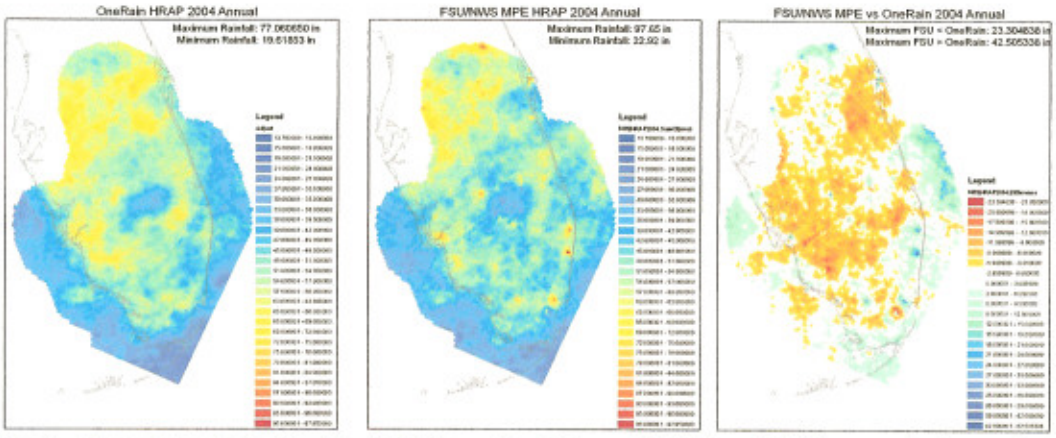

Fig. 2. Annual precipitation for 2004 from OneRain and MPE, and differences between the two products. Warm colors show greater estimates from OneRain. Cool colors show greater estimates from FSU/NWS.

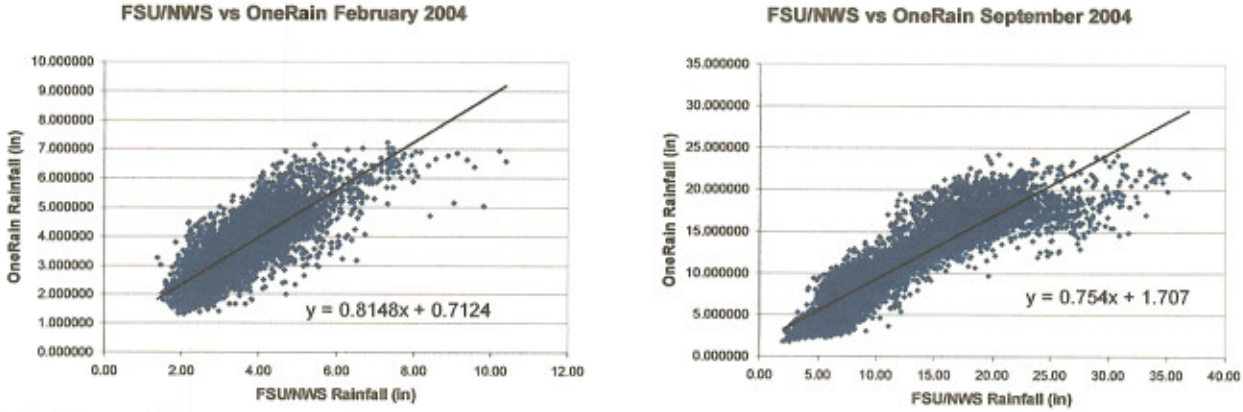

Fig. 3. Scatter diagrams comparing values of FSU/NWS pixel values with those from OneRain for February and September 2004.

Table 1. Comparison of Mean Areal Precipitation (MAP) for the Tamiami East Watershed.

Month/Year	MAP FSU/NWS (in.)	MAP OneRain (in.)	MAP Difference (in.)	Percent Difference
Jan 2004	2.378031	2.151367	0.226664	9.532 %
Feb 2004	3.482546	3.457805	0.024741	0.710 %
Mar 2004	1.278589	0.902159	0.376430	29.441 %
Apr 2004	3.935067	2.967373	0.967694	24.592 %
May 2004	2.582166	1.435037	1.147129	44.425 %
Jun 2004	3.778446	2.632247	1.146199	30.335 %
Jul 2004	7.677876	6.886893	0.790983	10.302 %
Aug 2004	10.503016	12.410105	-1.907089	-18.158 %
Sep 2004	13.585865	9.677520	3.908345	28.768 %
Oct 2004	6.930458	5.161953	1.768505	25.518 %
Nov 2004	1.009164	0.919753	0.089411	8.860 %
Dec 2004	0.855655	0.421506	0.434149	50.739 %
Annual 2004	57.996878	49.023713	8.973165	15.472 %

Publications During Last Year

Fuelberg, H.E., S.M. Martinaitis, J.L. Sullivan, Jr., and C.S. Pathak, 2007: An intercomparison of precipitation values from the OneRain Corp. algorithm and the National Weather Service Procedures. World Environmental and Water Resources Congress, Tampa, May 2007, in press.

Fuelberg, H.E., D.D VanCleve, Jr., and T.S. Wu 2007: An intercomparison of mean areal precipitation from gauges and a multisensor procedure, World Environmental and Water Resources Congress, Tampa, May 2007, in press.

D.D. VanCleve, and H.E. Fuelberg, 2007: An intercomparison between mean areal precipitation from gauges and a multisensor procedure, 21st Conf. on Hydrology, Amer. Meteor. Soc., San Antonio, January 2007, in press.

Martinaitis, S.M., H.E. Fuelberg, J.L. Sullivan, Jr., and C. Pathak, 2007: An intercomparison of precipitation values from the OneRain Corp. algorithm and the National Weather Service procedure. 21st Conf. on Hydrology, Amer. Meteor. Soc., San Antonio, January 2007, in press.

Presentations During Last Year

Seminar at the South Florida Water Management District Headquarters on October 4, 2006.

Seminar at the Florida Department of Environmental Protection on December 5, 2006

6. Related Research Cited Above

Baeck, M.L., and J.A. Smith, 1998: Rainfall estimation by the WSR-88D for heavy rainfall events. *Weather and Forecasting*, 13, 416-436.

Bedient, P.B., B.D. Hoblit, D.C. Gladwell, and B.E. Vieux, 2000: NEXRAD radar for flood prediction in Houston. *J. Hydrolog Engrg.*, Vol. 5, Issue 3, 269-277.

Fulton, R.A., J.P. Breidenbach, D.J. Seo, D.A. Miller, and T. O'Bannon, 1998: The WSR-88D rainfall algorithm. *Weather and Forecasting*, 13, 377-395.

Gourley, J.J., and B.E. Vieux, 2005: A method for evaluating the accuracy of quantitative precipitation estimates from a hydrologic modeling perspective. *Journal of Hydrometeorology*, 6, 115-113.

Hoblit, B.C., P. Bedient, B. Vieux, and A. Holder, 2000: Urban hydrologic forecasting application issues using the WSR-88D radar. Joint Conf. on Water Resource Engineering and Water Resources Planning and Management 2000, ASCE Conference Proceedings.

Klazura G.E., J.M. Thomale, D.S. Kelly, and P. Jendrowski, 1999: A comparison of NEXRAD WSR-88D radar estimates of rain accumulation with gauge measurements for high- and low-reflectivity horizontal gradient precipitation events. *Journal of Atmos. and Oceanic Tech.*, 16, 1842-1850.

Marzen J., and H.E. Fuelberg, 2005: Developing a high resolution precipitation dataset for Florida hydrologic studies. 19th Conf. Hydrology, Amer. Meteor. Soc., San Diego, paper J9.2, available on CD.

Nelson, B.R., W.F. Krajewski, A. Kruger, J.A. Smith, and M.L. Baeck, 200x: Archival precipitation data set for the Mississippi River Basin: Algorithm development. *J. Geophys. Res.,* 108 (D22), 8857, doi:10.1029/2002JD003158.

Ogden, F.L., and H.O. Sharif, 2000: Rainfall input for distributed hydrologic modeling: The case for radar. Watershed Management and Operations Management, ASCE Conference Proceedings.

Quina, G., H. Fuelberg, B. Mroczka, R. Garza, J. Bradberry, and J. Lanier, 2003: The effects of rainfall network density on river forecasts—A case study in the St. Johns basin. Proceedings of the 2003 Georgia Water Resources Conference, University of Georgia, Athens, paper available on CD.

Seo, D.J., J.P. Breidenbach, and E.R. Johnson, 1999: Real-time estimation of mean field bias in radar rainfall data. *Journal of Hydrology*, 223, 131-147.

Smith J.A., D.J. Seo, M.L. Baeck, and M.D. Hudlow, 1996: An intercomparison study of NEXRAD precipitation estimates. *Water Resources Research*, 32, 2035-2045.

Steiner, M., J.A. Smith, S.J. Burges, C.V. Alonso, and R.W. Darden, 1999: Effect of bias adjustment and rain gauge data quality control on radar rainfall estimation. *Water Resources Research*, 35, 2487-2503.

Stellman, K., H. Fuelberg, R. Garza, and M. Mullusky, 1999: Utilizing radar data to improve streamflow forecasts. Preprints, Twenty-ninth Intl. Conf. on Radar Meteor., Amer. Meteor. Soc., Montreal, in press.

Stellman, K., H. Fuelberg, R. Garza, and M. Mullusky, 2000 Investigating forecasts of streamflow utilizing radar data. Preprints, Fifteenth Conf. on Hydrology, Amer. Meteor. Soc., Long Beach, 115-118.

Stellman, K.M., H.E. Fuelberg, R. Garza, and M. Mullusky, 2001: An examination of radar- and rain gage-derived mean areal precipitation over Georgia watersheds. *Wea. and Forecasting*, 16, 133-144.

Walch, M.P., and P. Jelonek, 2002: Managing urban watersheds with the use of NEXRAD radar virtual rain gauges: The Miami-Dade county experience. 9th Intl. Conf. on Urban Drainage, ASCE Conference Proceedings.

Wang, D., M.B. Smith, Z. Zhang, S, Reed, and V.I Koren, 2000: Statistical comparison of mean areal precipitation estimates from WSR-88D, operational and historical gage networks. 15th Conf. on Hydrology, Paper 2.17, American Meteorological Society.

Watkins, D.W., Jr., H. Li, K.A. Thiemann, and T.E. Adams III, 2003: Radar rainfall estimates for Great Lakes hydrologic models, World Water and Environmental Resources Congress, ASCE Conference Proceedings.

Wride, D., M. Chen and R. Johnstone, 2004: Characterizing the spatial variability of rainfall across a large metropolitan area. World Water and Environmental Resources Congress 2004, ASCE Conference Proceedings.

7. Training Potential

One graduate student, Steven Martinaitis, is supported by this project and thereby receives training from it. Mr. Martinaitis collaborates with another graduate student, John Sullivan, who is supported by the FDEP and whose graduate research utilizes the FSU/NWS dataset. Thus, two graduate students will benefit from the project.

Measurement of evapotranspiration, recharge, and runoff in a transitional water table environment

Basic Information

Title:	Measurement of evapotranspiration, recharge, and runoff in a transitional water table environment
Project Number:	2006FL142B
Start Date:	3/1/2006
End Date:	2/29/2008
Funding Source:	104B
Congressional District:	2
Research Category:	Climate and Hydrologic Processes
Focus Category:	Climatological Processes, Hydrology, None
Descriptors:	
Principal Investigators:	Mark Ross

Publication

1. Trout, Ken and Mark Ross, Estimating Evapotranspiration in Urban Environments, Urban Groundwater Management and Sustainability, J.H. Tellam, et al., editors, pgs 157-168, Springer 2006.
2. Shah, N., M. Nachabe, and M.Ross. 2007. Extinction Depth and Evapotranspiration from Ground Water under Selected Land Covers. Ground Water, Paper # GW20060417-0057R, doi: 10.1111/j.1745-6584.2007.00302., published online March 12, 2007, awaiting paper publication, submitted 4/17/2006 Accepted December 2006, In Press.
3. Shah, N., M.Ross. 2006. Variability in Specific Yield for Different Drying and Wetting Conditions. Vadose Zone Journal, In Review.
4. Shah, N., J.Zhang, and M.Ross. 2006. Long Term Air Entrapment Affecting Runoff and Water Table Observations. Water Resources Research, In Review.
5. Zhang, Jing and Mark A. Ross, 2007. Conceptualization of a 2-layer Vadose Zone Model for Surface and Groundwater Interactions, J. Hydrologic Engrg., HE/2005/022952, in press.
6. Nilsson, Kenneth A., Ken Trout and Mark A. Ross, 2006. Analytic Method to Derive Wetland Stage-Storage Relationships Using GIS Areas, J. Hydrologic Engrg., manuscript number HEENG-07-55, In Review.
7. Shah, N., J.Zhang, and M. Ross, 2006. Long Term Air Entrapment Affecting Runoff and Water Table Observations, Water Resources Research, AGU Paper # 2006WR005602, In Review.
8. Rahgozar, Mandana, Nirjhar Shah, and Mark Allen Ross, 2006. Estimation of Evapotranspiration and Water Budget Components Using Concurrent Soil Moisture and Water Table Monitoring, Journal of Hydrology, paper no. HYDROL5813, In Review.

Measurement of Evapotranspiration, Recharge, and Runoff
in
Transitional Water Table Environments

Year One Progress Report

Prepared by
Center for Modeling Hydrologic and Aquatic Systems
Department of Civil and Environmental Engineering
University of South Florida

Funding Agency

Southwest Florida Water Management District
Brooksville, Florida

March, 2007

Table of Contents

List of Figures

1. Summary of First-Year Progress

The first year of the USF eco-site hydrology study has been completed. The primary objectives of the first year were to: 1) obtain permission to install wells at the USF eco-site; 2) identify potential sites for data collection; 3) install both surficial aquifer and Floridan aquifer monitor wells at the chosen sites; 4) install soil moisture probes at each well site; 5) install pressure transducers in each well and data loggers to record high-resolution measure (at 10-minute intervals) water levels and soil moisture; 6) install an evaporation pan to measure real-time open-pan evaporation rates; 7) install a weather station to continuously monitor atmospheric conditions; and 8) begin collecting all data above plus background topologic and hydro-geologic data to characterize the site. All of these tasks have been completed. The wells were installed by the Southwest Florida Water Management District (SWFWMD) and cores were recovered at each location. All of the data collection equipment was installed by USF personnel and all instrumentation is operational and recording data. Also, a database (Microsoft Access) has been created to organize and facilitate further assessment of the data.

The sites selected for aquifer water level and soil moisture data were chosen by topography and accessibility and so that they would lie on a general down-slope flow path. The sites range from the top of a ridge, approximately at 55 feet in elevation, to a low-lying area near the Hillsborough River at approximately 28 feet elevation. The vegetative cover transitions from a pine forest at the top of the ridge to a predominately palmetto scrub with scattered slash pine trees.

The upper site is characteristic of a deep water table. It is covered by dry very-fine (D_{50} ~ 0.5 mm) dune sand. The predominant vegetative cover is pine and scrub oak forest. The two upper-most shallow wells have not contained water since they were installed. Both of those wells are in a relatively thin unit of very-fine dune sand overlying a thick clay lens. Precipitation has been unusually light this year and the sand unit has remained unsaturated. All other shallow wells have contained water since installation.

A Florida aquifer monitor well was installed next to the upper-most dry surficial well. The purpose of this Floridan well was to evaluate the geologic structure of the ridge, determine if any actual or potential aquifer units exist above the Floridan aquifer and below the surficial, and to obtain measurements of Floridan aquifer water elevations from a second location. No additional aquifer units were located in the unconsolidated sediments above the Floridan limestone. Below the top 14 feet of dune sand were primarily clay and sandy-clay lenses. If a water table forms on the upper portion of the ridge, it will probably be an ephemeral appearance, present only during the wet season and perched above the underlying clay.

The well at the lowest elevation is approximately ¼ mile from the Hillsborough River and is in a high (shallow) water-table environment. A second well, screened from the bottom of the well to the ground surface, was installed approximately 20 feet away. The purpose of the second well is to compare the water levels in a well fully screened to water levels in a monitor well of standard construction where the well screen is present only at the bottom portion of the well. If the water level in a well is influenced by air pressurization due to an infiltrating wetting front, the water level in a cased well should be more responsive than the water level in a fully-screened well where the air pressure inside the well can equilibrate to the air pressure outside of the well.

A Floridan aquifer monitor well was installed next to the ECO-4 surficial aquifer well to measure the head gradient between the surficial and Floridan aquifers. The ECO-4 well was drilled to a depth of 27 feet, where limestone was encountered. No significant clay (confinement) was detected. For the Floridan well installed approximately 18 feet from ECO-4, limestone was encountered at 44 feet with a total depth of 58 feet. Significant clay units were found at 22 and 37 feet bls. Despite the difference in depths to the limestone (and the

difference in clay content) between the two wells, the water elevations in the wells are almost identical. It is believed that both wells reflect the Floridan aquifer water elevations.

Active data collection is now in progress. USF personnel visit the site weekly to download data and maintain the equipment. Water levels in the wells and in the evaporation pan are measured manually and compared to the transducer measurements for validation. Also the total rainfall recorded by the tipping-bucket gauge is compared to a manual gauge.

Data collection will continue this year and slight modifications to the network may be made to utilize new insights gained from the project.

2. Study Area

The study area, shown in Figure 1, was inspected by the faculty, staff and the graduate students involved in the project. A formal request for permission to use the USF Ecological Research Area was sent to the designated authority, Dr. Gordon Fox. The permission and access was granted subject to specific terms and conditions. (Ref. *Appendix A*: Use of USF Eco-site to Establish and Monitor Hydrologic Processes)

A reconnaissance survey was conducted and the instrument installation sites were identified. The sites were identified based on topographic elevation, soil type, and existing vegetation coverage. The selected sites were flagged. These sites were approved by the USF Eco Area committee and were later instrumented (Figure 2).

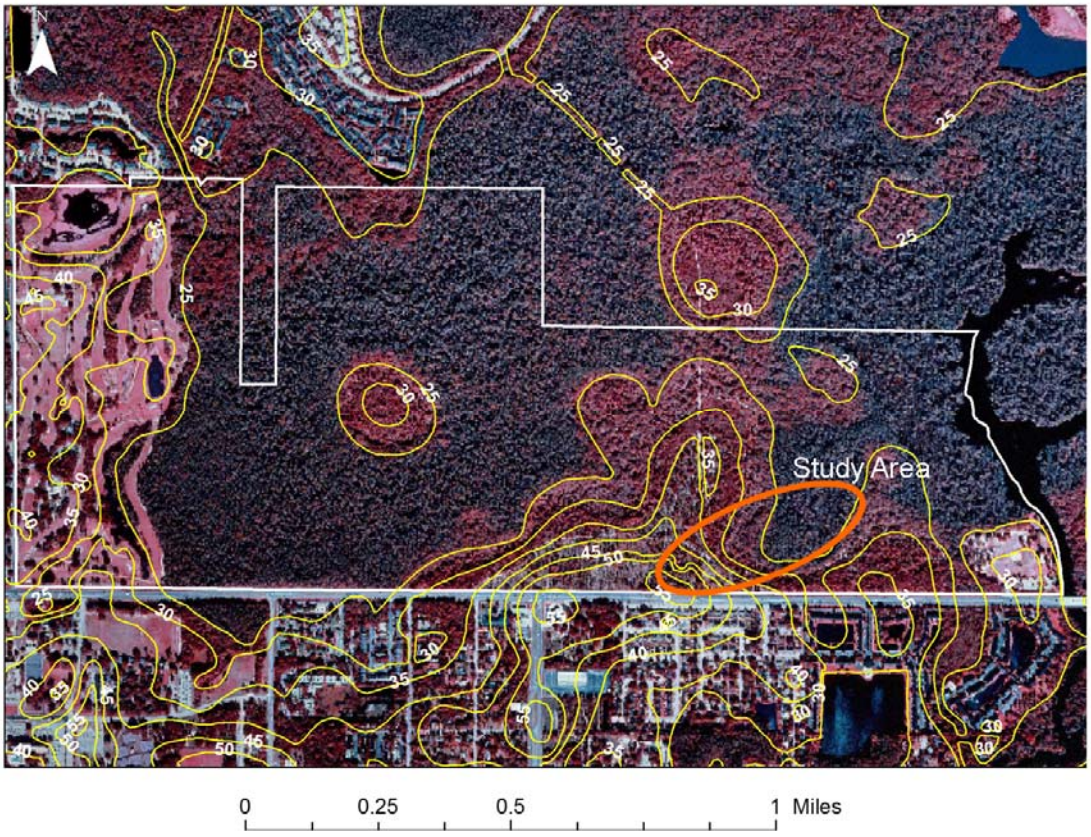

Figure 1. The Orange oval identifies the study area with white line showing the boundary of the USF Eco Area flanked by Fletcher Ave (CR-582A) on the south side. See detailed view in Figure 2.

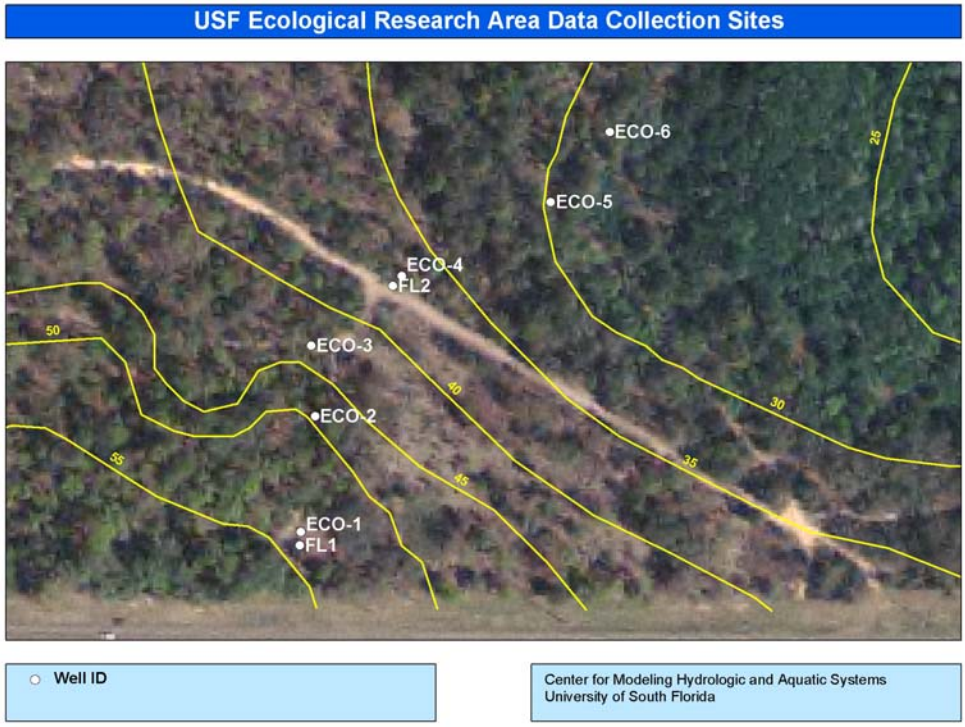

Figure 2. Data collection sites with contour lines showing the land elevation feet above National Geodetic Vertical Datum (NGVD). Floridan wells have an FL prefix.

3. Equipment

3.1 Water-level Monitoring Wells

SWFWMD installed six surficial wells and two Floridan wells at identified sites in the USF Ecological Research Study Area (Figure 2). At the time of well installation, a core was taken and stratigraphic well logs were compiled. Well logs are shown in Tables 1-8 and Cores are shown in Figures 4-16. All wells, with the exception of the most recently installed Floridan well, were then surveyed. Water-level data collection began immediately using Solinst Leveloggers® (Solinst Canada Ltd., Figure 3).

Figure 3. Solinst Levelogger® transducers with built-in data logger.

3.2 Soil Moisture Monitoring

Along with the monitoring wells, EnviroSMART® soil moisture probe (Sentek Pty. Ltd Australia) was installed at the data collection sites to measure water content of the soil profile at high vertical resolution. Figure 4 (a) shows the soil moisture probe with multiple sensors mounted on the rail. Figure 4 (b) shows the soil moisture probe as connected to the Starlogger PRO® (Unidata Ltd., Australia) data logger used to log the water content readings.

(a)

(b)

Figure 4. (a) EnviroSMART soil moisture probe with multiple soil moisture sensors and (b) The probe as installed a with the data logger.

3.3 Weather Monitoring

3.3.1 Weather Station

Campbell ET-106 (Campbell Scientific Inc., Logan, Utah) weather station was installed in the study area. The weather station measures rainfall, wind velocity, solar radiation, temperature and relative humidity (Figure 5).

Figure 5. Campbell Scientific weather station installed in the study area.

3.3.2 Evaporation Pan

A standard USGS Class A evaporation pan was also installed to give a direct measure of the open water evaporation rate. A Geokon Model 4675LV water level monitor (Geokon Inc., Lebanon, New Hampshire) along with Geokon 8001 LC-1 single channel data logger was used to record the fluctuation in the water level in the evaporation pan. The installation of the evaporation pan and water-level monitor beside the weather station is shown in Figure 6.

Figure 6. Class A ET pan with GeoKon water level monitoring device installed next to the weather station.

4. Stratigraphic Logs

Table 1. Stratigraphic well log for ECO-1

Eco-1	
Well Log	6/1/2006
Depth (ft)	Soil Description
0-1	Brown Fine Sand
1-4	Light Brown Fine Sand
4-6	Light Brown-Red Fine Sand
6-10	Very Light Brown Fine Sand
10-12	Very Light Brown Fine Sand
12-12.5	Light Brown Fine Sand
12.5-13.5	Tan Clayey Sand
13.5-16	Gray Clay

Notes:
Total Depth: 16 ft
Screen Length: 5 ft
Screened Interval: 11-16 ft

Figure 7. ECO-1 Core, 0-16 ft.

Table 2. Stratigraphic well log for ECO-2

Eco-2	
Well Log	6/1/2006
Depth (ft)	Soil Description
0-1.5	Light Brown Fine Sand
1.5-6.5	Very Light Brown Very Fine Sand
6.5-10	Very Light Brown Very Fine Sand-almost white
10-10.7	Light Brown Fine Sand
10.7-11.3	Brown Fine Sand (maybe fall)
11.3-13.5	Very Light Brown Very Fine Sand
13.5-14.5	Red-Tan Very Fine Sand
14.5-18	Red Clayey Sand
18-22	Light Brown Sandy Clay

Notes:
Total Depth: 21 ft
Screen Length: 10 ft
Screened Interval: 11-21 ft
Top of screen in Very Light Brown Very Fine Sand

Figure 8. ECO-2 Core, 0-14 ft.

Figure 9. ECO-2 Core, 14-22 ft.

Table 3. Stratigraphic well log for ECO-3

Eco-3	
Well Log	6/1/2006
Depth (ft)	Soil Description
0-4	Brown Fine Sand
4-10	Light Brown Fine Sand
10-19	Light Brown Fine Sand
19-24	Light-Red Clayey Sand, with Red Lenses

Notes:
Total Depth: 22 ft
Screen Length: 10 ft
Screened Interval: 12-22 ft
wet at 14 ft; water table possible at 17 ft

Figure 10. ECO-3 Core, 0-22 ft.

Table 4. Stratigraphic well log for Eco-4

ECO-4	
Well Log	6/2/2006
Depth (ft)	Soil Description
No Core taken	

Notes:
Total Depth: 27 ft
Screen Length: 10 ft
Screened Interval: 17-27 ft
No obvious confining layer observed when well installed
Rock (may be Limestone or Chert) at 27 ft

Table 5. Stratigraphic well log for ECO-5

ECO-5	
Well Log	6/2/2006
Depth (ft)	Soil Description
0-1	Gray Fine-Medium Sand
1-2	Brown Fine-Medium Sand with Organics
2-4	Light Brown Fine Sand
4-5.5	Brown Fine Sand with darker brown Organics
5.5-13	Light Gray Fine Sand
13-13.5	Light Gray to Orange Grading Fine Sand
13.5-14	Orange Clayey Sand
14-19	Light Gray Clayey Sand - Grading to More Clay Content

Notes:
Total Depth: 19 ft
Screen Length: 10 ft
Screened Interval: 9-19 ft

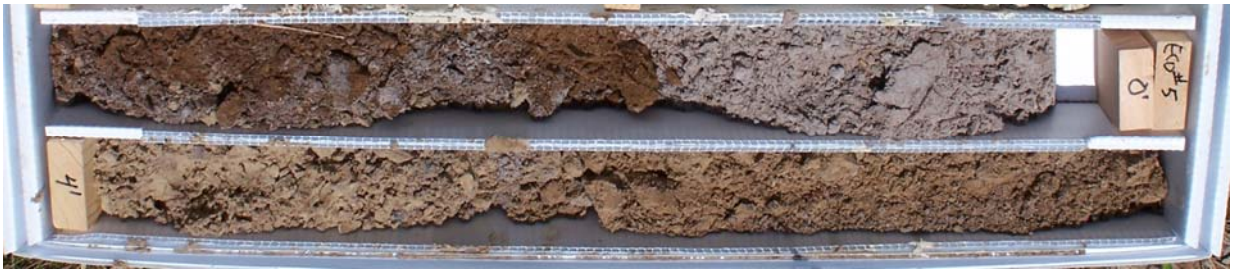

Figure 11. ECO-5 Core, 0-4 ft.

Figure 12. ECO-5 Core, 4-19 ft.

Table 6. Stratigraphic well log for ECO-6

ECO-6	
Well Log	6/5/2006
Depth (ft)	Soil Description
0-2	Dark Brown Medium-Fine Sand
2-9	Light Brown Fine Sand
9-10	Very Light Fine Sand-Clean Quartz, Well Rounded and Sorted
Notes: Wet at 5 ft Standing Water inhole at 6 ft below land surface	

Figure 13. ECO-6 Core, 0-10 ft.

Table 7. Stratigraphic well log for FL-1 (ECO-8)

Well Log	9/11/2006
Depth (ft)	Soil Description
0-6	Light Red-Brown Fine Sand - Hollow Stem
6-14	Very Light Brown Fine Sand
14-19	Brown Clayey Sand
19-28	Gray Clay - Tight
28-31	Clayey Sand
31-32	Very Light Brown Dry with Small Limestone Nodules
32-33	Red-Brown Clayey Sand - Wet
33-36	Very Light Brown Clayey Sand with Limestone Pieces
36-37	Gray-Brown Sandy Clay
37-38	Blue-Gray Clay with Limestone Pieces
38	Stopped core sampling, began mud drilling; Lost circulation at 40 ft

Notes:
Total Depth: 60 ft
Screen Length: 15 ft
Screened Interval: 45-60 feet

Figure 14. FL-1 Core, 0-40+ ft

Table 8. Stratigraphic well log for FL-2 (ECO-7)

Well Log	6/2/2006
Depth (ft)	Soil Description
0-8	Light Brown Fine Sand-loose
8-12	Very Light Brown Fine Sand-damp
12-13	Very Light Brown Fine Sand-damp
13-21	Light Gray Fine Sand-water table near 16 ft
21-21.5	Reddish Fine Sand
21.5-22	Orange Silty Fine Sand, some clay
22-29.5	Gray Clay with Orange Staining
29.5-30	Orange Clay with weathered Limestone
30-30.5	Gray Clay with Orange Staining
30.5-32	Red-Gray Clay with Limestone nodules
32-33	Orange Wet Sandy Clay with Limestone
33-34	Gray Silty Medium Sand
34-35	Orange-Gray Sandy Clay with Small Chert Fragments
35-36	Gray Sandy Clay
37-37	Wet (sat) Sandy Clay with Limestone Pieces
37-37.8	Orange-Gray Clay with Limestone fragments
37.8-38	Light Gray Limestone Chips
38-40	Tan-Gray Sandy Clay with Limestone
40-42.5	Light Brown Silty Clay with Limestone Pieces
42.5-43.7	Light Tan Silty Clay with Limestone pieces (up to 2.5 inch diameter)
43.7+	Rock at 44 feet; Stopped core sampling, began mud drilling

Notes:
Total Depth: 58 ft
Screen Length: 15 ft
Screened Interval: 43-58 feet
Well drilled into limestone to 64 feet with button bit.
When augers removed, 6 feet of casing pulled out of well.
When pumped, yield from well was good as was water clarity.

Figure 15. FL-2 Core, 0-28 ft.

Figure 16. FL-2 Core, 28-43.7 ft.

5. Data Collection

The data from all the equipment are collected at a 10 minute intervals and stored in a Microsoft-Access database. Figure 17 illustrates data collected at site ECO-5 during a nineteen-day period in December 2006. Soil moisture sensors near the land surface respond rapidly to rainfall event. Deeper sensors respond more slowly, and the deepest sensors show little change during this period. The water table responds to major rainfall events but more slowly.

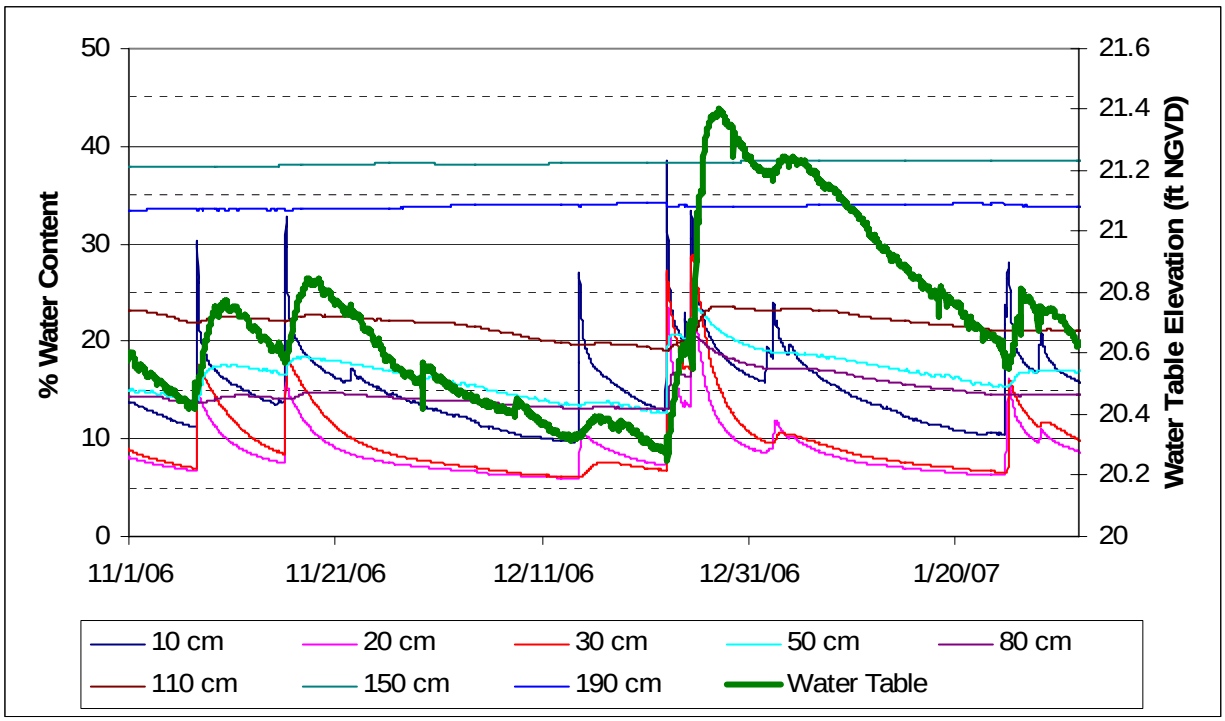

Figure 17. Soil moisture content and water table fluctuations at ECO-05.

5.1 Soil Moisture Data

Soil moisture probes were installed at sites ECO-1 through ECO-6. Each probe has eight moisture sensors at depths below the land surface of 10 cm to 190 cm, except at ECO-6. Site ECO-6 is in a high water-table environment and the deepest moisture sensor at that site is 140 cm. Figures 18-23 show the moisture content at each of the sites through 1/31/2007. In general, shallower sensors respond more quickly to rainfall and subsequent evaporation.

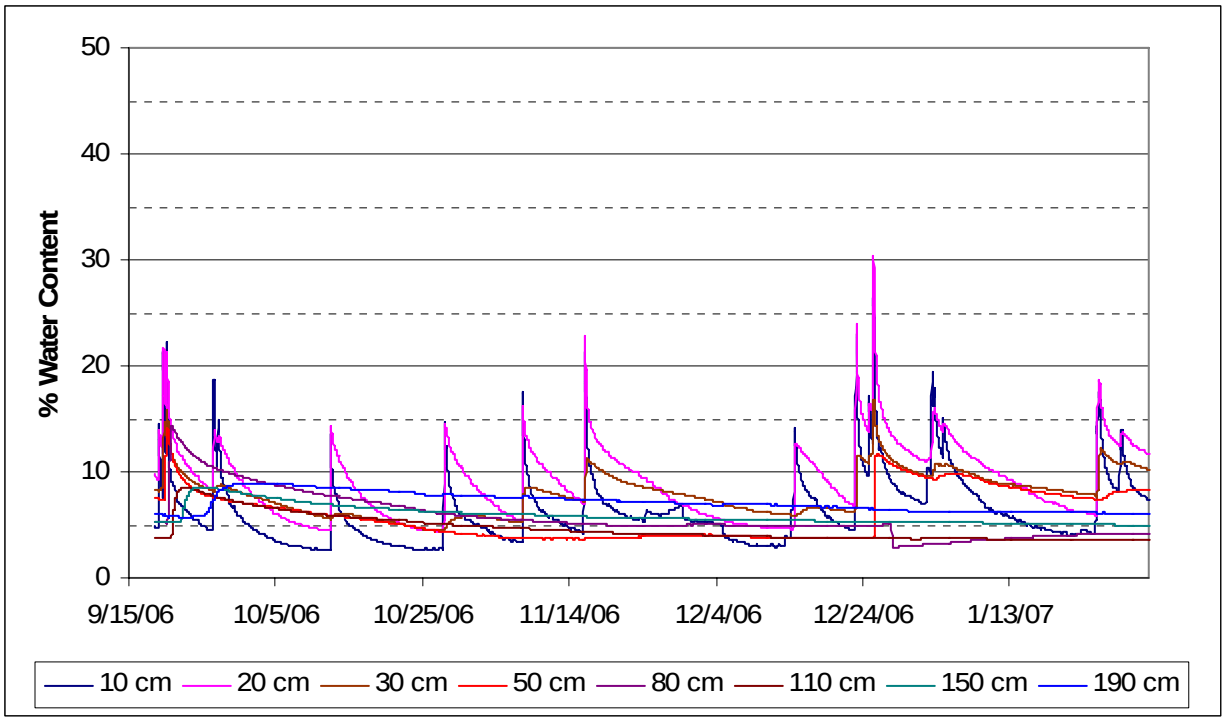

Figure 18. Soil moisture data at ECO-1.

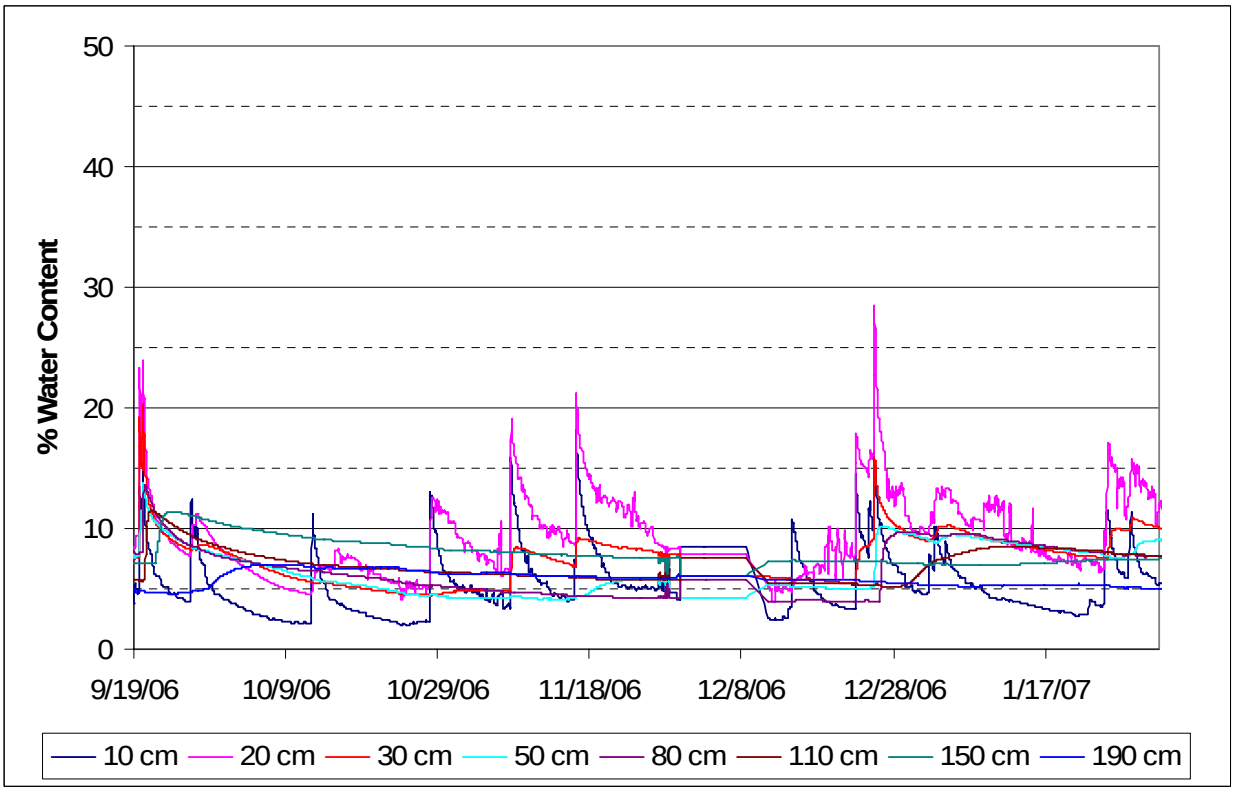

Figure 19. Soil moisture data at ECO-2.

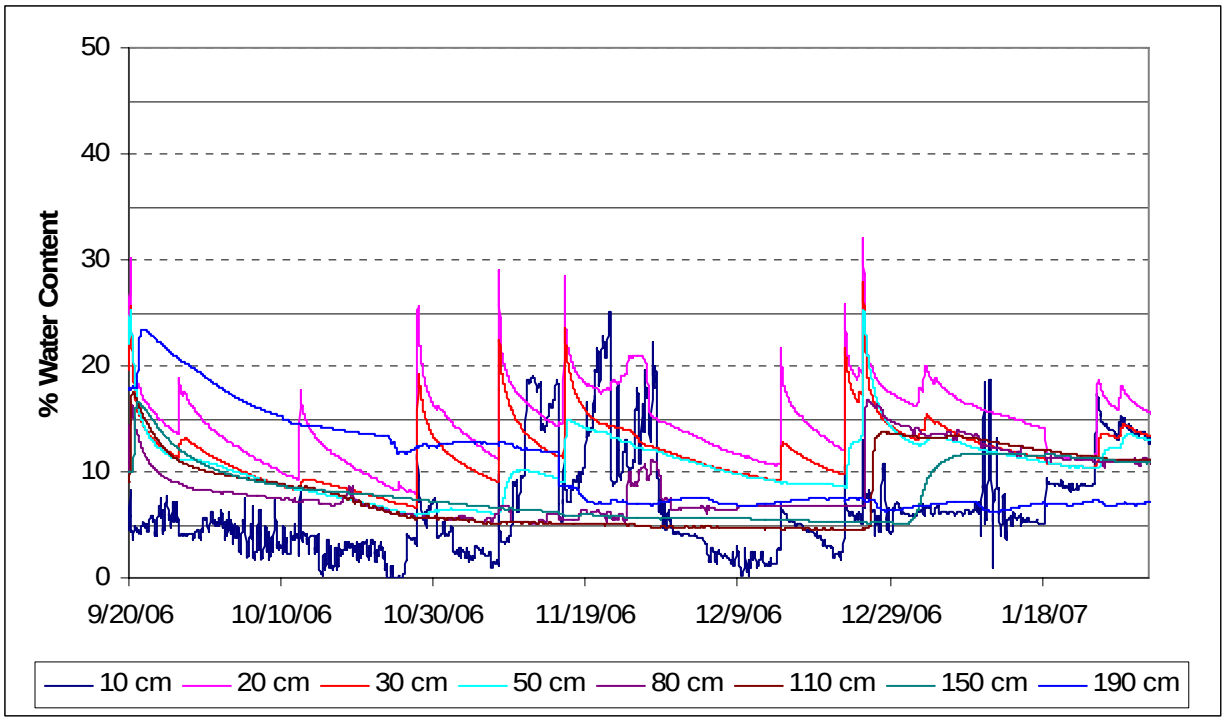

Figure 20. Soil moisture data at ECO-3.

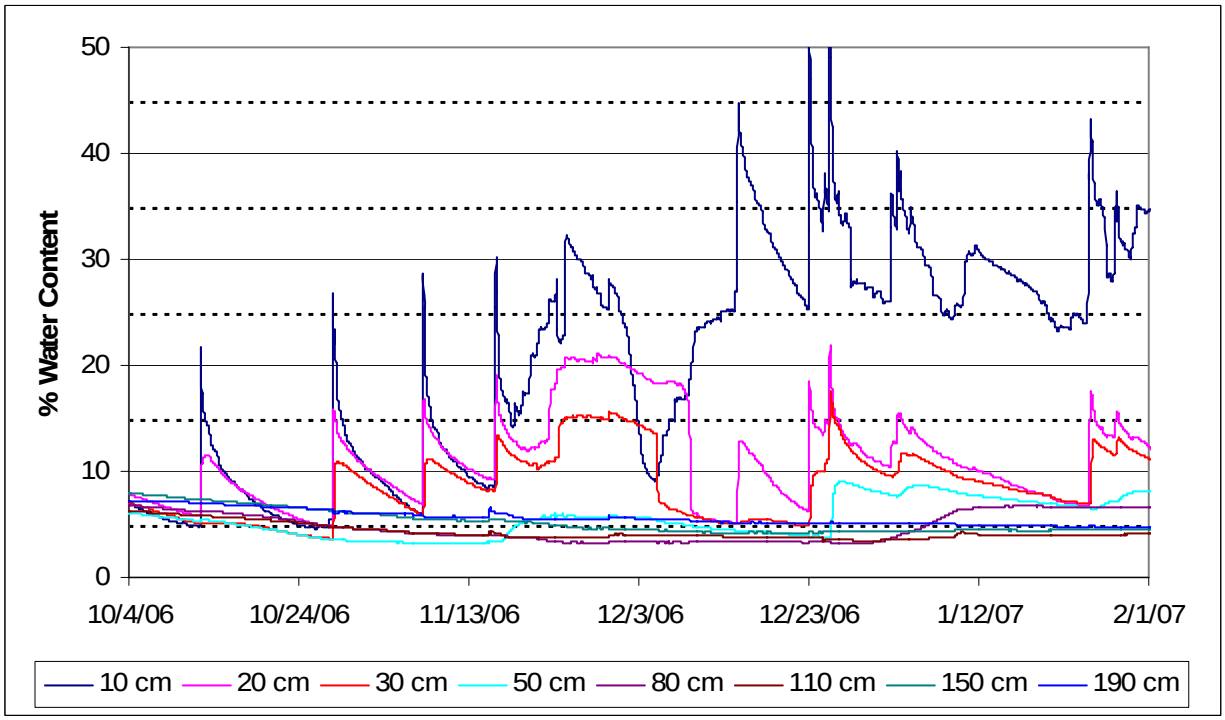

Figure 21. Soil moisture data at ECO-4.

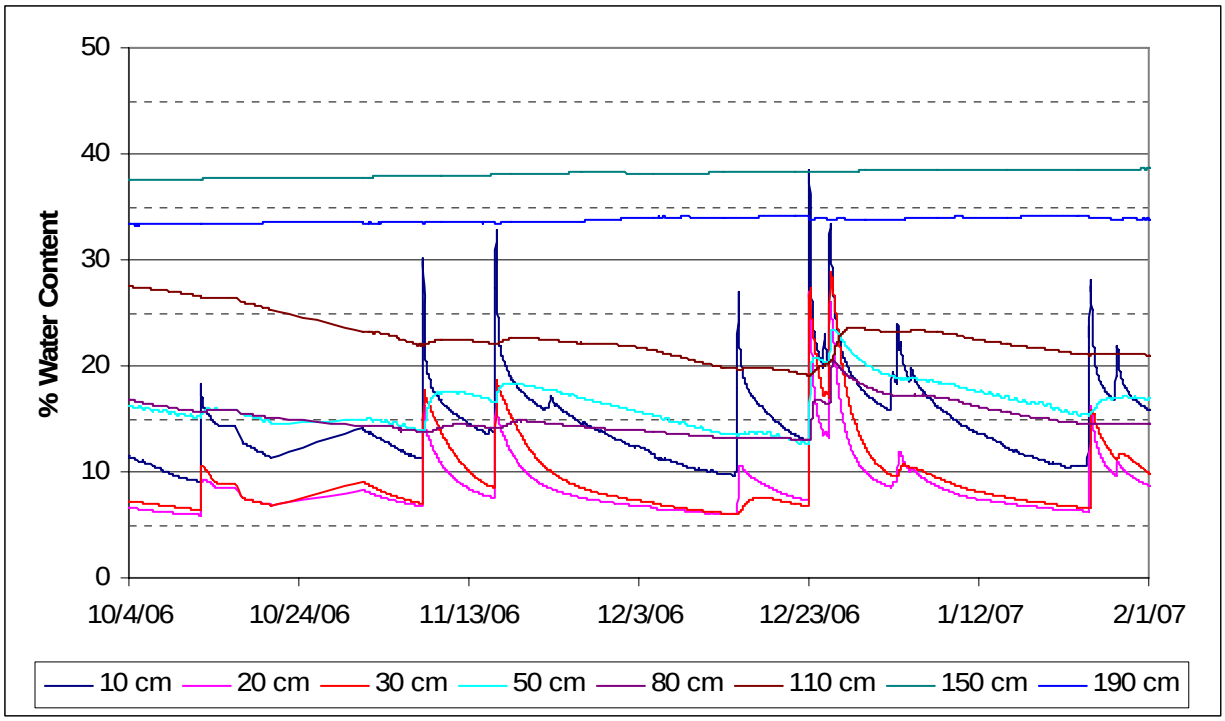

Figure 22. Soil moisture data at ECO-5.

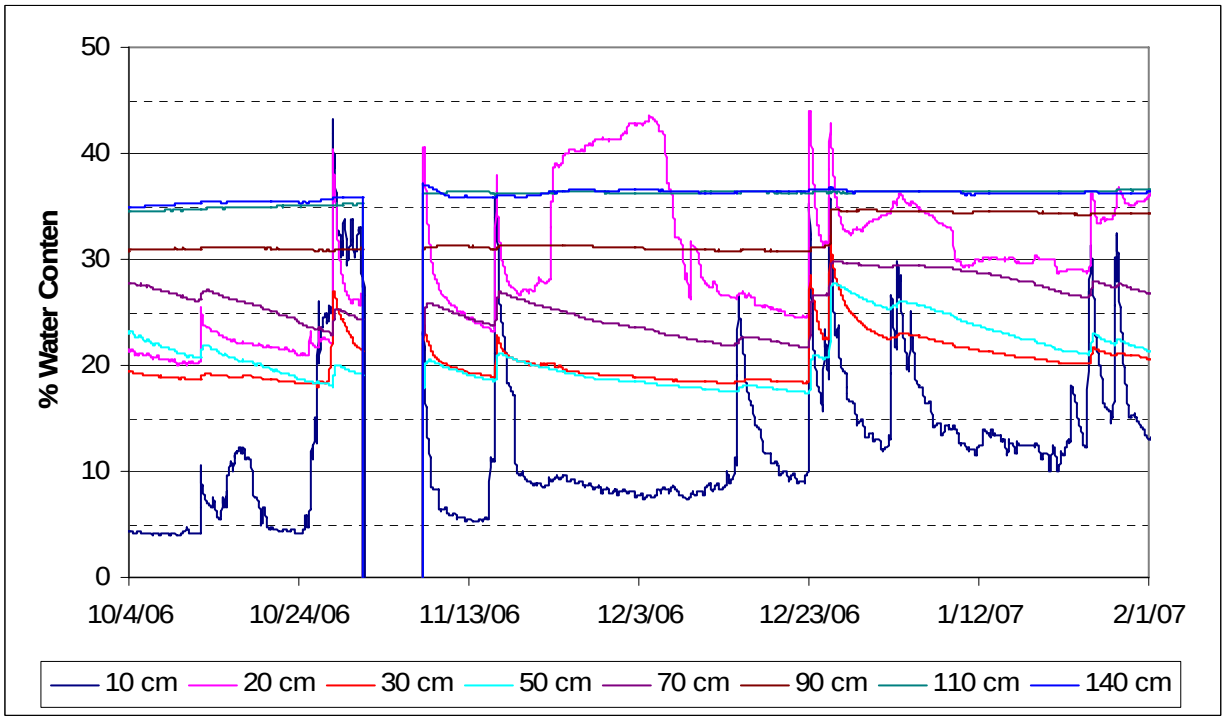

Figure 23. Soil moisture data at ECO-6.

5.2 Water Table Elevations

Pressure transducers were installed in the monitor wells to record ground water levels. ECO-1 and ECO-2 have been dry since they were installed. The wells with the ECO prefix were intended as surficial aquifer monitor wells; they were installed to the first competent clay unit or, in the case of ECO-4, to rock as no clay was encountered. The wells with the FL prefix were installed into the first competent limestone unit which is the Upper Floridan Aquifer. Initially, one Floridan well (FL-2) was installed near ECO-4 to provide head gradient information between the surficial and Floridan aquifers. A second Floridan well (FL-1) was then installed near ECO-1. All the wells except FL-1 have been surveyed and their water levels corrected to NGVD. Figures 24-29 display the continuously recorded water-level elevations (blue line) and the manual measurements (red box) for each of the wells. The water-levels in ECO-3 are the deepest of any of the surficial wells and that well shows very little response to rainfall. The water levels in the Floridan wells exhibit pronounced diurnal fluctuations while the diurnal fluctuations in the surficial wells are less obvious.

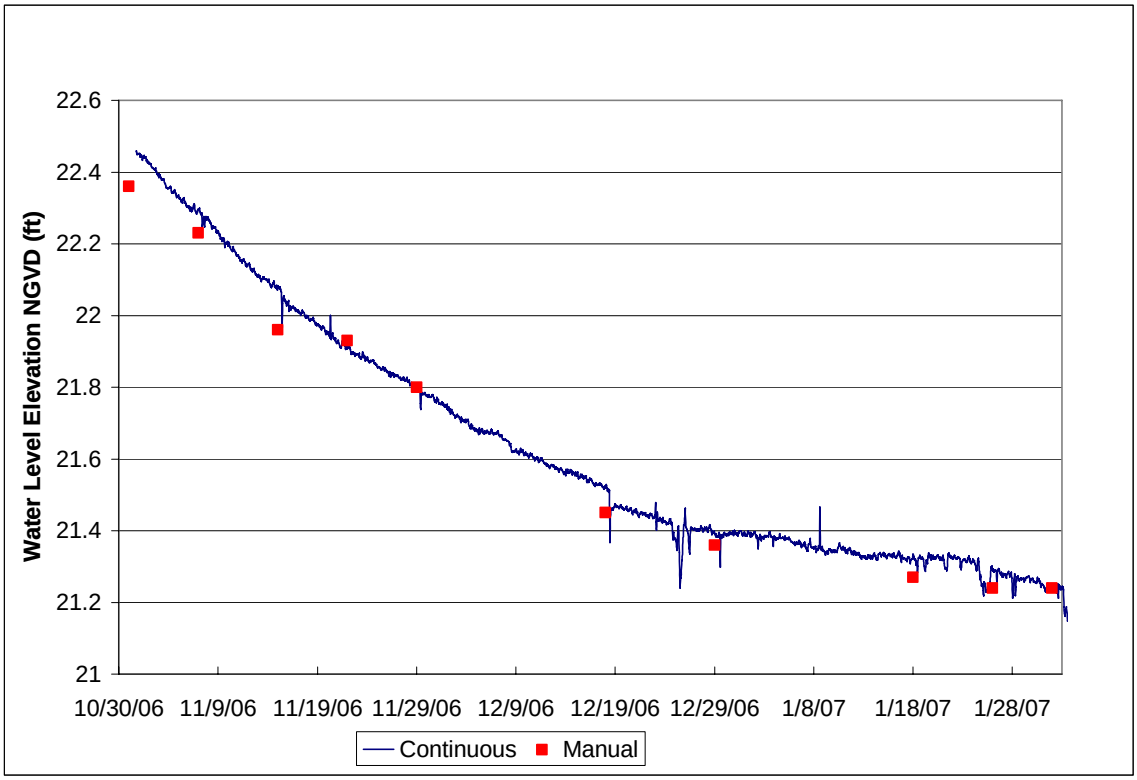

Figure 24. Continuous water-table measurements at ECO-3 with weekly manual measurements.

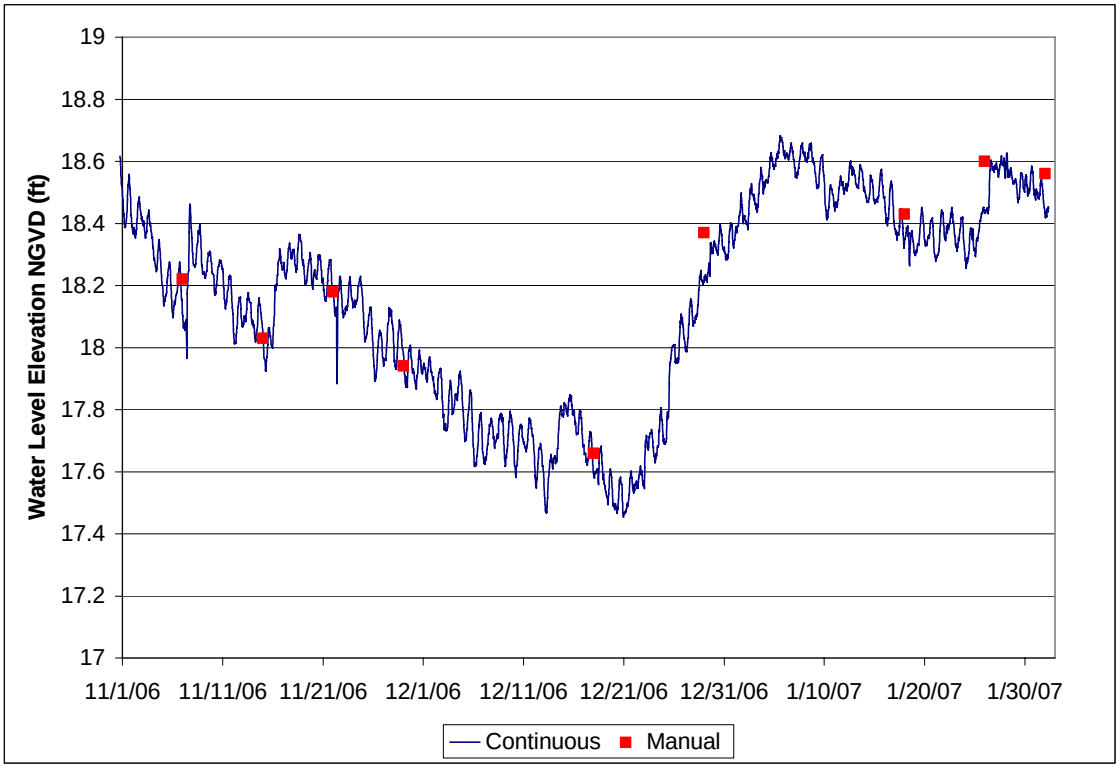

Figure 25. Continuous water-table measurements at ECO-4 with weekly manual measurements.

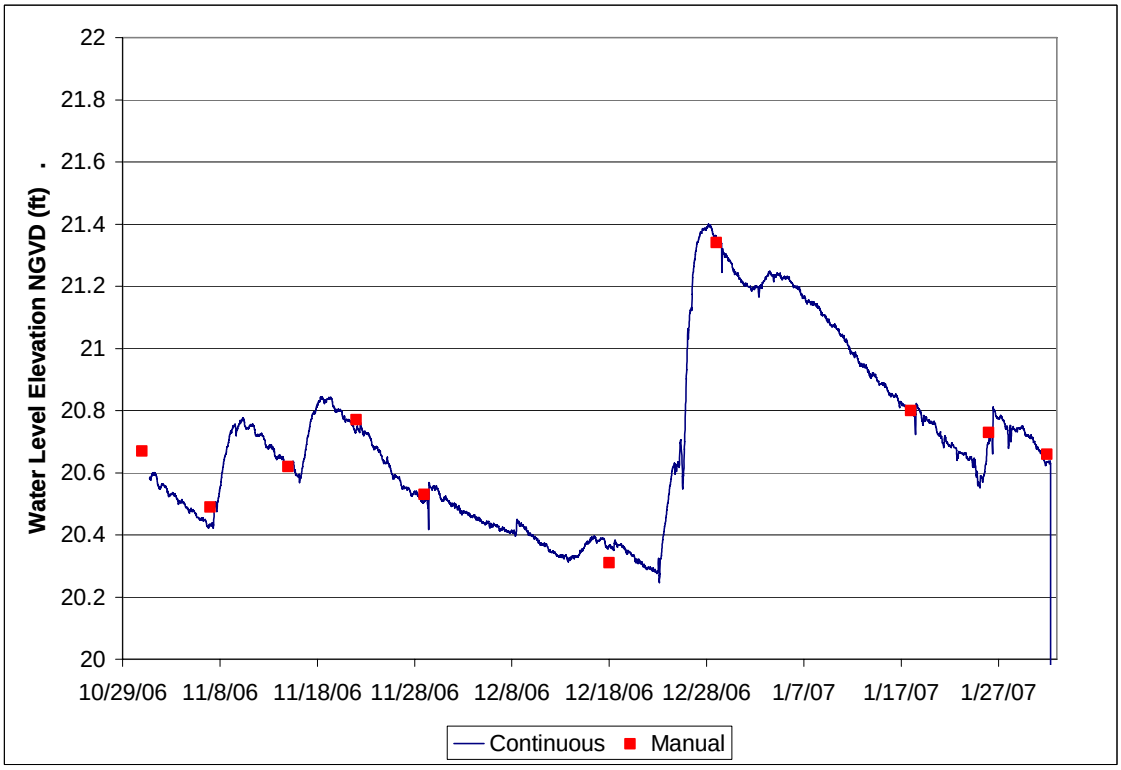

Figure 26. Continuous water-table measurements at ECO-5 with weekly manual measurements.

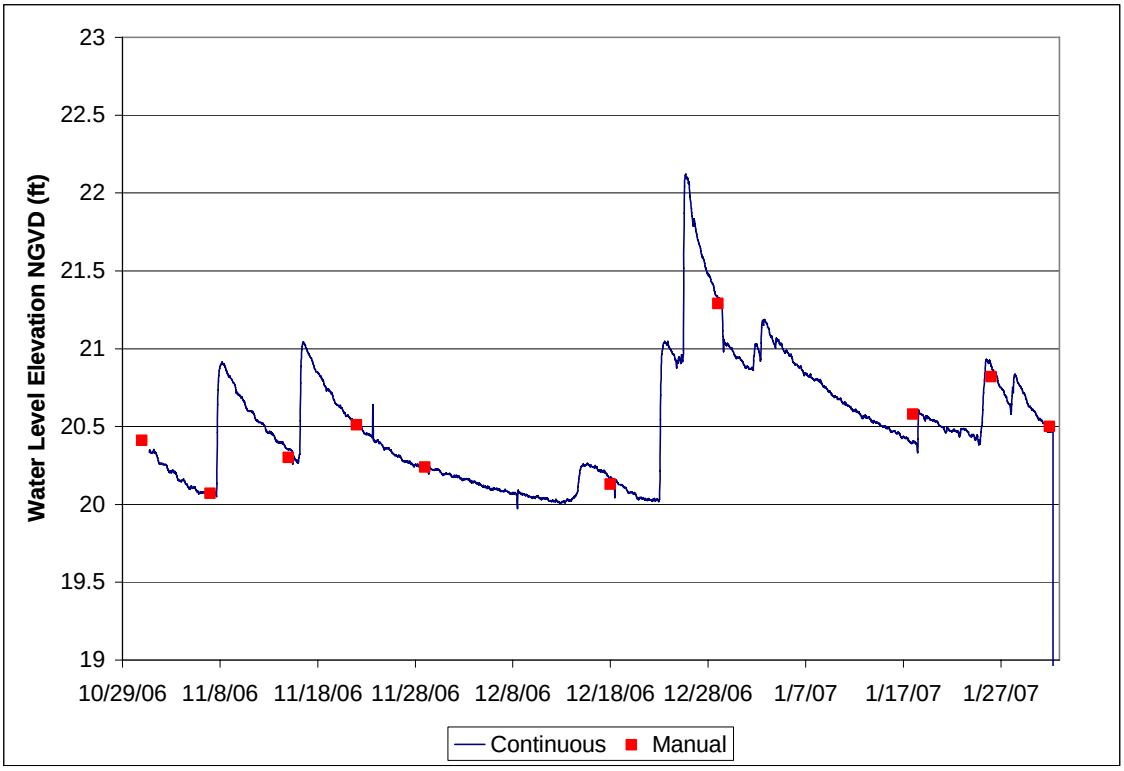

Figure 27. Continuous water-table measurements at ECO-6 with weekly manual measurements.

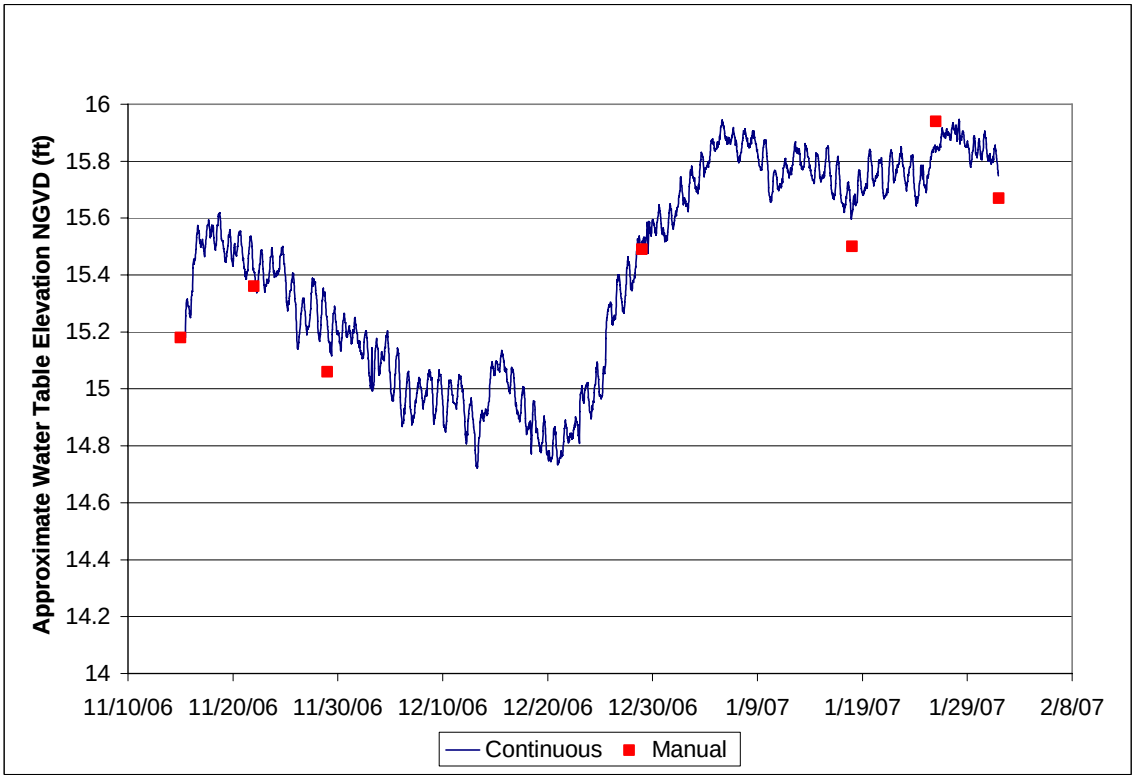

Figure 28. Continuous approximate Floridan Aquifer water levels at FL-01 with weekly manual measurements.

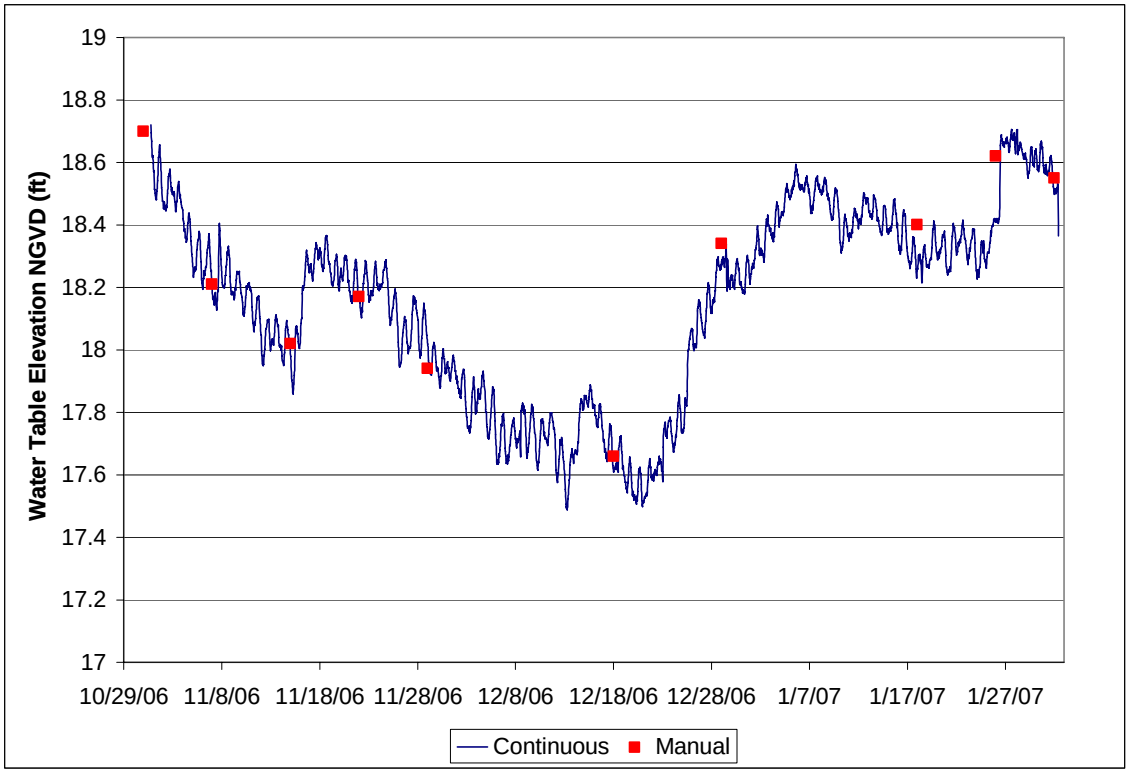

Figure 29. Continuous water-table measurements at FL-02 with weekly manual measurements.

ECO-4 was installed as a water-table monitor well. However, no significant clay unit was penetrated. The well was ended at 27 feet below land surface when rock was encountered. The well was screened from 17-27 feet below land surface (bls).

Approximately 18 feet from ECO-4, a Floridan Aquifer well was installed, FL-2. FL-2 passed through two significant clay units, one between 22 and 32 feet bls and the other between 37 and 44 feet bls. Several smaller clay layers or lenses were encountered between the two thickest clay units. Rock was encountered at 44 feet bls. The well was continued for an additional 20 feet through the limestone to a total depth of 64 feet. A 15-foot well screen was installed in the well, but the bottom six feet of the well was lost when the auger flight was extracted and the well casing pulled up. The final depth of the screen is from 43 to 58 feet bls.

Although ECO-4 is only 27 feet deep and FL-2 is 58 feet deep and finished in limestone, the water elevations in both wells match. Figure 30 illustrates the correspondence between the water elevations in the two wells. Both wells reflect water elevations in the Floridan Aquifer.

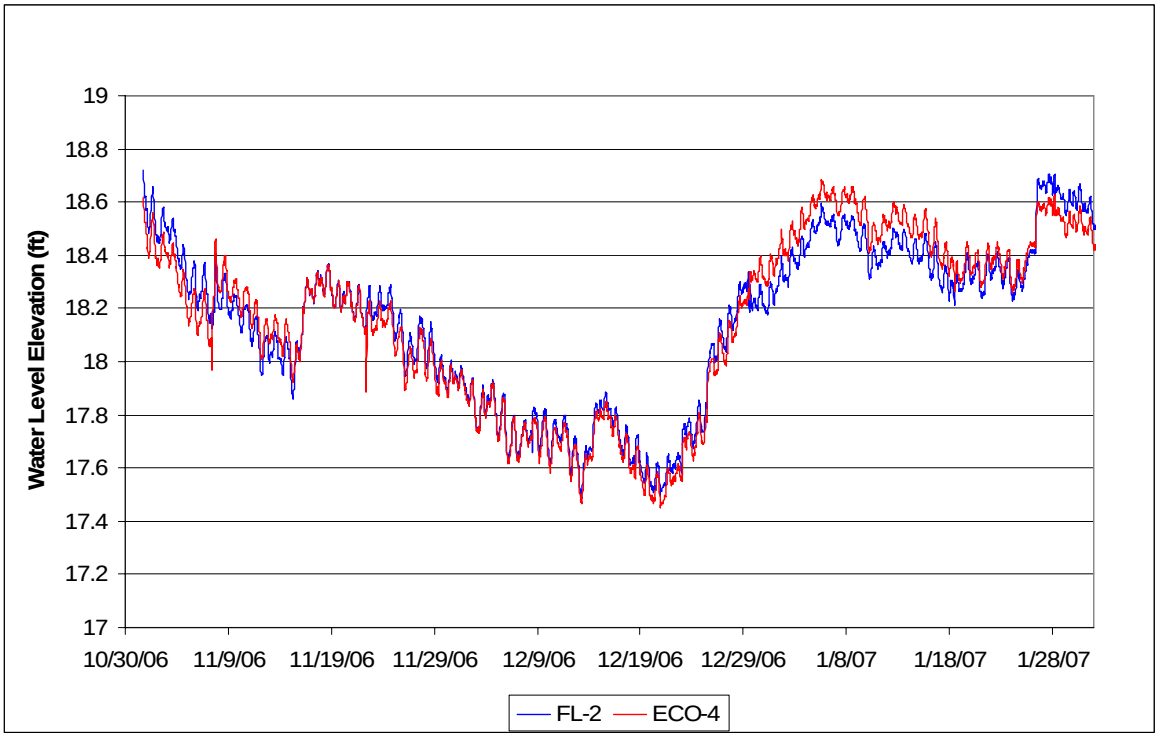

Figure 30. Water elevation comparison between FL-2 and ECO-4.

A second well was manually installed at the ECO-6 location to a depth of approximately four feet. This well is screened for its entire length below the ground surface. Because air entrapment or compression is believed to play a role in the rapid water-table response to rainfall events, this second well will provide a water-table comparison to the partially screened initial well. A water-table response in the cased well that is not present in the fully-screened well may indicate a water-table change due to air pressurization. Figure 31 illustrates the water levels recorded in the two wells and a possible air pressurization response.

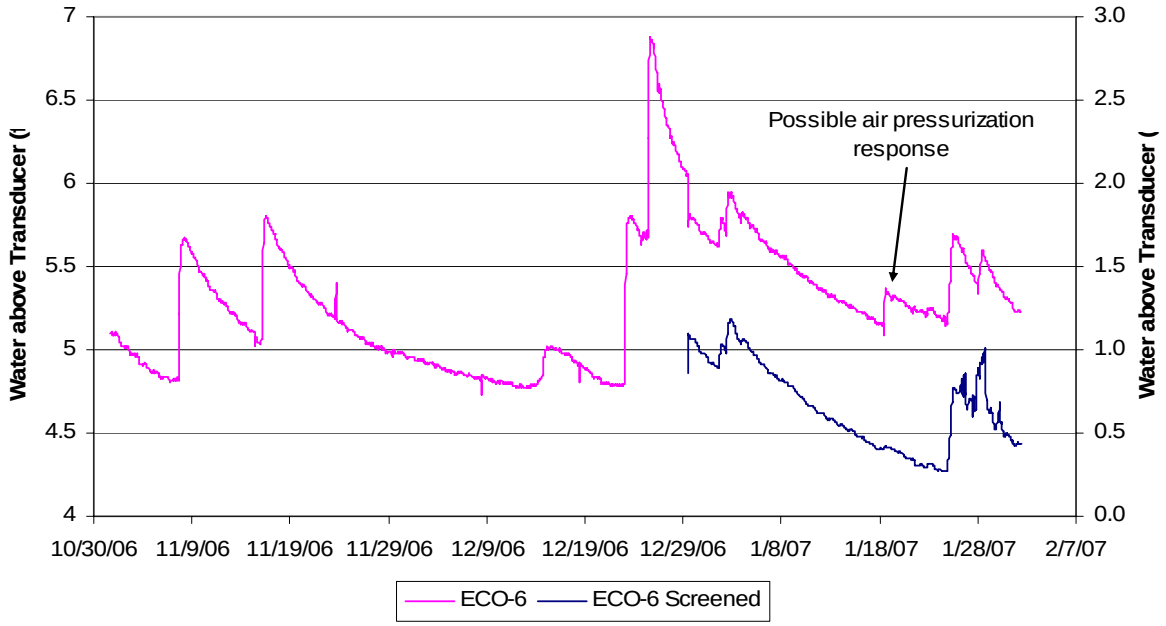

Figure 31. Water levels above the transducers at the ECO-6 wells illustrating a possible air pressurization event.

Appendix

Use of USF Eco-site to Establish and Monitor Hydrologic Processes

Brief explanations are included here. Please refer to the proposal for details on methodology and instruments used.

1. What is the general purpose of your research?

   The objective of the study is to measure evapotranspiration, recharge, and groundwater elevations in a transitional water-table environment. These measurements will be used to understand major hydrologic processes and their interdependence. The Findings from the study should be of immediate importance and use to water management entities. It will provide useful information for parameterization and conceptualization of processes for emerging integrated surface and groundwater computer models of the region.

2. Describe the methods you intend to use – number of plots, types of markers, etc.

   - Rainfall: Tipping-bucket rainfall gauge
   - Evapotranspiration:
     - Central Weather Station
     - Evaporation Pan
   - Soil Moisture: EnviroSMART soil moisture Probes
     - A 2-meter rail that slides vertically into a 2" PVC-cased dry well to a desired depth, accompanied by a data logger enclosed in a small box
   - Runoff: Doppler flow velocity meter
     - Runoff from a small basin will be routed to a channel where this velocity meter will be installed
   - Water Table: Ground water monitoring wells

   Survey Flags will be used to mark the location of instruments. There will be six soil moisture probes and seven wells installed.

3. Describe how you will minimize damage to soils and plants.

   Once the wells are installed, trips made to the site will only be to collect data from the loggers and to repair or replace equipment.

   The instruments described above (in section 2) are designed to have minimum damage to soils and plants. The study and the instruments require us to collect all the data in an undisturbed and natural state, which itself means we will try to minimize the damage. Also, we are aware of the importance of maintaining the health of the eco-area.

4. Identify (on a map) where you intend to conduct this work. Explain why these spots are desirable; this information may be used to suggest other locations in the EcoArea if there are problems of heavy or concurrent use.

   (Ref. Fig. 1)
   The Orange oval identifies the study area. The instruments will be installed along hill slope transect (towards the river).

5. How will your markers, plots, etc., be labeled so that we can tell they are yours? Describe your plan to repair damage, remove markers, etc., at the end of the study.
   All instrumentation sets will have labels saying “USF-CMHAS-SWFWMD Eco Area Project” and the Instrument Identification Number or the Location Number. Survey flags will be used to mark the instrument locations.
   The markers and instruments will be removed at the end of the study.

6. If you are working with vertebrates, provide information on your IACUC permit. We will not approve any use that violates IACUC rules.
   Not Applicable. We are not working with vertebrates or other animals.

7. Over what time period will your work be conducted? Any time extensions must be approved.
   The study will be conducted for a period of three years.

8. Permission to use the EcoArea is conditional on your providing the EAAC with reprints of all relevant publications and links to all web sites referring to this work. Seminars and publications must acknowledge the use of the EcoArea.
   Agreed.

Investigating arsenic mobilization during aquifer storage recovery (ASR)

Basic Information

Title:	Investigating arsenic mobilization during aquifer storage recovery (ASR)
Project Number:	2006FL143B
Start Date:	3/1/2006
End Date:	2/29/2008
Funding Source:	104B
Congressional District:	6
Research Category:	Ground-water Flow and Transport
Focus Category:	Hydrogeochemistry, Hydrology, Water Supply
Descriptors:	
Principal Investigators:	Mike Annable

Publication

1. Norton, S. Quantifying the Near-Borehole Geochemical Response During ASR. Masters Thesis. University of Florida. May, 2007.

Status Update

Investigating Arsenic Mobilization During Aquifer Storage Recovery (ASR)

Project Background

Due the growing demand on water resources within the State of Florida, alternative water supply and water storage technologies are becoming increasingly attractive to municipalities. Aquifer Storage Recovery (ASR) has the potential to provide much of the seasonal storage need for many municipalities within areas of increased water demand. However, as with any engineered water supply process, ASR must meet stringent Federal and State regulations to insure the protection of human health and the health of the environment.

Recently, facilities in southwest Florida utilizing the Suwannee Limestone of the Upper Floridan Aquifer for ASR have reported arsenic concentrations in recovered water at levels greater than 112 µg/L (Arthur et al., 2002). On January 23, 2006 the Maximum Contaminant Level for arsenic was lowered from 50 µg/L to 10 µg/L (FDEP: Chapter 62-550 F.A.C., Table 1).

Research has been conducted to determine the abundance and mineralogical association of arsenic within the Suwannee Limestone (Pichler, et al., 2006). This research suggests that the bulk matrix of the Suwannee Limestone generally contains low concentrations of arsenic. However, according to this research, arsenic is concentrated within the Suwannee Limestone in arsenic bearing minerals such as pyrite.

The potential mechanisms by which arsenic may be mobilized during ASR have been investigated (Arthur, et al., 2002) and suggested by others (Pichler, et al., 2006). The conclusions of this research suggest that the introduction of the injectate containing oxidants, such as oxygen and chlorine, into a highly reduced groundwater environment produces a geochemical response that releases arsenic from the aquifer matrix.

Several ASR projects are under testing in southwest Florida. Of these, the recently constructed Bradenton Potable ASR facility presents several benefits for further research including the following:

- Only a few small volume recharge and recovery cycles have been performed at the facility. Therefore, the aquifer matrix has not been repeatedly exposed to water with high levels of oxidizers.
- One large volume cycle was recently completed (Cycle 6) with recharge being initiated immediately at the end of the recharge event. Because no storage occurred during this cycle it may be possible to determine the rate at which the oxidizers are consumed in the matrix.
- The data sets collected to date at this facility are fairly extensive.
- The City of Bradenton has authorized the use of the data set in this study.
- Site access has been granted by the City of Bradenton.

Work Scope

Based on the research completed to date, it appears that one of the primary mechanisms by which arsenic is mobilized during ASR is by the introduction of oxidizers into the aquifer. Therefore, the following work scope was developed to further evaluate the role of oxygen and other oxidizers in the mobilization of arsenic during ASR:

- Compile and evaluate in-situ measurements collected at the Bradenton ASR site during recovery for Cycle 6 to include field measurements (pH, temperature, dissolved oxygen,

conductivity, and ORP) and laboratory measurements (sulfate, sulfide, hydrogen sulfide, carbonate, bicarbonate, total chlorine, total phosphorous, and ortho-phosphate).

- Review the data being collected per the FDEP temporary operations (cycle testing) permit for this facility and additional data being collected by FGS.
- Employ Istok's approach to data analysis and compare Istok's push pull test method to the current method of Cycle Testing regulated by FDEP.
- Utilize the existing Bradenton ASR data to:
    - Attempt to quantify the consumption rates (reaction rates) of oxygen and other oxidizers (i.e. chlorine) during ASR.
    - Investigate the applicability of solute transport models to predict the behavior of arsenic during ASR to suggest future studies.
- Make suggestions for further studies.

Schedule and Deliverables

The timeline to complete this research and submit a paper for publication will be as follows:

- In-Situ data collection occurs January 2006.
- FGS grant awarded by end of February 2006.
- WRC funding awarded by end of March 2006.
- Funds dispersed over three semesters; Summer 2006, Fall 2006, and Spring 2007.
- Thesis defense Spring 2007.
- Thesis submitted for publication Spring 2007.

Project Status

Funding was awarded from the FGS and WRC, through the State Water Resources Research Institute (WRRI) Program and the following research components are underway.

In-Situ data collection and review was extended through March 2006 to include Cycle 6a conducted at the Bradenton ASR facility. The available field data and laboratory analytical data have been reviewed. Istok's push-pull analytical model has been employed to quantify DO consumption rates. Results are similar for three of the four cycle tests completed to date. The results indicate that DO undergoes first order decay during ASR. Variability in the measured decay rates appears to be due to a reaction rate dependence on temperature (Prommer, 2005). While recharge water temperatures were similar for three of the four cycle test, one of the test was conducted during the summer with recharge water temperatures exceeding 30°C. Therefore, additional computations are underway to correlate the decay rate at varying temperatures.

A review of potential reactive transport (geochemical transport) models is nearly complete. The reactive transport model PHT3D appears best suited for modeling arsenic mobilization during ASR. PHT3D couples the geochemical model PHREEQC-2 with the multi-component transport model MT3DMS. The model is being maintained by Henning Prommer at the University of Western Australia. Future studies may include the application of PHT3D to the Bradenton dataset, or others.

A project status update was presented, in power-point format, to the graduate committee (Dr. Mike Annable and Dr. Kirk Hatfield) and Dr. Jon Arthur of FGS on November 9, 2006. Two committee members, Dr. Mark Newman and Dr. Jean-Claude Bonzongo could not attend the presentation. Therefore, separate review meetings will be held with these members in the near future. Comments received by the committee members and FGS will be incorporated into the draft thesis due April 2007.

Dr. Arthur has expressed his interest in providing funding support for continuing the project during the following year. A prospectus will be drafted for review by the graduate committee and subsequent submittal to FGS for approval.

References

Arthur, Jonathan D., Dabous, Adel A., and Cowart, James B., 2002, Mobilization of arsenic and other trace elements during aquifer storage and recovery, southwest Florida: USGS Open-File Report 02-89

Price, Roy E., and Pichler, Thomas, 2006, Abundance and mineralogical association of arsenic in the Suwannee Limestone (Florida): Implications for arsenic release during water-rock interaction: Chemical Geology, Vol. 228, pp. 44-56

Prommer, Henning, and Stuyfzand, Pieter J., 2005, Identification of temperature-dependent water quality changes during a deep well injection experiment in a pyritic aquifer: Environmental Science and Technology, Vol. 39, pp. 2200-2209

Cooperative Graduate Research Assistantships Between the Florida Water Resources Research Center-South Florida Water Management District UF/ABE in Critical Water Resources Areas for South Florida

Basic Information

Title:	Cooperative Graduate Research Assistantships Between the Florida Water Resources Research Center-South Florida Water Management District UF/ABE in Critical Water Resources Areas for South Florida
Project Number:	2006FL144B
Start Date:	3/1/2006
End Date:	2/29/2008
Funding Source:	104B
Congressional District:	6
Research Category:	Climate and Hydrologic Processes
Focus Category:	Hydrology, Ecology, Solute Transport
Descriptors:	
Principal Investigators:	Rafael Munoz-Carpena, Wendy D Graham, Gregory Alan Kiker

Publication

1. Jawitz, J.W., R. Muñoz-Carpena, K.A. Grace, S. Muller, A.I. James. 2007. Spatially Distributed Modeling of Phosphorus Reactions and Transformations in Wetlands. Scientific Investigations Report 2006-XXXX. U.S. Department of the Interior. U.S. Geological Survey (under review).
2. Muller. S. and R. Muñoz-Carpena. 2007. Effect of variable model structure in modelling wetlands phosphorus water quality in South Florida. (in review, Adv. Water Resources).
3. Muñoz-Carpena,R. Z. Zajac, Y.-M. Kuo. 2007. Evaluation of water quality models through global sensitivity and uncertainty analyses techniques: application to the vegetative filter strip model VFSMOD-W. (in review, Trans. of ASABE)
4. Lagerwall, Kiker, Muñoz-Carpena. 2007. TaRSE-ECO: Ecological algorithms for the RSM model. FL-Section of ASABE, MAy 31, 2007, St. Pete Beach, FL.
5. Zajac, Z., R. Muñoz-Carpena, Y-M. Kuo. 2007. Application of Global Sensitivity and Uncertainty Analysis Techniques to the Vegetative Filter Strip Model (VFSMOD). University of Florida, Department of Agricultural and Biological Engineering. FL-Section of ASABE, MAy 31, 2007, St. Pete Beach, FL.
6. Muller. S., R. Muñoz-Carpena and G. Kiker. 2007. Global Sensitivity and Uncertainty of a Wetland Phosphorus Water-Quality Model, Accounting for Variable Model Structure. FL-Section of ASABE, May 31, 2007, St. Pete Beach, FL.
7. Muller. S. and R. Muñoz-Carpena. 2007. Towards an objective framework for evaluation of hydrologic models: state-of-the-art methods. ASABE Paper No. 072212. St. Joseph, Mich.: ASABE.

Cooperative Graduate Research Assistantships Between the Florida Water Resources Research Center-South Florida Water Management District UF/ABE in Critical Water Resources Areas for South Florida

Project Description

Two specific research projects have been agreed and contracted with South Florida Water Management District (SFWMD). The status of each research project is presented followed by more specific program details and long-term objectives.

Topic 1: Sensitivity Analysis Of South Florida Regional Modeling
Topic 2: Addition of Ecological Algorithms into the RSM Model

Progress report: Topic 1

Sensitivity Analysis for the SFWMM

PI: Dr. Rafael Muñoz-Carpena[1], Co-PI: Dr. Wendy Graham[2]

[1] *Department of Agricultural and Biological Engineering, University of Florida*

[2] *Water Institute, University of Florida*

1. Review of Previous Sensitivityy Analysis of the SFWMM

We conducted a detailed review of the sensitivity analysis performed on the South Florida Water Management Model (SFWWM), as presented in the Model Documentation of SFWMM Version 5.5). The traditional approach of varying one parameter at a time was used for this analysis. The results indicated that most geographical regions, of the model's domain were most sensitive to WPET (Wetland Potential ET) and that, coastal areas were strongly influenced by CPET (Coastal Potential ET). However, this review found that the methods applied for the different inputs and modeling subdomains are often inconsistent and at times subjective. Examples of this are the different and insufficiently explained variational ranges applied to the parameters (which changed for the different regions where the model is applied), or the varying criteria selected to identify a parameters as sensitive or not. As a result, the sensitivity analysis performed appears too simplistic and not appropriate for the level of complexity and importance of the SFWMM as a regional management tool. Our findings are in agreement with those of the "SFWMM Peer Review Panel", which recommended a more thorough approach towards sensitivity analysis of SFWMM, including global sensitivity techniques.

2. Review of Alternative Global Sensitivity and Uncertainty Methods

We performed a review of modern global sensitivity analysis techniques suitable for application to SFWMD models. Hydrological and water quality models are often

complex and require a large number of parameters and other inputs. Mathematical models like these are built in the presence of uncertainties of various types (input variability, model algorithms, model calibration data, and scale). The role of uncertainty analysis is to propagate all these uncertainties, using the model, onto the model output of interest. Complementarily, sensitivity analysis is used to determine the strength of the relation between a given uncertain input and the output. As a result of these analyses, the model user can learn what model input factors affect the output of interest the most, and possibly quantify the uncertainty of the model due to the most sensitive inputs. This knowledge is critical to efficiently guide the model calibration as well as to document the validity of the model outputs for management or decision tasks. In spite of their importance, these analyses are not usually performed in many model development and application efforts today. Even if they are performed, the procedures used are often arbitrary and lack robustness. Usually derivation techniques (variation of the model output over the variation of the model input) are employed. These methods are applied just over a prescribed (and usually small) parametric range, only can handle one-parameter-at-a-time (OAT techniques), and can consider efficiently but a few parameters. When the model output response is non-linear and non-additive, as with most complex model outputs, the derivative techniques are not appropriate. As an alternative, new global sensitivity and uncertainty techniques are available that evaluate the input factors of the model concurrently over the whole parametric space (described by probability distribution functions). So far, two modern global techniques, a screening method (Morris method) and an analysis of variance one (Fourier Analysis Sensitivity Test-FAST) were identified as potentially suitable for performing the sensitivity analysis of the SFWMM. An initial application of these techniques to the new water quality component of the SFWMD RSM model has been recently performed (Jawitz et. al. 2007), as well as to the water quality model VFSMOD (Muñoz-Carpena et. al. 2007).

3. Publications

Jawitz, J.W., R. Muñoz-Carpena, K.A. Grace, S. Muller, A.I. James. 2007. Spatially Distributed Modeling of Phosphorus Reactions and Transformations in Wetlands. Scientific Investigations Report 2006-XXXX. U.S. Department of the Interior. U.S. Geological Survey (under review)

Muñoz-Carpena, R. S. Muller, and Z. Zajac. 2007. Application of Global Sensitivity and Uncertainty Analyses Techniques to a the vegetative filter strip model VFSMOD (Invited paper for Soil and Water Centennial Collection, Trans. of ASABE, in preparation)

Progress Report: Topic 2
Addition of Ecological Algorithms into the RSM Model

CoPIs: Gregory Kiker, Rafael Muñoz-Carpena, Wendy D. Graham,
SWFMD Coordinator: Naiming Wang
Ph.D. Student: Gareth Lagerwall
Collaborator: Andrew James

Progress to Date:

This research project aims to systematically review, design and develop selected ecological algorithms for the RSM model using a similar methodology to the development of recent water quality algorithms (RSM-WQ).

Activities for this project have included the usual startup related activities including formation of Mr. Lagerwall's supervisory committee and the design/submission of a coursework plan. The graduate committee consists of the following persons:

Dr G A Kiker (Dept of Agr. & Bio. Engineering) Chair

Dr R Munoz-Carpena (Dept of Agr. & Bio. Engineering) Co-Chair

Dr K Hatfield (Civil and Coastal Engineering)

Dr A James (Soil and Water Sciences)

Dr N Wang (SFWMD) (to be added shortly)

Research activities have been primarily focused on a review of the RSM and RSM-WQ models (including their fundamental designs, code layout/design and input/output structures). Weekly meetings were conducted with Dr Andy James, Prof Munoz-Carpena and Prof Kiker to understand and explore potential design challenges in adding ecological components to the RSM structure. In addition, other integrated regional models (FT-LOADS/SICS/TIME) were included in review discussions to provide a variety of design viewpoints for upcoming object/code design discussions. It is expected that increased communications/discussions with SFWMD modelers will be required to establish upcoming design and implementation strategies for code expansion.

Program Details and long-term objectives:

Cooperative Graduate Research Assistantships Between the Florida Water Resources Research Center-South Florida Water Management District UF/ABE in Critical Water Resources Areas for South Florida

As mentioned previously, two specific research projects have been agreed and contracted with South Florida Water Management District (SFWMD): ***Topic 1: Sensitivity Analysis Of South Florida Regional Modeling and Topic 2: Addition of Ecological Algorithms into the RSM Model.***

Topic 1: Sensitivity Analysis Of South Florida Regional Modeling

CoPIs: Rafael Muñoz-Carpena, Wendy D. Graham, Gregory Kiker
SWFMD Coordinator: Jayantha Obeysekera
Ph.D. Student: Zuzanna Zajac

Introduction

Mathematical models are built in the presence of uncertainties of various types (input variability, model algorithms, model calibration data, and scale) (Haan, 1989; Beven, 1989; Luis and McLaughlin, 1992). Propagating via the model all these uncertainties onto the model output of interest is the job of uncertainty analysis. Determining the strength of the relation between a given uncertain input and the output is the job of sensitivity analysis (Saltelli et al., 2004). The evaluation of model sensitivity and uncertainty must be an essential part of the model development and application process (Reckhow, 1994; Beven, 2006). Although sensitivity analysis is useful in selecting proper parameters and models, and model uncertainty provides much needed assessment of results, they are rarely used in most water quality modeling efforts today (Muñoz-Carpena et al., 2006). If uncertainty is not evaluated formally, the science and value of the model will be undermined (Beven, 2006). The consideration of model uncertainty should be linked to the availability or efficient collection of data. This combination will allow: a) to improve the representation of the inputs and boundary conditions; b) refine the evaluation of the model complexity structure; c) indicate what models are adequate for specific applications; and d) constrain feasible sets of effective parameter values at particular applications (Beven, 2006).

"Input factor" in a broad sense refers to anything that changes the model prior to execution. This not only includes the model parameters, but entirely different conceptualizations of the system. Input parameters of interest in the sensitivity analysis are those that are uncertain; that is, their value lies within a finite interval of non-zero width. Traditionally, model sensitivity has been expressed mathematically as model output derivatives; these are normalized by either the central values where the derivative is calculated or by the standard deviations of the input parameter and output values. These sensitivity measurements are "local" because they are fixed to a point or narrow range where the derivative is taken. Local sensitivities are used widely and are the basis

of many applications, such as the solution of inverse problems. These local sensitivity indexes, used in "one parameter at a time" methods, quantify the effect of a single parameter by assuming all others are fixed (Saltelli et al., 2005). Sometimes a crude variational approach is selected in which incremental ratios are taken by moving factors one at a time from the base line a fixed amount (for example, 5 percent). This is often done without prior knowledge of the factor uncertainty range or the linearity of the output response.

Techniques that vary one parameter at a time relative to a chosen initial value have some inherent drawbacks. Using such local sensitivity indexes for the purpose of assessing relative importance of input factors can only be effective if the effects of model parameters are all linear, unless some kind of average over the parametric space can be made (Saltelli 2004). Often, the models are non-additive (non-linear) and an alternative "global" sensitivity approach is more appropriate. Exploring the entire parametric space of the model may answer questions such as (1) which of the uncertain input parameters largely determine uncertainty of a specific output, or (2) eliminating uncertainty in which input parameter would reduce output uncertainty by the greatest amount (Saltelli et al., 2005).

Different types of global sensitivity methods can be selected based of the objective of the analysis. For computationally expensive models or if a large number of parameters need to be evaluated simultaneously, it is usually more efficient to apply a screening method. This type of method provides a parameter ranking in terms of relative effect over output variation. Screening tools yield a qualitative parameter ranking that allows the user to focus the calibration or development effort on the most sensitive parameters. If quantitative information is desired, an analysis of variance technique is usually required.

The South Florida Water Management Model (SFWMM) is a regional-scale computer model that simulates the hydrology and the management of the southern Florida water resources system from Lake Okeechobee to Florida Bay. The model simulates all the major components of the hydrologic cycle in southern Florida on a daily basis using climatic data for the 1965-1995 period. The SFWMM is widely accepted as the best available tool for analyzing regional-scale structural and/or operational changes to the complex water management system in southern Florida (http://www.sfwmd.gov/org/pld/hsm/models/sfwmm/index.html). A derivative based local sensitivity analysis was performed by the South Florida Water Management District (SFWMD) for 8 parameters of the SFWMM for a number of sites to which the model was differentially calibrated based on land use characteristics and availability of historical hydrological data (SFWMD, 2005). As parameters ranges characteristic for South Florida conditions were not found in the literature, they were assessed in an unconventional way: “for each parameter, a series of model runs were completed to determine the range of acceptable values such that each parameter within the range can be used without significantly affecting the calibration”. A recommended permissible variation of the parameters was thus determined to be ±10% for WPET (Wetland PET), ±20% for CPET (Coastal PET) and ±50% for other parameters.

Such derivative-based techniques as were applied in this work were found inadequate by the “SFWMM Peer Review Panel” and in a recent report (Bras et al., 2005). The panel recommended that the District adopts effective and quantitative measures of sensitivity.

Objectives

In the proposed research, global sensitivity approaches and alternative sensitivity techniques will be undertaken. Global sensitivity measures will provide a measure of the overall model sensitivity to a parameter across the entire distribution of its possible values. Choice of sensitivity analysis techniques will depend on the following criteria: 1) the computational cost of running the model, 2) the number of input parameters, 3) the degree of complexity of model coding, 4) the amount of time available to perform the analysis and 5) the ultimate the objectives of the analysis. For computationally expensive models, or when large numbers of parameters need to be evaluated simultaneously, a screening technique can prove more efficient. These kind of methods provides a qualitative measure of the relative importance of each of the parameters. For quantitative comparisons of parameter sensitivity variance-based methods will be used

Scope of Work:

Year 1

- Literature review on sensitivity analysis methods and theory
- Understanding the fundamental principles, inputs and parameter requirements of the model
- Selection of an application case (domain/subregion) for sensitivity analyses

Year 2

- Identification parameters and the distribution of each parameter from existing data at the application site and literature (for the intended area of application i.e. South Florida).
- Selection of sensitivity analysis method(s) to be applied, tools and training.
-

Years 3

- Carry out the sensitivity analysis.
- Interpretation of results.

D**eliverables:**

These are proposed to permit the evaluation of the project by the three partners of this project as included in the UF/SFWMD Cooperative Agreement:

1) One-page quarterly reports summarizing the progress in recruiting, enrolling, developing supervisory committees, developing plans of study, developing research proposals, courses taken, and research conducted by the Ph.D. student.
2) Annual summary report.
3) Regular progress meetings at UF and/or SFWMD.
4) A final report at the completion of each students degree program (the content of this report will be close to that of the students dissertation).

5) One or more papers submitted to a peer-reviewed journal, co-authored with the student's adviser and the South Florida Water Management District Staff that actively works with the student in his research study. The paper(s) should cite the financial, in-kind, and technical support received from the South Florida Water Management District and the Water Resources Research Center.

References:

Beven, K. (1989), Changing Ideas in Hydrology -- The Case of Physically Based Models. Journal of Hydrology, 105: 157.

Beven, K (2006), On undermining the science? Hydrological Processes, 20:1-6.

Bras, R.L., A. Donigian, W.D. Graham, V. Singh, J. Stedinger (2005), The South Florida Water Management Model, version 5.5: Review of the SFWMM Adequacy as a Tool for Addressing Water Resources Issues. Final Panel Report, Oct. 28, 2005. SFWMD : West Palm Beach.

Haan, C. T. (1989), Parametric Uncertainty in Hydrologic Modeling. *Transactions of the ASAE, 32*(1): 137-.

Luis, S.J., and D. McLaughlin (1992), A Stochastic Approach to Model Validation. Advances in Water Resources, 15:15.

Muñoz-Carpena, R., G. Vellidis, A. Shirmohammadi and W.W. Wallender (2006), Evaluation of modeling tools for TMDL development and implementation. Transactions of ASABE 49(4):961 -965.

Reckhow, K. H. (1994), Water-Quality Simulation Modeling And Uncertainty Analysis For Risk Assessment And Decision-Making, *Ecological Modelling*, *72*, 1-20.

Saltelli A., Ratto M., Tarantola S. Campolongo F. (2004), Sensitivity analysis in chemical models, Chemical Reviews, 105, 2811-2827.

Saltelli, A., M. Ratto, S. Tarantola, and F. Campolongo (2005), Sensitivity analysis for chemical models, *Chemical Reviews*, *105*, 2811-2827.

SFWMD (2005), Final Documentation for the South Florida Water Management Model (v5.5). South Florida Water Management District and the Interagency Modeling Center West Palm Beach, Florida, November, 2005.

Topic 2: Addition of Ecological Algorithms into the RSM Model

CoPIs: Gregory Kiker, Rafael Muñoz-Carpena, Wendy D. Graham,
SWFMD Coordinator: Naiming Wang
Ph.D. Student: Gareth Lagerwall
Collaborator: Andrew James

Introduction

Alterations to the natural delivery of water and nutrients into the Everglades of the southern Florida peninsula have been occurring for nearly a century. Major regional drainage projects, large-scale agricultural and urban development, and changes to the hydrology of the Kissimmee River-Lake Okeechobee-Everglades watershed have resulted in substantial changes in ecological components of all these systems. The highly connected nature of groundwater and surface water systems over large spatial areas has necessitated the development of integrated regional modeling approaches to adequately represent the unique hydrological and ecological conditions of southern Florida.

The Regional Simulation Model (RSM) was developed to provide an integrated surface and subsurface hydrological model for the development and exploration of water management and habitat restoration objectives (SFWMD, 2005). One of the primary challenges in developing RSM and its concomitant implementation within southern Florida (SFRSM) is to provide a flexible and adaptable framework for new code additions and expanded functionality while maintaining stable simulations for management analysis. Recent RSM code addition projects have successfully added generic water quality components into the model structure (RSM-WQ: Jawitz et al., 2006). This approach used an innovative mixture of conceptual model design, XML implementation and global sensitivity analysis to provide water quality algorithm designs for multiple modeling platforms while being implemented and tested within RSM. Given the initial success of the RSM-WQ module additions, interest has been growing to utilize elements of this approach to add ecological algorithms with a similar methodology. Ecological components and their representation within modeling platforms present a significant challenge as a variety of algorithm designs exist ranging from simplified Habitat Suitability Indices (USFWS, 1981; Tarboton et al., 2004) to Spatially Explicit Species Index (SESI) and individual models (DeAngelis et al., 1998; Curnutt et al., 2000) to more complex, high resolution, individual-based models (Goodwin et al., 2006).

Objectives

This research project aims to systematically review, design and develop selected ecological algorithms for the RSM model (RSM-ECO) using a similar methodology to the development of water quality algorithms (RSM-WQ). To this end, the objectives of this research are the following:

- Review of relevant ecological models, design concepts and code implementation tools for development of RSM-ECO ecological algorithms.

- Selection of ecological species (habitat, plant and/or animal) to be included in the initial development and testing of RSM-ECO.
- Development of the conceptual model of RSM-ECO organisms
- Prototype model development and testing on the "10x4" mesh (Jawitz et al., 2006)
- Selection of a test site for model calibration and testing
- Model implementation and testing on selected test site
- Systematic global sensitivity analysis

Scope of Work:

Evolution of the RSM-ECO model and its associated simulation results will be posted on-line with reports and deployed software (Years 1-3). A basic schedule is listed as follows:

Year 1: Review of relevant models and concepts

- Review current RSM and RSM-WQ design and code structure
- Current ecological model designs/algorithms (*i.e.* HSI models, ATLSS, ELM, ELAMS)
- Object-oriented design and code implementation (Java and C++)

Year 2: Development of conceptual models for selected organisms

- Selection of organisms for initial RSM-ECO inclusion and testing.
- Development of the "10x4" site with selected organisms for prototype testing
- Selection and development of parameters for a South Florida test site for RSM-ECO

Year 3: Model implementation on selected test site

- Sensitivity Analysis
- Calibration/Validation with SFWMD ecological data
- Development of technical documentation

D**eliverables:**

These are proposed to permit the evaluation of the project by the three partners of this project as included in the UF/SFWMD Cooperative Agreement:

6) One-page quarterly reports summarizing the progress in recruiting, enrolling, developing supervisory committees, developing plans of study, developing research proposals, courses taken, and research conducted by the Ph.D. student.
7) Annual summary report.
8) Regular progress meetings at UF and/or SFWMD.
9) A final report at the completion of each students degree program (the content of this report will be close to that of the students dissertation).

10) One or more papers submitted to a peer-reviewed journal, co-authored with the student's adviser and the South Florida Water Management District Staff that actively works with the student in his research study. The paper(s) should cite the financial, in-kind, and technical support received from the South Florida Water Management District and the Water Resources Research Center.

References:

Curnutt, J.L., J. Comiskey, M.P. Nott, and L.J. Gross. 2000. Landscape-based spatially explicit species index models for Everglades restoration. *Ecological Applicat*ions 10:1849-1860.

DeAngelis, D.L., L.J. Gross, M.A. Huston, W.F. Wolff, D.M. Fleming, E.J. Comiskey, and S.M. Sylvester. 1998. Landscape modeling for Everglades ecosystem restoration. *Ecosystems* 1:64-75.

Goodwin, R.A., Nestler, J.M., Anderson, J.J., Weber, L.J. and Loucks, D.P. 2006. Forecasting 3-D fish movement behavior using a Eulerian–Lagrangian–agent method (ELAM). *Ecological Modelling* 192: 197–223

Jawitz, J., Muñoz-Carpena, R. Grace, K., Muller, S. and James, A.I. (2006). Spatially Distributed Modeling of Phosphorus Reactions and Transformations in Wetlands. USGS Draft Report.

South Florida Water Management District (SFWMD), 2005. Regional Simulation Model (RSM): Theory Manual. South Florida Water Management District, Office of Modeling (OoM), 3301 Gun Club Road, West Palm Beach, FL 33406. Web: http://www.sfwmd.gov/site/sub/m_rsm/pdfs/rsmtheoryman.pdf#RSM_Theory

Tarboton, K. C., Irizarry-Ortiz, M. M., Loucks, D. P., Davis, S. M., and Obeysekera, J. T. (2004). Habitat Suitability Indices for Evaluating Water Management Alternatives. Office of Modeling Technical Report. South Florida Water Management District, West Palm Beach, Florida. December, 2004..

USFWS. (1981). Standards for the Development of Habitat Suitability Index Models forUse in the Habitat Evaluation Procedures. Report ESM 103, Interagency, Interdisciplinary Development Group, Division of Ecological Services, U.S. Fish and Wildlife Service, U.S. Department of the Interior, Washington, DC.

Related research.

As described above, these training efforts will complement existing research conducted by the PIs. Currently this includes work with NSF, FDEP, FDACS, USGS and SFWMD that will provide a foundation for the new assistantships. Within the first year the PIs, with the close cooperation of SFWMD staff, have recruited the listed students and have developed supervisory committees, plans of study and Ph. D. research proposals that match the interests formulated by the SFWMD. These research areas encompass, but are not limited to, global sensitivity analysis and uncertainty of hydrologic/water quality models, ecological modeling in South Florida. These research proposals are co-funded with matching funds from SFWMD.

Training potential.

Two Ph.D. graduate students will be trained through this effort.

Investigator's qualifications.

Resumes from the project PIs and collaborator are included in the next pages.

Measurement of erosion around hydraulic structures

Basic Information

Title:	Measurement of erosion around hydraulic structures
Project Number:	2006FL145B
Start Date:	3/1/2006
End Date:	2/29/2008
Funding Source:	104B
Congressional District:	6
Research Category:	Engineering
Focus Category:	Sediments, Models, None
Descriptors:	
Principal Investigators:	Tian-Jian Hsu

Publication

Erosion at Hydraulic Structures

Tian-Jian Hsu
Civil and Coastal Engineering
University of Florida

1 Introduction

1.1 The problem addressed in this report

As a result of recent active hurricane seasons, many District waterways experienced bank and bed erosion. The erosion was more severe downstream of flow control structures, particularly spillways and weirs. These erosions cause several undesired problems, for example, erosion on the discharge canal potentially endangers the structural stability of the flow control structure. In addition, bank erosion may also result in damages to the levees. The eroded sediments may also be carried by the flow to the lakes and reservoirs and causing undesired sedimentation, and resulting in reduction of storage capability for water supply and deterioration of the water quality.

The primary objective of this report is to summarize an effort on literature survey for existing experimental studies of erosion problems, specifically at hydraulic structures and river banks and to recommend a process-based experimental approach to further investigate erosion problem at selected District field sites. A process-based approach based on physical principles allows effective field experimental design and data analysis so that eventually a general formulation for evaluating erosion problem can be proposed for District's management purposes.

In the past several decades, there have been extensive studies on bridge pier and abutment scour for both cohesionless and cohesive sediments. Many of these studies adopted process-based approach and had greatly advanced our physical understanding on local scour and common sediment erosion processes. Therefore in this report, after a general discussion on scour types, we begin our investigation by summarizing some of the major finding from bridge pier scour studies (section 2). Some of the lessons learned from these studies, such as the concept of equilibrium, timescale to equilibrium and differences between noncohesive and cohesive sediments, are very important guidelines to our major objective regarding erosion at hydraulic structures and bank erosion. In section 3, erosion below spillway and culvert outlets are discussed, respectively. Section 4 focuses on bank erosion. In each of the sections 3 and 4, we begin with a general description of the problem, and a literature survey on existing approaches. By the end of each section, recommendations for new field experiments to improve our current predictive capability are described and planned. Finally, in section 5 a brief literature survey on recent advances in sediment transport modeling and three-dimensional numerical approach based on computational fluid dynamics (CFD) for erosion at structures is discussed. Major conclusions from this investigation are remarked in Section 6.

1.2 Scour types

Scour is the loss of soil by erosion due to the flow. Scour is generally divided into several types (e.g., Mueller & Wagner 2005; Briaud et al. 1999) and each scour type does not necessarily have a precise definition in all physical aspects when compared to other types. Therefore, for the purpose of clarity and relevance to this report, they are first defined here.

In terms of the mechanism, scour is a result of acceleration of the flow (and possibly enhancement of flow turbulence) and it is generally a time-dependent process. Considering the stream flow and the sediment bed as one system in equilibrium at a specific time, then the scour is a process that represents how the streambed morphology is in respond to the local flow acceleration through sediment erosion/accretion and eventually arrives at another equilibrium state. The acceleration of the local flow can be resulted from increase of stream flow velocity due to flooding or due to local obstructions (e.g., contraction) to the water flow, or both. The type of flow disturbance can be due to the enhanced shear flow and bottom/wall stress near the streambed/bank (e.g., bridge scour, bank erosion) or the direct impact to the soil through a jet-like flow (scour below spillway, culvert outlets).

The *long-term scour* is the general aggradation or degradation of streambed elevation due to natural and human causes. In this study, we focus more on the *short-term scour* in which the streambed respond to short-term stream-flow runoff cycles, e.g., a stream's storm hydrograph. Within the context of short-term scour, we can further distinguish between the *contraction scour* and the *local scour*. The contraction scour is resulted from the increase of normal stream flow due to natural or manmade contractions. It includes removal of soil from a river's bed and banks and is a concern of the overall channel stability. The local scour refers to removal of soil from around piers, abutments or of more concerns here, the hydraulic control structures.

The local scour can be further classified based on the mode of sediment transport due to the approaching flow (e.g., Melville and Chiew 1999; Barbhuiya and Dey 2004). The *clear-water scour* occurs when the approaching flow intensity is not sufficient to initiate ambient sediment transport (except around the structure). Hence, there is no upstream supply of sediment relative to the local scour. On the other hand, *live-bed scour* occurs when the approaching flow is energetic enough to entrain bed sediment from the upstream and hence the local scour is continuously fed with upstream supply of sediment. The time-dependent behavior of the scour processes is rather different for clear-water scour and live-bed scour (Fig 1). The equilibrium scour depth is attained more rapidly during live-bed scour and strictly speaking, it is a quasi-equilibrium state due to for example, the migration of bedforms. The clear-water scour reaches its equilibrium more slowly. However, the resulting magnitude of the maximum equilibrium scour depth is greater (about 10%) than that for live-bed condition (Graf 1998).

If the interest here is erosion due to storm, live-bed scour may be more likely to occur. However, the duration of the storm becomes another critical factor to be incorporated. In this case, the timescale to reach equilibrium must be a competing factor with the storm duration. It is well-known that the erodibility for non-cohesive (sand) and cohesive (clay, fully consolidated) sediments are rather different and hence the timescale to reach equilibrium must also depend on the cohesion property of the sediment. In the field condition the size of sediment is often non-uniform and hence the armoring effects due different sizes of sediments become another concern. Also because of the non-uniform sediment, most upstream approaching flow may consist of the fines (or at least some washloads) which is recently shown to be sensitive to the local scour (Sheppard et

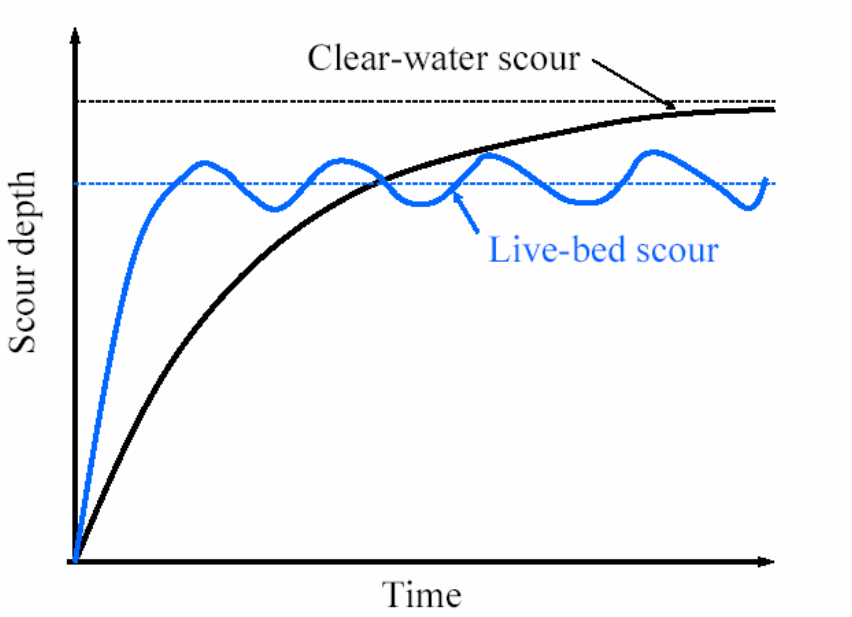

Fig. 1: Schematic descriptions for clear water scour (black curve) and live-bed scour (blue curve). See Graf (1998) for a similar plot.

al. 2004). Therefore, the definition of clear-bed and live-bed scour can not be definite. These are the critical issues that are relevant to both the fundamental sediment transport and various kinds of erosion problems that we will address in this report through a comprehensive literature survey.

2 Lessons Learned from Bridge Scour

In the Unite States, there are about 500-thousand bridges that are over water (National Bridge Inventory 1997). In the past 30 years, about 60% of the bridges failed were due to scour (Shirole & Holt 1991; Briaud et al. 1999). Therefore, there has been an extensive research on bridge scour ranging from theoretical analyses, laboratory/field experiments, and numerical modeling. Research findings resulted from these studies, especially those related to the physical processes of erosion, can certainly provide useful guidelines for other type of erosion problems relevant to District's interests. Hence, this section concentrate on summarizing important lessons learned from extensive bridges scour studies that will be useful for our major objective regarding erosion at hydraulic structures and bank erosion

2.1 Dimensional analysis

Bridges scour is a rather complex problem form the fluid mechanics point of view. It involved interactions among turbulent fluid flow, sediment and the geometry of the structure. Dimensional analysis is a very useful tool as the first step toward a more comprehensive study. Here we utilize a framework for analysis following Melville & Chiew (1999). This framework is concise but provides considerable insights into the dynamical processes and is also used by other researchers recently for interpreting measured scour data (Sheppard et al. 2004; Sheppard & Miller 2006).

The local scour is caused by the presence of structure that alters the original flow field from an equilibrium state. Therefore, it is reasonable to expect that after the installation of structure, flow and sediment bed may evolve to another equilibrium state through the removal of soil and the adjustment of bed morphology. The maximum equilibrium scour depth d_{sm} is perhaps the most important quantity in the scour prediction. The maximum scour depth at a bridge pier generally depends on flow parameters, bed sediment properties, pier geometry and time.

Assuming uniform sediment properties, fully turbulent flow and simple pier geometry, the maximum scour depth at a cylindrical pier of diameter D can be written as (Melville & Chiew 1999):

$$\frac{d_{sm}}{D} = f\left(\frac{U}{U_c}, \frac{h}{D}, \frac{d}{D}\right) \tag{1}$$

where U is the averaged stream velocity at a significant distance upstream of the structure (stream velocity without the obstruction of structure), U_c is the critical velocity for sediment entrainment, h is the mean flow depth, and d is the mean sediment particle diameter, usually calculate from d_{50}.

The 1st parameter on the right-hand-side of (1) represents the nondimensional flow intensity. This parameter not only characterizes the intensity of the stream flow but also differentiates between the clear-water scour ($U/U_c < 1$) and live-bed scour

($U/U_c > 1$, see their definitions in section 1). The 2nd parameter represents the effect of flow shallowness. The 3rd parameter represents the sediment coarseness. The dependence of maximum scour depth with respect to these parameters reveals important mechanisms controlling scour processes and is discussed in more details in section 2.2.

The timescale to reach the equilibrium scour depth and the time-dependent behavior of scour are not incorporated in equation (1). However, this is another important aspect of the scour processes and has been studied in details by several studies (e.g., Melville & Chiew 1999; Briaud et al. 1999) for both non-cohesive and cohesive sediments. The importance of timescale in scour processes is discussed in section 2.3 and 2.4.

2.2 Prediction for the maximum equilibrium scour depth

The maximum equilibrium scour depth is the most important quantity for a scour prediction and has received the most investigations in the literature. It represents the maximum scour damage that can occur for a given flow condition, sediment properties and structure dimension if the duration of the flow forcing (i.e., a storm) is long enough to attain the equilibrium. Therefore, the maximum equilibrium scour depth is also the most conservative engineering design guideline.

Using the dimensional analysis described in section 2.1. Melville (1997) and Melville and Chiew (1999) proposed an empirical relation using several laboratory data sets conducted in 4 different flumes (totally 70 cases). The data used in this study is for relatively small structure due to the constraint of the laboratory facility and hence the largest ratio D/d is about 200. This value is smaller than what typically encounter in the field condition. Following Melville and Chiew (1999), Sheppard et al. (2004) and Sheppard and Miller (2006) further utilize a proto-type scale flume facility (at USGS and University of Auckland), extend the database for D/d as high as 4155, and propose a new empirical formulation to estimate the maximum equilibrium scour depth. On the other hand, one of the most commonly used scour prediction equation is the HEC-18 equation (Richardson and Davis 2001) recommended by Federal Highway Administration, U.S. Department of Transportation. Since the original HEC-18 was proposed, it has been revised few times by calibrating with new field data (Mueller & Wagner 2005). Other empirical equations for scour prediction can be found in a recent review paper by Barbhuiya and Dey (2004).

Before presenting several widely-used formulae for predicting maximum equilibrium scour depth, it is useful to exam the general dependence of d_{sm} on each of the nondimensional parameters on the right-hand-side of (1). Summarizing the results and analyses presented by Melville and Chiew (1999) and Sheppard et al. (2004), their most important conclusions are shown here graphically in Fig 2-4.

As the nondimensional flow intensity increases, the scour depth has two peak values (Fig. 2). The maximum clear-water scour occurs when $U/U_c = 1$. Subsequent increment of flow intensity initiates sediment movement over the entire streambed (not

just the scour hole area). In such live-bed condition, the upstream flow (before approach the scour hole) already consists of suspended sediment and the suspension capacity of the overall flow is reduced (e.g., suspended sediment reduces flow turbulence, Hsu et al. 2003). The maximum equilibrium scour depth thus reduces according (usually about 10-20%). Even at the live-bed scour maximum (the second peak in Fig. 2), its magnitude is still smaller than that at clear-bed scour maximum (i.e., at $U/U_c = 1$ in Fig 2).

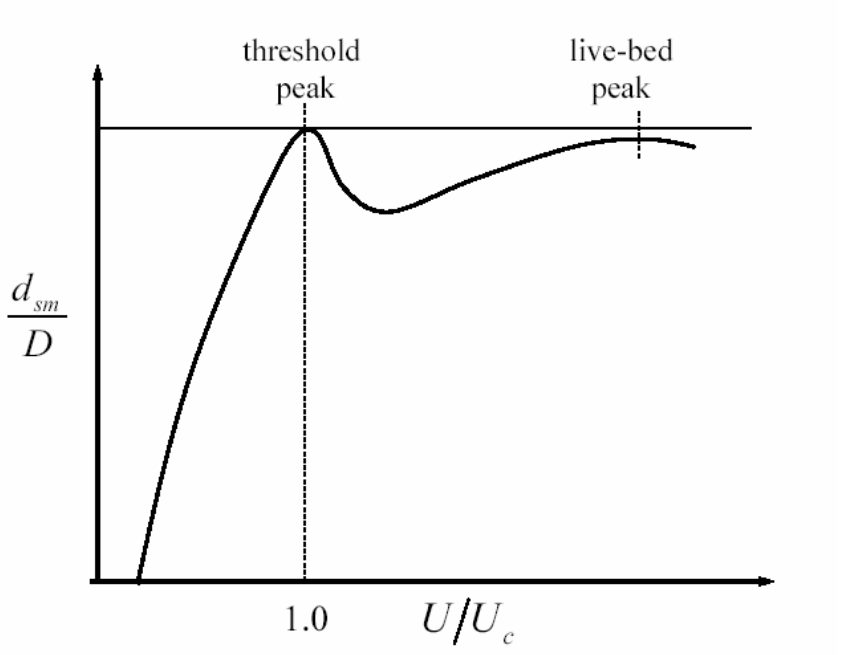

Fig2: Influence of flow intensity U/U_c on nondimensional scour depth. $U/U_c = 1$ differentiates clear-water scour and live-bed scour.

As the flow shallowness increases, the nondimensional scour depth increases until it reaches an asymptotic value (Fig. 3). Approximately, when the water depth is about several times larger than the pier diameter, further increment of water depth has no effect on the scour depth. The flow turbulence around the pier, which more or less determines the amount of sediment transport, can be approximately characterized by the largest size of the turbulent eddy. When the water depth is sufficiently deep, it has no effect on the local flow and the largest turbulent eddy size is determined by pier diameter and the so is the scour depth. On the other hand, when the water depth is relatively small compared to the pier diameter (or relatively wide pier), the largest turbulent eddy size must be confined by the water depth and the scour depth must scale with the water depth.

Based on most of the small-scale laboratory results, it is generally believe that then grain size has no effect on scour depth except for relatively coarse grain (*D/d<50*, Fig 4, black curve), the scour depth decreases because coarse grains provide significant bed roughness and porous effect that dissipate the flow energy (e.g., Ettema 1980). However, this conclusion is made from small-scale laboratory results with limited size of

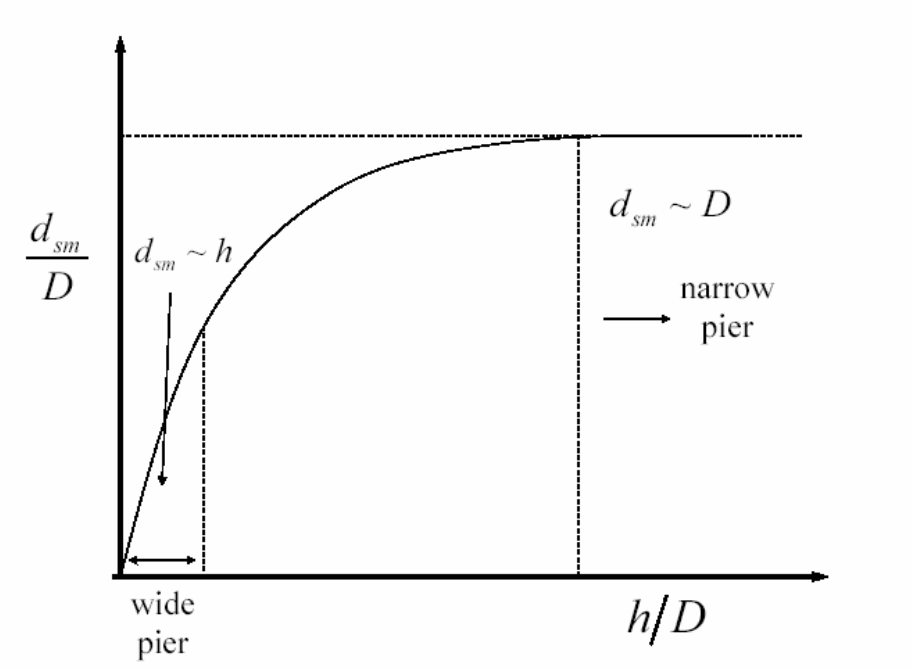

Fig. 3: Influence of flow shallowness on nondimensional scour depth.

pier and *D/d* value is no more than about ~100. Recently, new evidences based on prototype experiments, with *D/d* as large as 1000~4000 suggest nondimensional scour depth clearly decreases as *D/d*>>50 (Sheppard et al. 2004). There is no definite explanation at this point for the reason why nondimensional scour decreases for fine sediment (Sheppard, personal communication). One possible explanation could be due to the effect of suspended sediment on damping the flow turbulence (Ross and Mehta 1988; Hsu et al. 2003; 2006), which has been proved to be important in controlling the lutocline dynamic of soft fluid mud at estuary or continental shelf (Trowbridge and Kineke 1994) when mud concentration is greater than about 10g/l. This important finding in scour process by Sheppard et al. (2004) also demonstrates the importance and the justification for pursuing field experiments on scour processes.

The scour prediction equation proposed in Melville and Chiew (1999) is a function flow-pier width, flow intensity and particle size. However, the equation is dimensional (even though they propose equation (1) that is nondimensional). Sheppard et al (2004) and Sheppard and Miller (2006) later followed equation (1) and propose scour formulae for bridge pier that is more complete. The Sheppard's equations are given as, for clear water scour,

$$\frac{d_{sm}}{D} = 2.5 \tanh\left[\left(\frac{h}{D}\right)^{0.4}\right] f_d\left(\frac{D}{d}\right)\left\{1 - 1.75\left[\ln\left(\frac{U}{U_c}\right)\right]^2\right\} \tag{3.1}$$

and for scour above live-bed peak

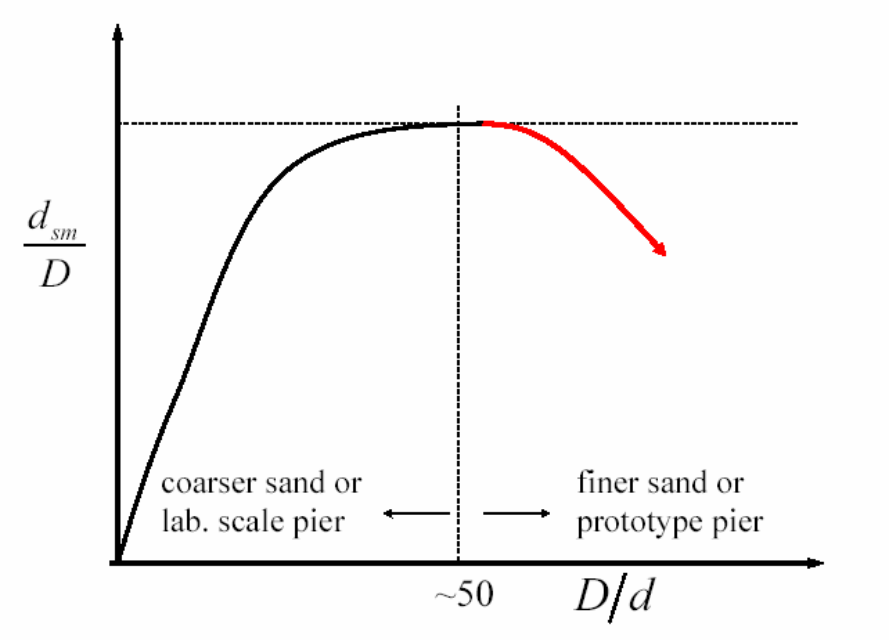

Fig.4: Influence of sediment coarseness on nondimensional scour depth. The red curve represents new findings based on prototype scale experiments.

$$\frac{d_{sm}}{D} = 2.2\tanh\left[\left(\frac{h}{D}\right)^{0.4}\right]. \tag{3.2}$$

A linear interpolation can be used in between live-bed scour range up to live-bed peak. In (3.1), a complete functional dependence of D/d is obtained through large-scale flume experiment as:

$$f_d\left(\frac{D}{d}\right) = \frac{D/d}{0.4(D/d)^{1.2} + 10.6(D/d)^{-0.13}} \tag{3.3}$$

The HEC-18 equation, which is used and calibrated in the field, is nondimensionalized in a rather different way as compared to Melville's and Sheppard's formula. HEC-18 formula is based on the Froude number (Richardson and Davies 2001):

$$\frac{d_{sm}}{D} = 2.0K_3\left(\frac{h}{D}\right)^{0.35} F_r^{0.43} \tag{4.1}$$

where K_3 is a numerical coefficient that account for bedforms (1.1 for plane bed and small dunes and up to 1.3 for large dunes). The Froude number F_r is defined as

$$F_r = \frac{U}{\sqrt{gh}} \tag{4.2}$$

2.3 Time-dependent scour behavior

The timescale to attain the equilibrium maximum scour depth has received less investigation than the equilibrium scour depth itself. This is partly because for sandy environment, the timescale to attain equilibrium is relatively short (or on the same order of magnitude) when compared to typical duration of an extreme event (e.g., storm). In addition, the maximum equilibrium scour depth already provided the most conservative design criterion (but costly). However, as our capability for predicting the scour depth advances, the time-dependent behavior received more and more interests in the past several years (Melville and Chiew 1999; Briaud et al. 1999; Sheppard et al. 2004). Predicting the time-dependent scour depth is essential when considering storm of relatively short duration or even more importantly when considering fully consolidated cohesive soil erosion (see section 2.4 for details).

Following the nondimensional form in (1), the time t for scour depth evolution can be normalized by T_e, the timescale to reach the equilibrium maximum scour depth. Hence, we can add the 4th nondimensional quantity t/T_e into equation (1) for predicting the general time-dependent scour depth d_s:

$$\frac{d_s}{D} = f\left(\frac{U}{U_c}, \frac{h}{D}, \frac{d}{D}, \frac{t}{T_e}\right). \tag{2}$$

According to Melville & Chiew (1999), the time evolution of scour depth d_s approaching the final equilibrium maximum scour depth d_{sm} can be well represented by the following equation:

$$\frac{d_s}{d_{sm}} = \exp\left\{-0.03\left|\frac{U_c}{U}\ln\left(\frac{t}{T_e}\right)\right|^{1.6}\right\} \tag{3}$$

This equation requires an estimate of T_e. Existing data suggest (Melville & Chiew, 1999) T_e itself when normalized by D/U, depends on flow intensity, flow shallowness and sediment coarseness. An empirical formula is suggested to predict T_e as:

$$\begin{aligned} T_e(\text{days}) &= 48.26\frac{D}{U}\left(\frac{U}{U_c} - 0.4\right), \qquad \frac{h}{D} > 6 \\ T_e(\text{days}) &= 30.89\frac{D}{U}\left(\frac{U}{U_c} - 0.4\right)\left(\frac{h}{D}\right)^{0.25}, \qquad \frac{h}{D} \le 6 \end{aligned} \tag{4}$$

Notice here that when the water depth is large enough (6 times the structure diameter), the effect of water depth on scour vanishes, consistent with that observed for maximum equilibrium depth.

An estimate of the typical time evolution for scour to reach equilibrium is insightful at this point. Considering a peak flood velocity of *U=0.8m/s*, sand diameter *d=0.22mm*, structure diameter *D=1.0m*, and water depth *h=1.2m*. The threshold velocity in this case can be confidently estimated as $U_c = 0.32$ m/s (Melville 1997). The time scale for the scour to reach equilibrium, according to (4) is calculated as 84.87 days, which is seemingly a very long time. However, the time-dependent behavior described in (3) is rather nonlinear (see Fig 5, for an example). In fact, in simply 1 day, the scour depth is as deep as 93% of the final equilibrium depth. Therefore, when considering the uncertainties in estimating maximum equilibrium scour depth itself, the scour processes reach its maximum scour depth in a rather short period of time (~1day) when compare to typical flood duration.

On the other hand, a fully consolidated cohesive soil (clay) has a rather low erodibility and the threshold velocity can be several times higher than that for sand. Let's now assuming equation (3) and (4) are equally applicable to cohesive sediment. Using a typical threshold velocity for clay of $U_c = 1.0$ m/s (Briaud et al. 2004) but with other parameters unchanged, it will take 4 day to reach 93% of the final equilibrium scour depth. This is about 4 times slower as compared to sandy condition. Therefore, for cohesive sediment the scour process is much slower and the duration of a storm is often not long enough for the scour to attain its maximum equilibrium depth. Notice that in reality, equation (3) and (4) may only qualitatively applicable to cohesive sediment and one would expect the empirical coefficient involved in (3) and (4) different from that used in sandy condition. As we will discuss in the next section (section 2.4), the scour processes for cohesive sediment is even much slower than our crude estimate here using (3) and (4) (see Fig. 5).

2.4 Scour for cohesive soils

Previous sections focus on bridge scour for non-cohesive, sandy environments (coarse-grained). The major difference between a non-cohesive and a cohesive sediment scour is that the erodibility for a fully consolidated, cohesive clay material is much less (sometime 1000 times less, Briaud et al. 2004; Ansari et al. 1999) than that of sand. Therefore, the scour depth for cohesive soil develops much slower than that for non-cohesive sandy material. An example for comparing sand scour and clay scour demonstrated by Brandimarte et al (2006) is reproduced in Fig 5.

For typical peak flow duration due to storm of say 1 day, it is sufficient for sandy scour to develop to its maximum equilibrium scour depth. Hence, simply estimating the maximum equilibrium scour depth at sandy environment is sufficient for engineering purposes. However, 1-days of storm duration are too short for cohesive soil to develop to the maximum scour depth. Hence, using an estimated maximum scour depth in a cohesive sediment condition usually over-predicts the scour and hence provides a design criterion that is too conservative. For scour in cohesive sediment, it is important to study the time-dependent behavior. Accurate descriptions on the time-dependent scour process for cohesive soil can save lots of money in building a reliable structure.

Briaud et al. (1999, 2004) developed a useful approach to predict the time-dependent behavior of scour depth for cohesive soil. This method is called SRICOS (Scour Rate In Cohesive Soils). In this approach, the maximum scour depth in clay is in fact considered to be similar to that in sand (same formulae presented in section 2.3 can be use). SRICOS is more complicated in predicting the time-dependent behavior. Briefly, SRICOS method can be described in several steps:

1. Estimate maximum initial bottom shear stress around the structure (i.e., structure with an initial flat bed). This can be estimated by measurements, or CFD simulations.
2. Obtain the initial scour rate. Again, if it were non-cohesive sediment, the initial scour rate can be estimated with good confidence using the maximum bottom stress obtained in (1) and a power law (Graf 1998). However, for cohesive clay material, such a simple relation does not exist. The erodibility of cohesive sediment is too complicated to allow for developing effective mathematical formulae to relate the bottom stress and erosion rate. In SRICOS, samples of cohesive material is taken from the field and tested in a laboratory facility, called EFA (Erosion Function Apparatus) to estimate the initial scour rate.
3. Estimate maximum equilibrium scour depth using well-developed method for non-cohesive sediment (e.g., formulae presented in section 2.3).
4. Using the initial scour rate (obtained from step 1 and step 2) and maximum equilibrium scour depth (obtained in step 3), the time-dependent behavior of scour can be calculated by a hyperbolic model. It is basically a nonlinear interpolation scheme to get "scour depth versus time". This method has been validated by extensive experimental data.

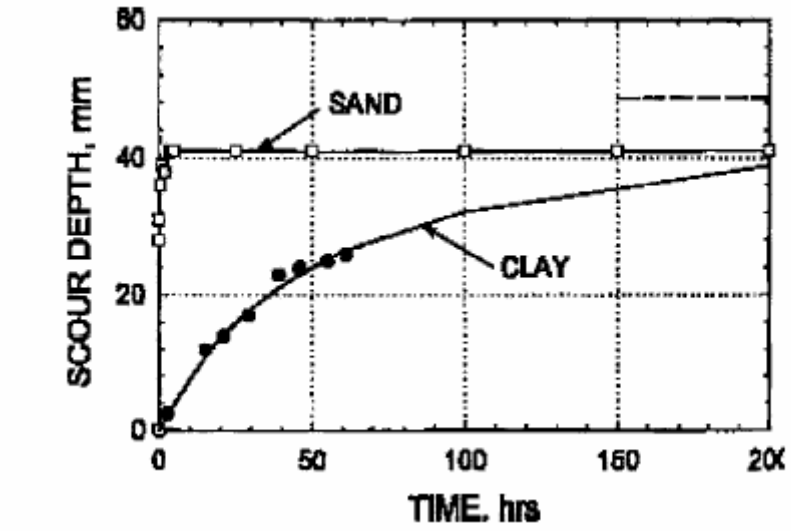

Fig 5. Scour development in clay is much slower than that in sand. (adopted from Brandimarte et al. 2006, see also Briaud et al. 2002)

The basic concept of this method appears to be rather general and hence may be applied to other type of erosion problems involving cohesive soil. For other type of erosion problem, different empirical formulae or experimental setups in getting the initial scour rate, the maximum erosion depth and the hyperbolic interpolation relation are required.

2.5 Summary

Several important experiences learned from extensive bridge scour studies that may be useful for other type of erosion problems for the District are summarize here:

(1) An equilibrium state exists for bridge scour and possibly other type of scour problems. The state of equilibrium provides the most important step toward simplifying the erosion problem from a engineering point of view because the maximum equilibrium scour can be estimated as the most conservative design criterion. Predicting the maximum equilibrium scour is the most fundamental step to study a scour problem.

(2) The time scale to attain the equilibrium state is another important parameter that needs to be estimated. The relative magnitudes between the equilibrium time scale for a specific scour problem and the duration of the episodic forcing (e.g., flooding) determine whether the time-dependent behavior of the scour needs to be further explored; or simply estimating the maximum equilibrium scour is sufficient. In general, the time scale for non-cohesive sediment (e.g., sand) scour is much shorter than that of cohesive sediment scour. If the driving force for scour is short-term stream-flow runoff, then predicting the maximum equilibrium scour depth is sufficient for non-cohesive sediment. However, for cohesive sediment the problem is more complex and time-dependent behavior of scour need to be further estimated or parameterized. The SRICOS method developed by Briaud et al. (1999, 2004) appears to be effective for predict bridge scour in cohesive soil. The concept of this method may also be applicable to other type of scour for cohesive soil.

(3) The general believe based on laboratory-scale experiment that fine sediment has no effect on scour is disproved by new prototype scale experimental finding (Sheppard et al. 2004). New finding suggests fine sediment scour is smaller than previously predicted and old design principle may be too conservative and the criterion may be too costly. This provides an important lesson for sediment transport: It is easy to match the similitude principles for pure hydrodynamics experiments but it is impossible to also match the sediment parameters concurrently. Hence for sediment transport study, it is extremely important to consider field or proto-type scale experiments.

(4) From a fluid mechanics point of view, scour formulae developed based on laboratory experiments are more complex and perhaps more complete. On the other hand, formulae developed from field studies are usually simpler. This is partly because in an idealized laboratory environment, some of the parameters are

easier to define than that in the field condition (or difficult to measure in the field). Additionally, the uncertainties in the field may also prevent more detailed calibrations if too many parameters are involved. However, we must note that the empirical coefficients in a laboratory-developed formula may suffer from scale effect and hence are often not as robust as compared to those simple formulae calibrated with extensive field data. The field scale erosion problem is certainly of more concern to the District. Hence, the suggestion is to start with formulae developed for field condition. Then, according to more detailed laboratory experimental results, we can identify one or two major mechanisms that may greatly improve the existing field-based formula. Using this hypothesis-driven approach, we can then define and design the scope of the field experiment that we will conduct.

3 Erosions below Spillway and Culvert Outlet (Plunge Pool Scour)

3.1 General

The capability to predict and control erosion near hydraulic structure is of great importance for the District. In the previous section, bridge scour problems are reviewed. Scour at bridge piers can be considered as a special case of a more general sediment erosion problem due to a shear flow (and vortices) that is primarily parallel to the bed. On the other hand, we must consider another important type of erosion problem that is due to the direct impact of the flow perpendicular (or arbitrary impact angle) to the sediment bed. This type of problem can be generally named as *plunge pool scour*. Plunge pool scour process is very important to, for example, the erosion downstream of a ski-jump bucket of a spillway or scour below a culvert outlet.

Spillways are widely used to dissipate the energy of floodwater. At the end of the long tunnels, ski-jump buckets are often used to deflect the flow, which throws the jet flow away into the air the then plunge into the tail water. Culverts are another common hydraulic control structure. Flows exiting a culvert outlet often drop from a distance into the downstream flow emulating a free jet. A the point of impact to the streambed, the free jet of water-air mixture enters the tail water, diminishes part of its energy but may eventually approach the streambed and excavating a scour hole.

There have been a great amount of empirical studies for estimating the scour depth below a ski-jump bucket of a spillway, dated back to as early as 1930's (e.g., Veronese 1937; Wu 1973; Martins 1975; Chee and Kung 1983; Mason and Arumugam 1985; Mason 1989, and reference therein). However, most of these formulae are either too simple to incorporate most of the important mechanisms or dimensionally incorrect to be generalized to various field conditions. For example, Azmathullah et al. (2005, 2006) conduct comprehensive evaluation of these formulae with 95 scour data observed at dams of India and Iran. They conclude that none of these formulae are satisfactory (correlations below 0.75). Anther study by Pagliara et al. (2004) also makes a similar conclusion.

Recently, detailed process-based laboratory study on plunge pool scour has been conducted and in the writer's opinion, has revealed systematically various critical mechanisms of jet-impinging type of scour processes and their dependence on flow and sediment parameters (e.g., Mason 1989; Aderibigbe and Rajaratnam 1996; Canepa and Hager 2003; Pagliara et al. 2006). However, none of the formulae proposed in these studies has been tested with field conditions and their practical applicability is not yet known.

In the following, several commonly used scour formulae downstream of a spillway are first summarizes, which consists of earlier empirical studies from 1930s to 1980s. More recent process-based laboratory studies on plunge pool scour is discussed later to assist our understanding on the physical processes involved in this type of scour. A new formulation following Pagliara et al. (2006) is review in more details. Finally, we will recommend a field experiment utilizing new sensors and process-based analytical

framework that may improves upon the existing knowledge on scour downstream of the spillways or culvert outlets.

3.2 Scour formulae commonly used in the field

Similar to bridge pier scour described in section 2, the concept of equilibrium for jet impingement still hold here. According to a vast amount of laboratory and field observations, after the initial impact of the jet flow, the scour continue for a period of time until it attains a maximum equilibrium scour depth. Such equilibrium is established because either the jet has insufficient energy at the point of impact to erode more sediment or the secondary currents are insufficient to sweep away the suspended sediment out of the scour hole (Mason and Arumugam 1985).

The time scale to attain equilibrium for plunge pool scour is not well-documented. However, generally it is believed that the time to reach equilibrium is rather fast for non-cohesive sediment (Aderibigbe and Rajaratnam 1996). According to our survey, there has been no detailed study of this problem for cohesive sediment condition.

There is a great amount of studies focus on predicting the maximum equilibrium scour depth under a spillway. Earlier studies for maximum scour depth are rather simple and empirical. According to Mason and Arumugam (1985), who analyzed 31 formulae from 1930s to 1980s with prototype and laboratory scale data, the most promising formulae are of the following form, which is of the Schoklitsch-Veronese type (Schoklitsch 1935; Veronese 1937):

$$d_{sm} = K \frac{q^x H^y}{d^z} \tag{3.1}$$

where q is the unit discharge at the point of impact, H is the head from upstream to downstream water level, d is the characteristic sediment size as defined before, and K, x, y, z are empirical coefficients. According to calibrations with data, x is about 0.6, y is less certain but ranges from 0.2 to 0.3 and it appears to be even larger variation for z ranging from 0 to 0.5 and K ranging from about 0.2 to 2.8. There is also debate on what type of grain size shall be used (d_{90}, d_{50}, or others).

Notice that several important parameters are not incorporated into equation (3.1), such as impact angle and tail water depth. Mason and Arumugam (1985) suggest a modification of (3.1) to incorporate tail water depth h:

$$d_{sm} = K \frac{q^x H^y h^w}{d^z g^v} \tag{3.2}$$

with g the gravitational acceleration included for dimensional balance such that K become a nondimensional coefficient with a numeric value of about 2~3.

Among these earlier formulations, it is worthwhile here to discuss that proposed by Martins (1975). This formulation is not necessary more accurate but the scour formula is expressed into several nondimensional parameters, which is useful for our later process-based discussion (section 3.3). We show here a more complete version of Martins' formula later modified by Chee and Kung (1983) to include the jet impact angle α:

$$\frac{d_{sm}+h}{H} = 3.3F_r^{0.6}\left(\frac{d}{H}\right)^{-0.1}\alpha^{0.1} \tag{3.3}$$

The sum of the scour depth and tail water depth $d_{sm}+h$ is normalized by the free fall height *H*. More importantly, the Froude number $F_r = q/\sqrt{gH^3}$ of the spillway system is considered. It is also noted here that the length scale used for nondimensionalization in (3.3) is the free fall height *H*. As we shall see in the next section, based on recent detailed laboratory experiments, the grain size appears to be the more appropriate length scale for nondimensionalization of local sediment scour process.

3.3 Process-based analysis

Since 1980s, more detailed process-based (laboratory) study has been conducted in order to understand various physical mechanisms involved in plunge pool scour. To facilitate our discussion next, a definition sketch for plunge pool scour under a submerged or unsubmerged flow is shown in Fig 6.

Based on their experimental observation on scour due to impinging jet, Aderibigbe and Rajaratnam (1996) characterize the flow regimes as *Strongly Deflected Jet Regime* (SDJR) and *Weakly Deflected Jet Regime* (WDJR) (similar classification has been proposed by Kobus et al. (1979)). For Strongly Deflected Jet Regime, the jet penetrates considerably into the sediment bed and hence also gets reflected more strongly. The eroded sediment in the scour hole is transported out by strong re-circulatory flow and turbulence. The time required for the scouring processes is relative short compare to WDJR. The side slope of scour hole is more or less equal to angle of repose and hence the overall shape of the scour hole is maintained by a constant depth-to-width ratio. On the other hand, Weakly Deflected Jet Regime is characterized by a relatively weak penetration into the sediment bed. The eroded sediment is transported out of the scour hole by flow that is mainly along the bottom boundary without re-circulatory flow structure. The depth-to-width ratio is very sensitive to the flow condition and sediment properties.

Another important scour depth definition for plunge pool scour is strongly related to the processes involved in SDJR and WDJR. The *Dynamic Scour Depth* refers to the maximum equilibrium scour condition in which the jet flow remains turned on. The *Static Scour Depth* refers to the maximum equilibrium scour condition when the jet flow stops. The reason to consider the scour condition with or without jet flow is because in SDJR, the strong re-circulation flow and turbulence maintain some sediment suspended in the scour hole (but not swept away) and when the jet flow ceases, these suspended sediments

settle back into the scour hole. Hence, for Strongly Reflected Jet Regime (SDJR), the dynamic scour depth is larger (sometimes much larger, depending on flow condition) than the static scour depth. On the other hand, there is no difference between the dynamic and static scours for Weakly Reflected Jet Regime (WDJR).

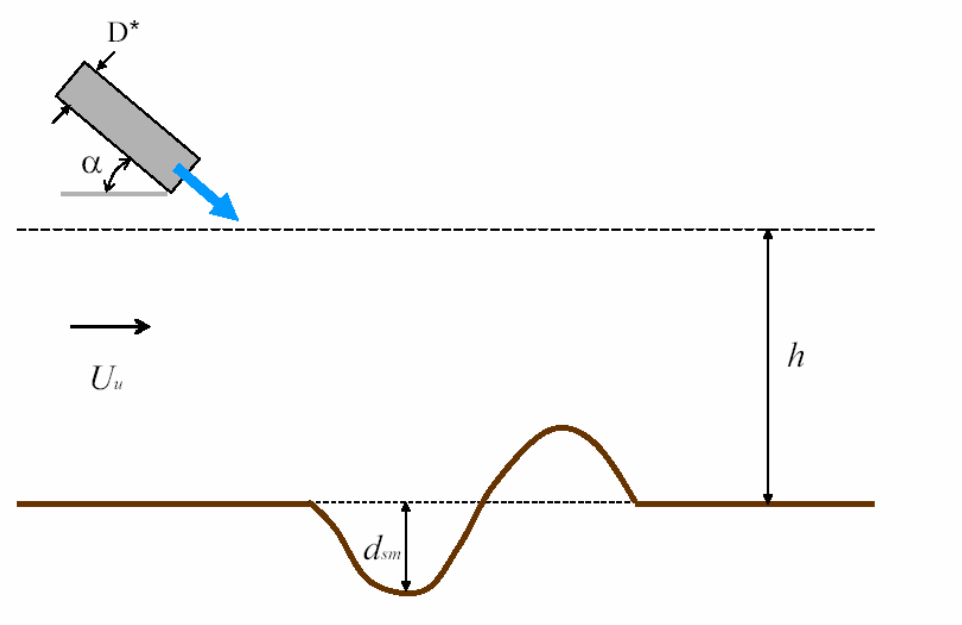

Fig 6: Definition sketch for plunge pool scour under an impinging jet.

Aderibigbe and Rajaratnam (1996) propose a semi-empirical formula for maximum (static) scour depth based on a simple theoretical formulation and laboratory data. Most importantly, they define a nondimensional parameter E_c that can appropriately parameterize the observed (static) scour depth:

$$E_c = \frac{q/h}{\sqrt{gd\,\Delta\rho/\rho}} \tag{3.4}$$

in which $\Delta\rho$ is the access density of sediment to the fluid flow. Notice that in Aderibigbe and Rajaratnam (1996) experiment, the jet nozzle is perpendicular to the bed and is placed right at the tail water depth. Therefore, h also represents the distance for the decay of jet velocity before it impinges to the bed. The numerator in (3.4) simply represents the approach jet velocity before impinging to the sediment bed while the denominator represents an equivalent weight (stabilizing force) of the sediment. Hence, E_c shown here for plunge scour is rather similar to the Shields parameter for shear flow (parallel to the bed) induced sediment transport. Equation (3.4) also suggests that for local scour processes, the appropriate length scale for nondimensionalization is the grain diameter.

Recently, Pagliara et al. (2006) and Canepa and Hager (2003) conduct one of the most comprehensive laboratory studies on plunge pool scour. They identify and test with several parameters that are important to the scour including, jet shape, jet velocity, jet air content, tail water depth, grain size sorting (nonuniformity), and the effect of upstream flow. A new formula for predicting the maximum equilibrium scour depth that incorporates all these effects is expressed as:

$$\frac{d_{sm}}{D^*} = f_1(F_r) f_2(\alpha) f_3(\beta) f_4(T) f_5(\sigma) f_6(F_{ru}) \tag{3.5}$$

with f_1 to f_6 the functions that each describes the dependence of normalized scour depth on a specific flow or sediment parameters, which we will discuss in details next.

Jet Shape The most important concern with these idealized laboratory studies is that whether they can well-represent the field applications. For example, idealized plane (rectangular) or circular jet is often used in the laboratory. However, the jet flow produced by spillway bucket or culvert outlet is of arbitrary shape. According to Pagliara et al. (2006), there is negligible effects of the jet shape provided that the equivalent diameter D^* is used and the corresponding velocity U is defined according to total flow rate and D^*. Therefore, for any arbitrary jet shape with cross-sectional area A, the equivalent diameter is defined as $D^* = \sqrt{4A/\pi}$ and mean jet velocity is simply $U = q/A$.

Froude Scaling After establishing that the equivalent diameter of the jet is the appropriate length scale to normalize scour depth (i.e., left-hand-side of (3.5)), the next major question is how to normalize the intensity of the jet. Even in the early days, the Froude scaling is acknowledged (e.g., Martins 1975; Mason and Arumugam 1985) to characterize the jet intensity. However, it is unclear what the appropriate length scale should be for the Froude scaling. Most existing scour formulae used in the field use the free fall height H as length scale. However, according to Pagliara et al. (2006) and Canepa and Hager (2003), detailed laboratory studies suggest that using the grain diameter as the length scale in Froude scaling gives very accurate fit. Therefore, the Froude number in equation (3.1) is defined as:

$$F_r = \frac{U}{\sqrt{g' d}} \tag{3.6}$$

with $g' = \Delta\rho g/\rho$ the reduced gravity. Notice that the Froude number defined here is consistent with the E_c adopted by Aderibigbe and Rajaratnam (1996) (see equation (3.4)). Based on extensive laboratory data Pagliara et al. (2006) suggest that when d_{90} is used the Froude number dependence is:

$$f_1(F_r) = 0.37 F_r, \qquad 2 \le F_r \le 20 \tag{3.7}$$

Jet Impact Angle Pagliara et al. (2006) conduct experiments on four different jet impact angle α=30, 40, 60 and 90 degree, and suggest the following dependence:

$$f_2(\alpha) = 0.38\sin(\alpha + 22.5^\circ), \quad 30^\circ \le \alpha \le 90^\circ \tag{3.8}$$

Notice that the maximum scour depth does not occur at 90 degree but at around 60 degree possibly because a slight jet angle encourages suspended sediment to be swept away by the flow more effectively.

Jet Air Content The jet air content defined as, $\beta = q_A / q_w$ with q_A and q_w the air and water flow rate respectively, is well-mixed in the idealized laboratory experiment, which is not necessarily the case in the field condition. However, it is the first attempt to consider the effect of air content. When air is present in the jet flow, the jet velocity of the water-air mixture is calculated as $U = q_w(1+\beta)/A$, and Pagliara et al. (2006) recommend:

$$f_3(\beta) = (1+\beta)^{-m} \tag{3.9}$$

m is an empirical coefficient and depends on whether the jet is submerged. The effect of submergence is generally not sensitive to the scour depth except when jet air content is significant. When jet is unsubmerged, *m* is found to be 0.75, and the effect of air content is more pronounced than that for submerged condition with *m=0.5*. Therefore, when the water-air mixture velocity is considered (which is larger than pure water velocity), the scour depth decreases with increasing air content. However, if consider the water velocity only, the addition of air increase the scour depth (Canepa and Hager 2003).

Tail Water Depth The parameter $T = h/D^*$ represents a nondimensionalized tail water depth. According to Pagliara et al. (2006), increasing the tail water depth reduces the scour depth. This is because firstly, higher tail water depth suggests a longer attenuation distance of the jet flow before it impinges the bed. Furthermore, when the tail water depth is very low, the downstream velocity is large and it is easier to transport sediment away from and around the scour hole. Specifically, smaller tail water depth suggests a smaller ridge. The presence of the ridge is usually considered to prevent (protect) the scour. Hence smaller ridge further encourage deeper scour. It is suggested that

$$f_4(T) = 0.12\ln\left(\frac{1}{T}\right) + 0.45, \qquad \text{for } T^{-1} > 0.05 \tag{3.10}$$

Notice that the E_c parameter proposed by Aderibigbe and Rajaratnam (1996), shown in equation (3.4) already considered the effect of tail water depth and is consistent with the combined effect of equation (3.7) and (3.10). According to Aderibigbe and Rajaratnam (1996), when tail water depth is large enough such that E_c<0.35, scour is not initiated.

Sediment Sorting (nonuniformity) The sediment nonuniformity is defined by a sorting coefficient $\sigma = \left(d^{84}/d^{16}\right)^{1/2}$, the larger the σ, sediment is more well-sorted. It is well-known that for nonuniform sediments, the coarse particles impose an armoring effect on the fine particles and hence the overall transport is reduced (e.g., Armanini and Di Silvio 1988). Based on laboratory data, Pagliara et al. (2006) suggest

$$f_5(\sigma) = 0.33 + 0.57\sigma \tag{3.11}$$

Therefore, as the grain size distribution is more uniform, scour depth is larger.

Upstream Velocity A Froude number for upstream velocity is defined as $F_{ru} = U_u / \sqrt{gh}$. As upstream flow velocity increases, more suspended sediments in the scour hole tend to be transported away in the tail water, resulting in a larger scour. In addition, the sediment accumulated in the ridge is easier to be eroded and hence further enhance scour. Based on 40 separate tests, Pagliara et al. (2006) suggest

$$f_6(F_{ru}) = 1 + F_{ru}^{0.5}, \quad \text{for } F_{ru} < 0.3 \tag{3.12}$$

In summary, based on dimensional analysis Pagliara et al. (2006) proposed equation (3.5) to predict maximum equilibrium scour depth. Further using comprehensive laboratory experiments (totally several hundred runs) empirical relations (3.7)-(3.12) are suggested. Because some of the experimental findings presented by Pagliara et al. (2006) are consistent with another study on a similar problem reported by Aderibigbe and Rajaratnam (1996), especially regarding to the Froude scaling and tail water depth, we can conclude that the physical processes involved in plunge pool scour in the idealized laboratory condition are relatively well-established. However, these new research results need to be further tested and calibrated in the field conditions before a new physical-based formulation for erosion under spillway or culvert outlet can be put forward.

3.4 Discussion and Recommendation

3.4.1 Summary on literature survey

Based on the literature survey presented in the previous sections on existing empirical scour formulae for spillways (section 3.2), and process-based laboratory study on plunge pool scour (section 3.3), several remarks can be made:

(1) It is clear that existing scour formulae for spillway are too simple (equations (3.2)-(3.3)) when compared to recent laboratory findings on plunge pool scour. Some of the physics are not included in the exiting scour formulae used for prototype, such as jet air content, sediment sorting and upstream velocity. The important effects of tail water depth and jet impact angle on spillway scour have been acknowledges in some earlier studies but are not incorporated consistently. In addition, most existing scour formulae for prototype are not developed using a complete dimensional analysis. When the number of relevant parameters increases, a formal dimensional analysis,

such as equation (3.5), needs to be adopted to provide a physical foundation for data analysis and to develop new scour formulae.

(2) From a process-based point of view, equation (3.5) used for plunge pool scour could be adopted for prototype erosion problems in the field. However, practically there are several major difficulties that need to be resolved. First of all, all laboratory studies on plunge pool scour use grain diameter as length scale to nondimensionalize local flow forcing (e.g., equation (3.4) or (3.6)). In such as formulation, the Froude number in fact becomes the ratio of two competing forces, namely, the driving force for scour in the numerator and the stabilizing force due to sediment buoyant weight in the denominator, e.g.,

$$F_r = \frac{U}{\sqrt{g'd}} \sim \frac{\text{impenging jet velocity}}{\text{immersed weigt of sedimet}} \sim \frac{\text{driving force}}{\text{stabilizing force}}$$

Using grain diameter as length scale is a plausible way to characterize the stabilizing force for sand or other cohesionless sediments. However, in the field, the sediment bed maybe of rock or fully consolidated clay (cohesive sediment). The stabilizing force for rock or clay soil is determined by intense internal bonding among particles and hence can not be solely described by its immersed weight in water. For cohesive sediment or rock, it is unclear whether one can define a simple parameter to characterize the stabilizing force based on soil strength tests (such as the EFA described in Section 2.4 for bridge scour).

(3) The effect of jet air content has not been addressed in the field condition. Even in the laboratory condition, the air is equally mixing with water in the jet. However, in field condition the air is mixing unequally with water as the jet flow coming down the spillway chute. Therefore, laboratory studies on jet air content as well as the formulae suggested (e.g., equation (3.9)) can only be used qualitatively at this point.

3.4.2 Plan for new field experiments

In order to better understand and further predict erosions below spillway or culvert outlets in the prototype field condition, new field experiments with careful planning are warranted. We recommend here to conduct a set of field experiments at selected sites in the District with several objectives. The main objective is to

- Obtain a complete field data set for erosions below spillways or culvert outlet structures, including bed scour processes, hydrodynamics, flow forcing and upstream flow conditions for at both sandy and muddy sites.

Using newly measured field data, further objectives are to

- Evaluate and calibrate existing scour formulae for erosions below spillway and culvert outlet structure.

- Incorporate several new physics into the existing formulae guided by process-based laboratory studies.

- Test the feasibility of extending the idealized process-based scour formulae to field/prototype condition.

Regarding the main objective, we propose to conduct a more complete field experiment using new sensors and guided by process-based laboratory experimental findings. Prior field experiments are designed to fit simple formulae developed in the earlier years and hence only limited flow and sediment parameters are measured. We believe that recent laboratory studies on plunge pool scour has reveals some important physical processes that need to be further investigated in the field condition and incorporated in predictive formulae in the future. We recommend conducting two set of field experiments, one at a sandy (non-cohesive sediment) site and the other one at a fully consolidated muddy (cohesive sediment) site. The specific locations will be later determined by consulting with the District. In each site, full bed survey at several instants (e.g., 1, 2, 5, 10, 20, 60, 180, 360 minutes) around the scour hole, including the downstream ridge will be recorded. Several acoustic sensors (2- or 3-components ADV) will be used to measure the flow velocity at

A. one or two locations along the jet trajectory to monitor the decay of jet velocity and final impact velocity.
B. one locations upstream of the scour hole to monitor the upstream flow conditions so that the effect of upstream flow condition can be studies (e.g., equation (3.12)).
C. one or two locations downstream of the scour hole, to monitor the flow condition and transport of sediment near the ridge. This will allow us to study the effect of the downstream ridge on the scour hole development.

Other measurements on the jet flow rate, shape (cross-sectional area), impact angle and tail water depth will also be conducted using traditional methods. Depending on District's interest, there is possible to also measure the void ratio (air content) in the jet flow using techniques well-developed in the surf zone processes. This will allows us to further characterize the air content in the jet. In addition, few OBS (optical backscatter sensor) can be deployed to measure the suspended sediment concentration (at same locations with the ADV described in B and C to see if sediment transport is initiated other than the local scour locations. This information will be related to whether the upstream flow is bringing in sediment into the local scour processes and its effect on local scour (i.e., clear-water or live-bed scour).

At the sandy site, samples will be taken to characterize the grain size and sorting coefficients. At the muddy site, it is expected that the problem is more complex. University of Florida has an in-house EFA system similar to that described in section 2.4 (this system at UF is developed by Prof. Sheppard in the Civil and Coastal Engineering Department). Samples of clay will be taken from the field site and tested in the laboratory of UF to characterize the strength of the clay.

The proposed new field experiments will provide the most comprehensive forcing, hydrodynamic and resulting scour and sediment transport processes which will allow us to not just validate/calibrate the existing scour formulae but also develop improved parameterizations on several new physical processes that have not been incorporated in the existing scour formulae but has been demonstrated to be important in the laboratory plunge pool scour experiments.

4 River Bank Erosion

4.1 General

River bank erosion, specifically at locations immediately downstream of the hydraulic structure, is another critical erosion problem in the District. Intense rainfall and flooding events can trigger sudden changes of stream flow intensity and causes bank erosion. On the other hand, land use or stream management, such as over-clearing of river bank vegetation can also trigger bank failure. River bank erosion has conventionally been studied in the context of fluvial geomorphology. Specifically, bank erosion is an important component for predicting river width adjustment in a time-dependent numerical modeling system for river channel morphology (e.g., Darby and Thorne 1996a, b; Nagata et al. 2000; Duan et al. 2001; Darby et al. 2002).

However, our current understanding on the mechanisms involved in bank erosion, specifically the mass failure, remain to be qualitative, despite several pioneering efforts has been put forward to improve our existing quantitative understanding (e.g., ASCE Task Committee 1998a,b, and reference therein). In this report, we will review the major findings in these studies and discuss the difficulties in characterizing the relevant parameters of a natural river system.

The overall stream flow, river morphology and local erosion are one inter-related system. Without considering the local flow disturbance due to hydraulics, one can predict the river bank stability as part of the width adjustment processes. There are existing empirical formulae (e.g., Huang and Warner 1995; Huang and Nanson 1998) that relate the river width with flow discharge, channel roughness, slope and bank material erodibility (i.e., bank strength). These formulae, when compared with measured data, have rather large uncertainties, because they attempt to parameterize a great amount of processes from small- to large-scale. Despite such empirical approaches are too simple for the present purposes, it can provide useful guideline to evaluate the vulnerability specific locations of a river, especially where District's hydraulic structures are installed.

The river bank erosion or the so-called bank stability consists of several sub-processes, including fluvial erosion, bank failure and basal removal (ASCE Task Committee 1998a). The fluvial erosion refers to removal of sediment at the river base and side banks. It is characterized by river flows imposing boundary layer shear on the river bed/bank causing sediment transport through bedload and suspended load processes. The fluvial erosion often results in the steepening of the bank slope and erosion of the bank toe, which eventually induces mass failure of the river bank soil and the river widening. The mass failure depends on the balance between gravitational force and friction/cohesion forces of the soil that resist the down-slope movement. It is generally characterized into planar failure, rotational failure, toppling failure, cantilever failure and more complex piping/sapping type failure (e.g., Darby et al. 2000), which are discuss in more details in the next section. The wasted sediment mass deposited into the toe or basal area can be entirely, or partially transported downstream. This is the basal removal stage. The balance between the removed deposits due to downstream flow and delivered debris

due to bank failure determines the medium- to long-term retreat rate of the bank or the possibility of the next episodic bank failure (Thorne 1982).

The entire erosion processes is further complicated when considering stratified bank soils (layered sand and cohesive soils), vegetation (Thorne et al. 1997), seepage effects, and man-made measures, such as sand piping (Hagerty et al. 1995).

4.2 Bank Mechanics

4.2.1 Fluvial Erosion

Stream flows entrain and transport sediment away from the river base and bank, increase the bank slope, destabilize the bank toe and eventually cause bank failure. Hence, understand fluvial erosion under a given flow and flood hydrograph is the fundamental step toward effective diagnosis for potential failure location or the so-called “hotspot”. In natural river, identifying such local hot-stop is non-trivial and may first require a large-scale numerical computation of fluvial hydraulics (e.g., Darby et al. 2002). In our case, our analysis is more localized to regimes downstream of the hydraulic structures.

However, to quantify fluvial erosion, information on bottom stress distribution over the river base/bank, main flow, secondary flow structures as well as flow turbulence must be obtained. Detailed field measurements or 3D numerical simulation (after model validations) can be utilized to obtain the required information. As described in the previous sections, the bottom stress is used to estimate sediment transport rate using a given sediment transport formula which generally requires specification of empirical coefficients and the critical bottom stress (erodibility). In alluvial bank, the deposition is stratified in a general fining-upward sequence and the erodibility of bank material varies with elevation.

4.2.2 Mass Failure

When significant bank toe is eroded or when the bank slope becomes steepened by fluvial sediment transport processes, episodic mass failure occurs. Mass failure generally relocate bank materials into the near-bank and basal regimes and hence effectively reduces the bank slope and enhance the subsequent stability of the newly-widened bank. The mass failure is a complex process that depends on various flow condition and bank materials and must be analyzed with a local, physically-based approach.

The Planar Failure often occurs for relative steep river banks (Fig 7). The analysis usually involved force balance on a potential failure plane (dashed curve in Fig 7), which gives a critical height for mass failure (e.g., Lohnes and Hardy 1968; Osman and Throne 1988). Recently, more detailed analysis on Planar Failure have been proposed by Darby and Thorne (1996), Darby et al. (2000) and Duan (2006), including some probabilistic approach. From an analytical point of view, Planar Failure has received most attentions compared with other type of failures.

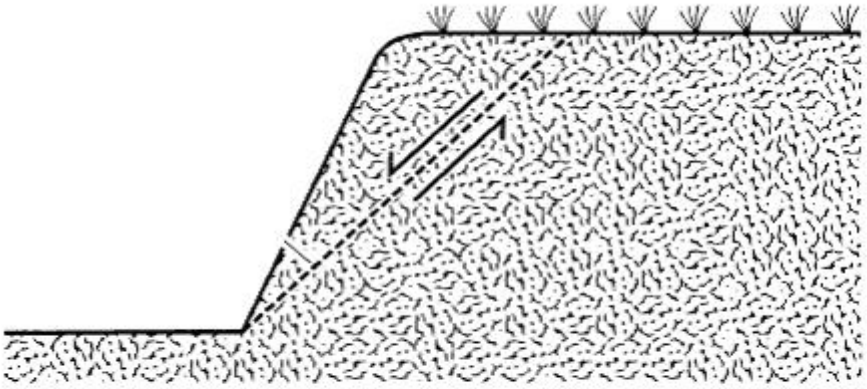

Fig 7. Planar failure occurs for relatively steep bank slope. The dashed line denotes the failure surface (Darby et al. 2000).

For banks with relatively mild slope (<60 degree), the failure slip surface is curved and is defined as Rotational Failure (Fig 8). Rotational failure can be further characterized as a base, toe or slope failure depending on where the failure arc intercepts the ground surfaces (ASCE Task Committee 1998a). Earlier analyses are based on conventional geotechnical procedures (Bishop, 1955). Later, Thorne (1982) developed a stability analysis of the slip circle called Method of Slice, which can be used as predictive guideline.

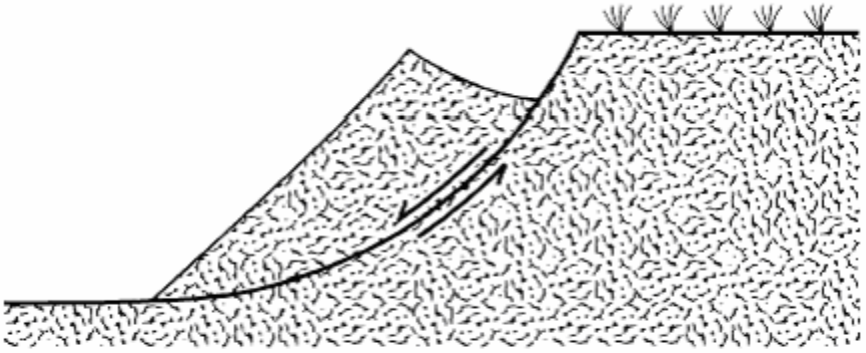

Fig 8. Rotational failure occurs for relatively mild bank slope (Darby et al. 2000).

In a stratified or composite bank (different layers of erodibility soil), the lower layer may be more erodible and undermines the overlying, more erosion-resistant layers. This is called Cantilever Failure. Fig 9 illustrates one such common scenario that a cohesive soil layer is overlying a non-cohesive sand layer. The sand layer is more easily to be eroded away and possibly by fluvial erosion process. Eventually, the overhanging

bank fails due to excess gravity force or moment and tensile shear through shear failure, beam failure or tensile failure depends on the cohesion of the overhanging layer, vegetation, and flow condition. Analysis of Cantilever Failure can be found in Thorne and Tovey (1981).

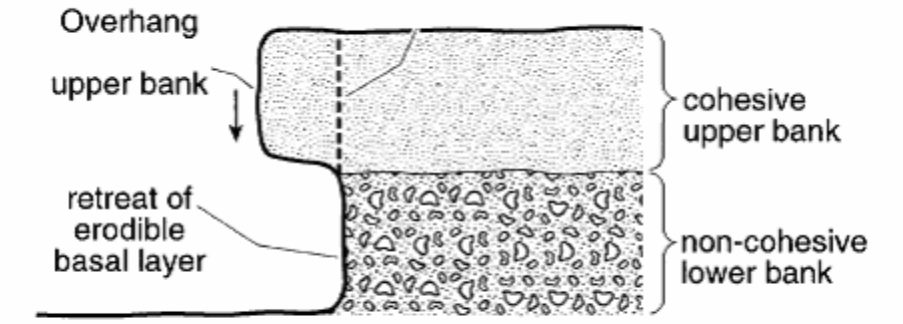

Fig 9. Cantilever Failure occurs in a stratified or composite river bank. The lower bank of cohesionless sand material is more erodible compared to the upper bank made of cohesive soil. The dashed line denotes the failure surface (Darby et al. 2000).

If piping or sipping is introduced in the sand bank. The sand layer is more erodible or more importantly destabilized by seepage outflow. In this case, the sand layer can also undermine the fine-grained upper soil layer (Hagerty 1991). This type of bank failure is more specific with respect to the site condition but shall not be overlooked.

4.2.3 Basal Removal

The failed bank sediment once deposited into the toe or basal area can be entirely or partially transported downstream. As described in the previous section, mass failure can be considered as an episodic event that changes the river geomorphology to another equilibrium state as far as the bank stability is concerned. The rate at which the deposited sediment to be eroded away determines how fast the next bank failure may occur. If the stream flow is not able to remove the debris downstream (or there are upstream supply of sediment), a berm or bench of failed material develops and bank is stable (Thorne 1982). Therefore, despite mass failure is a local process, its prediction, especially at more long-term scale, is closely related to the long-term fluvial sediment transport and geomorpology.

As was noted in ASCE Task Committee (1998a), for river banks of composite layer or man-made channel (such as piping), the basal removal guideline may not be useful. The process in composite bank is often more complicated because the upper bank

mass failure can continuous occur even when basal sediment or bank toe is stable (Hagerty et al. 1991).

4.2.3 Other Critical Processes

Two crucial, but less understood processes controlling bank erosions are discussed in this section.

Seepage Effect: The effects of pore-water movement within the river bank are important to bank erosion by is often overlooked (ASCE Task Committee 1998a). Seepage effects is the most prevailing during and following a high stream flow event. As flood water rises, the seepage flow enters the banks due to enhanced hydraulic head. However, as the flood recedes the hydraulic gradient reverses and drives the seepage flow out of the banks and into the stream. During the bank drainage stage, the outflow seepage destabilizes the bank sediment and transports sediment away from the bank. The seepage effect may contribute to lots of bank failure event during inundation of bank soil followed by rapid drops of water level after flooding. For bank of composite layer of sediment, seepage effect is of special concern because the permeability of sand layer is much higher then the overlying cohesive soil layer.

Vegetation Effect: The effects of vegetation on bank erosion are complex and poorly understood (ASCE Task Committee 1998a). Earlier studies (e.g., Carson and Kirkby 1972; Smith 1976) suggest that well-vegetated bank is one or two order of magnitude more stable than the unvegetated banks due to for example, restrain of soil by strong root system and reduced near-bank flow velocity. However, more recent studies on bank vegetation conclude that vegetation may have either a positive or negative effect on bank stability (Thorne et al. 1997). For example, the roots may invade cracks of the soil or rock and weaken the soil structure, or the weight of the vegetation itself may significantly enhance the gravitational force and destabilize the bank. It is generally believe that the effect of vegetation on bank stability can not be well-understood until other critical effects mentioned before are first quantified (Darby and Thorne 1996b).

4.3 Recommendation

River bank erosion, specifically the mass failure process is highly complex and of episodic nature. The complexities can be appreciated simply from the various failure types discussed in section 4.2. A complete study requires careful consideration in several key factors including the variability in soil properties (e.g., cohesion, permeability), composite nature of the bank (see Fig. 9), the vegetation effect and the turbulent flow fields near the bank (including secondary flow), etc. Therefore, to study the river bank erosion problem downstream of District's hydraulic structure, we recommend a two-stage study.

The first stage shall focus on a bulk survey at selected sites but without getting into the detailed flow structure and sediment measurements. Consultation with District's scientists/engineers shall start early in the investigation to identify several key locations downstream of District's hydraulic structures. A preliminary survey will be conducted at these sites, which includes

(1) Bathymetry survey downstream of the hydraulic structure. Acoustic sonar survey will provide comprehensive background information, such as the bank slope and more importantly the existing erosion condition at the bank toe. As described in section 4.2.1, the bank slope and the stage of bank toe erosion is the most important syndrome for potential mass failure.

(2) Historical hydrograph information on water depth and stream flow velocity during flooding condition. Few point measurements of flow velocity around the river bank downstream of the hydraulic structure are also necessary in order to estimate the local accelerated flow velocity (compared to the flow velocity far from the structure) due to the presence of hydraulic structure.

(3) Soil sampling at the river bank, including coring. This includes identifying the cohesion of the soil (cohesive sediment) or the average grain size (non-cohesive sediment) and the characterization of the layer structure of the bank. As shown in Fig 9, cohesive sediment layer overlying a sandy layer can cause cantilever failure.

The preliminary survey can assist us to obtained critical background information on the selected site and the vulnerability of the river banks that are useful for the District.

The second stage of the field study focuses on detailed measurement at one selected site. As discussed in section 4.2.3, the seepage effect on bank erosion and mass failure is the least studied area (ASCE Task Committee 1998a). However, there is no doubt that the seepage effect is a crucial mechanism determining the bank failure processes due to numerous evidences that bank failures often take place soon after the inundation of bank soils followed by rapid decrease of water level. Therefore, we suggest to studying the seepage effects on bank erosion as the major focus of the field investigation.

The first-stage preliminary survey results will provide the most appropriate site for detailed study and the background information on the selected site. Detailed measurements on bathymetry, flow velocity field, sediment suspension and seepage flows around smaller area downstream of the hydraulic structure will be conducted during a regular stream flow condition (before flood), a flooding condition and waning condition (after flood). Specific quantities that will be measured are

(1) Three-dimensional flow velocity measurement near the river bank, including secondary flow structure will be measured during regular flow condition. This will assist identifying the general bottom stress distribution and erosion pattern (such as bank toe erosion) without (before) the mass failure. We plan to deploy Acoustic Doppler Current Profiler to measure the stream flow velocity. Several three (or two) component ADV will be deployed to measure high frequency turbulent flow and secondary flows.

(2) Seepage velocity and pore pressure measurements within the river bank will be conducted. Detailed in-situ sampling will be used to measure the permeability of the soil in the bank. (Mark, please say more)

(3) Detailed bathymetry survey will be conducted before and after the flooding event (and possibly the bank failure event).

(4) We will conduct CFD numerical modeling to characterize more detailed 3D flow structure around the bank and seepage flow within the river bank.

Through detailed measurement, we will be able to understand the fluvial erosion processes around the bank, the seepage flow in the bank at different stages of the stream flow and the bathymetry response of the river bank and base. Measure flow and soil parameters will be used to test several existing analysis on mass failure (e.g., Throne 1982; Osman and Throne 1988).

References

Aderibigbe, O. O., and Rajaratnam, N., 1996. Erosion of loose beds by submerged circular impinging vertical turbulent jets, *J Hydraul. Res*., 34 (1), 19-33.

Armanini, A. and Di Silvio, G. 1988. A one-dimensional model for the transport of a sediment misture in non-equilibrium conditions, *J Hydraul. Res*., 26 (3), 275-292.

ASCE Task Committee on Hydraulics, 1998a, River width adjustment. I: processes and mechanisms, *J. Hydraulic Eng*., 124(9), 881-902.

ASCE Task Committee on Hydraulics, 1998b, River width adjustment. I: modeling, *J. Hydraulic Eng*., 124(9), 903-917.

Azmathullah, H. Md., Deo, M. C., and Deolalikar, P. B., 2005. Neural networks for estimation of scour downstream of a ski-jump Bucket, *J. Hydraulic Eng.*, 131(10), 898-908.

Azmathullah, H. Md., Deo, M. C., and Deolalikar, P. B., 2006. Estimation of dcour below spillways using neural networks. *J Hydraul. Res*., 44 (1), 61-69.

Barbhuiya A. K., and Dey, S., 2004. Local scour at abutments: A review, *Sadhana*, 29(5), 449-476

Briaud J.-L., Ting, C. K., Chen, H. C., Gudavalli, R., Perugu S., Wei, G., 1999. SRICOS: Prediction of scour rate in cohesive soils at bridge piers. *J Geotech. Environ. Eng.* 125(4), 237-246.

Briaud J.-L., Chen, H. C., Li, Y., Nurtjahyo, P., Wang, J. 2004. Pier and contraction scour in cohesive soils, National Cooperative Highway Research Program Report 516.

Canepa, S., and Hager, W. H., 2002. Effect of jet air content on plunge pool scour, *J. Hydraulic Eng.*, 129(5), 358-365.

Chee, S. P., and Kung, T., 1983. Theoretical configurations of scour basins. *Proc. 6th Canadian Hydrotechnical Conf.*, Ottawa, 569-579.

Darby, S. E., and Thorne, C. R., 1995. Developoment and testing of riverbank-stability analysis, *J. Hydraulic Eng*., 122(8), 443-454.

Darby, S. E., and Thorne, C. R., 1996. Numerical simulation of widening and bed deformation of straight sand-bed rivers. I: Model development. *J. Hydraulic Eng*., 122 (4), 184- 193.

Darby, S. E., Gessler, D. and Throne, C. R., 2000. Computer program for stability analysis of steep cohesive bank, *Earth Surf. Process Landform*, 25, 175-190.

Darby, S. E., and Alabyan, A. M., and Van de Wiel, M. J., 2002, Numerical simulation of bank erosion and channel migration in meandering rivers, *Water Resource Res.*, 38 (9), 1163.

Duan, J. G., 2005, Analytical approach to calculate rate of bank erosion, J Hydraulic Eng., 131(11), 980-990.

Ettema, R., 1980, Scour at bridge pier. Rep. No. 216, School of Engineering, University of Auckland, Auckland, New Zealand.

Graf, W. H., 1998 Fluvial Hydraulics: Flow and Transport Processes in Channels of Simple Geometry, John Wiley & Sons.

Osman, A. M., Throne, C. R., 1988. Riverbank stability analysis. I: Theory, *J. Hydraulic Eng.*, 114(2), 134-150.

Hagerty, D. J., Spoor, M. F., and Parola, A. C., 1993, Near-bank impacts of river stage control, *J. Hydraulic Eng*, 121 (2), 196-207.

Hsu, T-J, Jenkins, J.T. and Liu, P. L.-F., 2003. On two-phase sediment transport: dilute flow, *J. Geophys. Res., 108(C3), 3057*.

Hsu, T-J, Traykovski P. A., and Kineke, G. C. 2006b. On modeling boundary layer and gravity driven fluid mud transport, submitted to *J. Geophys. Res*.

Huang, H. Q., and Nanson, G. C., 1998, The influence of bank strength on channel geometry: an integrated analysis of some observations, *Earth Surf. Process Landform*, 23, 865-876.

Kubos,

Martin, R. B. F., 1975. Scouring of rocky riverbeds by free-jet spillways. *Water Power Dam Constr*. 27 (4), 152-153.

Mason, P. J., Arumugam, K., 1985. Free jet scour below dams and flip buckets, *J. Hydraulic Eng.*, 111(2), 220-235.

Mason, P. J., 1989. Effect of air entrainment on plunge pool scour, *J. Hydraul. Eng.*, 115(3), 385-399.

Melville, B. W., 1997. Pier and abutment scour: integrated approach, J. *Hydraul. Eng.*, 123(2), 125-136.

Melville, B.W., and Chiew, Y.-M., 1999. Time scale for local scour at bridge pier, . *Hydraul. Eng., 125(1), 59-65*.

Mueller, D. S., and Wagner, C. R., 2005. Field observations and evaluations of streambed scour at bridges, Federal Highway Administration, FHWA-RD-03-052.

National Bridge Inventory, 1997. Bridge management branch, Federal Highway Administration, Washington, D.C.

Nagata, N., Hosoda, T., Muramoto, Y., 1998. Numerical analysis of river channel processes with bank erosion, J. Hydraulic Eng., 126(4), 243-252.

Pagilara, S., Hager, W. H., and Minor, H.-E., 2006. Hydraulics of plane plunge pool scour, *J. Hydraul. Eng.,* 132 (5), 450-461.

Richardson, E.V., and Davis, S.R., 2001, Evaluating scour at bridges (4th ed.): Washington, DC, Federal Highway Administration Hydraulic Engineering Circular No. 18, FHWA NHI 01–001,

Ross, M. A., and Mehta A., 1989, On the mechanics of lutoclines and fluid mud, *J. Coast. Res.*, special issue 5, 51-61.

Schoklitsch, A. 1935. *Stauraumverlandung und Kolkabwehr [Reservoir sedimentation and scour prevention]*. Springer, Vienna.

Sheppard, D. M., Odeh, M, Glasser T., 2004. Large scale clear-water local scour experiments, *J. Hydraul. Eng., 130 (10),* 957-963.

Sheppard, D. M., and Miller W., 2006. Live-bed local pier scour experiments, *J. Hydraul. Eng.,* 132(7), 635-642.

Shirole, A. M., and Holt, R. C., 1991. Planning for a comprehensive bridge safety assurance program, Transp. Res. Rec. NO. 1290, Transportation Research Board, Washington, D. C.

Trowbridge, J. H., and Kineke, G. C., 1994, Structure and dynamics of fluid mud on the Amazon continental shelf. *J. Geophys. Res.*, 99(C1), 865-874.

Veronese, A. 1937. Erosioni di fondo a valle di un scarico [bottom edrosions downstream of a dam], *Annali dei Lavori Pubblici*, 75(9), 717-726.

Wu, C. M., 1973. Scour at downstream end of dams in Taiwan. *Proc. Int. Symp. on River Mechanics*, Bangkok, Vol. 1, A 13, 10-6.

Complex flows through culvert structures by CFD modeling

Basic Information

Title:	Complex flows through culvert structures by CFD modeling
Project Number:	2006FL146B
Start Date:	3/1/2006
End Date:	2/29/2008
Funding Source:	104B
Congressional District:	6
Research Category:	Engineering
Focus Category:	Models, Surface Water, None
Descriptors:	
Principal Investigators:	Tian-Jian Hsu

Publication

FLOW AROUND CULVERT STRUCTURES

Celalettin Emre Ozdemir and Tian-Jian Hsu

Civil and Coastal Engineering
University of Florida

Summary

Culvert is a control structure to convey streamflow through obstructions such as highway embankments. Culvert structures are important because they are control structures and act as boundary condition for large scale events such as flood mapping and mitigation. With the growth of environmental concerns, more accurate prediction on flow through culverts structures becomes necessary in the evaluation of, for example, the contaminants conveyed through it. Therefore the design and the discharge evaluation has become an important issue. Existing rating curves for flow through culverts contain empirical parameters which makes these evaluations with more stringent criterions questionable. With the advances in the computer technology and turbulent flow modeling, it possible to use computational fluid dynamics (CFD) as a tool to evaluate 3-D environmental flows with a variety of turbulence closures. However, CFD's potentials and limitations as a design tool for the flow field around the culvert structures have not been evaluated yet.

In this study, we report a literature survey on the culvert hydraulics for ungated and gated culverts including its theory, field and experimental studies. The applicability of CFD has been evaluated on the basis of what kind of errors it might contain with specific focus on turbulence modeling. Finally, we recommend an integrated approach, using CFD as a primary tool, with an aim to improve upon the existing algorithms to generate rating curves:

Considering the length scale of the problem, we recommend to utilize Reynolds-averaged approach as our primary tool to model the 3D flow field through the culvert structure. The CFD model results can directly resolve detailed flow field and energy dissipation in various components of the culvert structure. The CFD model results can be further analyzed to calibrate various empirical coefficients in the 1D hydraulics equations for culverts, which are difficult to measure directly in the field. The new approach proposed here may improve upon the existing rating curves generated based on lumped method.

From the view point of turbulence modeling, there are concerns regarding the accuracies of the existing Reynolds-averaged approach for complex flow condition. We acknowledge this problem and propose to conduct several detailed turbulent flow simulation using Large-eddy-simulation (LES) to evaluate the accuracy of various turbulence closure scheme in the Reynolds-averaged approach.

Accurate field data remains to be necessary in any model development study. Existing field data obtained by the District is useful for our model-data calibration at the overall culvert system level. However, more detailed flow field data, including turbulence quantities, is highly desirable for a reliable model development.

1.Introduction

A culvert is a conduit that evacuates the streamflow through flow obstruction such as roadway and embankment. Although designed under several considerations such as service time, economy and structural stability, most importantly from the hydraulics point of view it should convey the flow as efficient as possible. Hence within the design limits, flooding at the upstream of the culvert can be avoided. Different types of culverts with various shapes (e.g., elliptic to box culverts, Normann et al. (1985)) and hydraulic features such as tapered inlets are employed in the design process.

Apart from its practical purposes described above, culverts are control structures of a large-scale fluvial system. In other words we can obtain discharge-headwater relationship, i.e. rating curves in the culverts. The rating curves are critical parameterizations of local fluid flow processes in estimating the extreme events in a large scale river system such as flood mapping and flood mitigation. Therefore, the correct estimate of the relation between the headwater and the discharge is critical. For example to determine the flood map of the Lower Deer Creek, numerical study was carried out by using UnTRIM code (MacWilliams et al. 2004). In the aforementioned study there were three culvert boundaries in addition to five others which are either hydraulic structures or gauging stations. The necessary rating curves are developed by means of HEC-RAS using 1-D hydraulic equations. Any errors pertaining to these calculations might propagate throughout the river system. Therefore, the accuracy of HEC-RAS calculations which utilizes the FHWA (Federal Highway Administration) formulae affects the reliability of the large scale computational results.

Existing studies on the flow around the culverts are mostly design oriented. Most of these studies were classical modeling of culverts without the need to resolve the 3-D and unsteady turbulent flow characteristics. Though recently there are some model studies to seek for answers to the fish passage design in the culvert and the performance of the culverts against lock and dam operation. This report is organized as follows. Section 2 reviews the classical approach and design of culvert structures for both gated and ungated and the lessons learned from them. The third section discusses using the computational fluid dynamics (CFD) approach and its reliability with respect to sources of errors and applicability to complex domains. This report is concluded with some recommendations.

2. Theory of Culvert Flow

The flows through the culverts are affected by the flow conditions at the inlet, geometry of culvert, headwater (HW), tailwater and the flow conditions at the outlet (Gonzalez, 2005). Taking all these into account the flow conditions can be classified as inlet controlled flow and outlet controlled flow. This classification is made on the basis of the following fact: if the control section is at the end of the inlet, it is called as inlet controlled flow; while if the control section is at the outlet end or further downstream it is outlet controlled flow. Possible flow patterns for each case are illustrated in Figure 1. According to Figure 1, there is a critical flow formation at the inlet for inlet controlled flow. On the other hand, for the outlet controlled flows there is either a critical flow formation at the outlet or the flow is submerged at both ends.

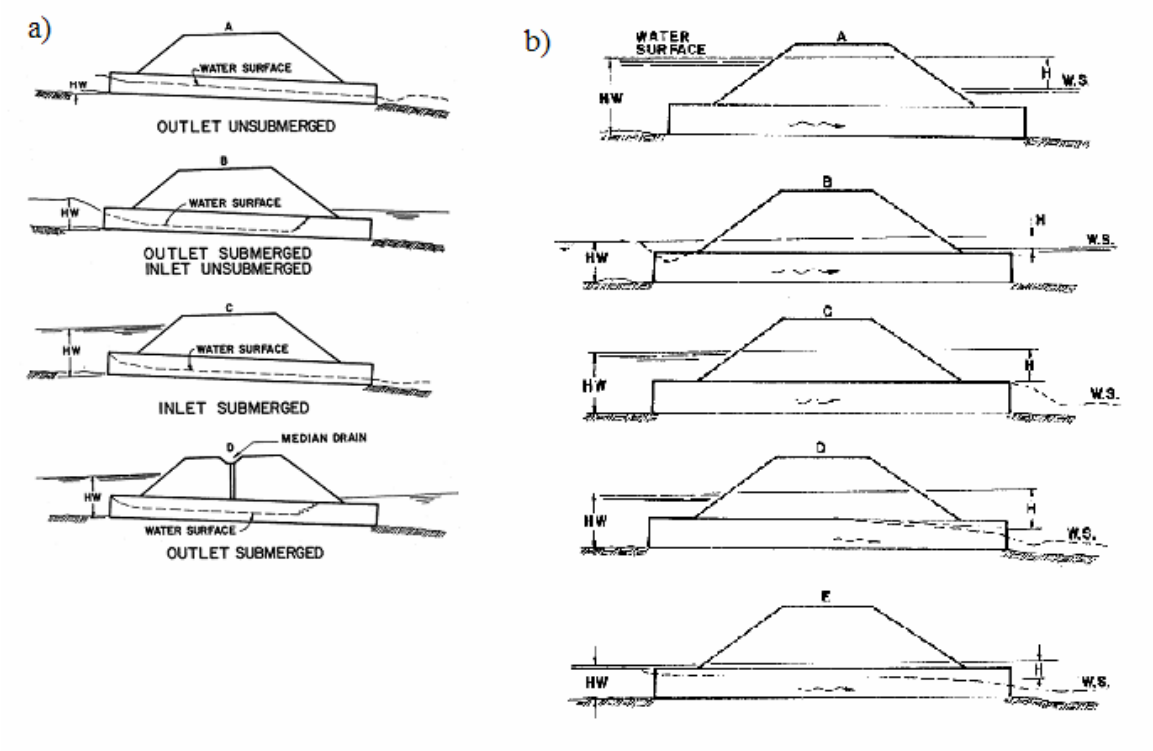

Figure 1 Inlet (a) and the outlet (b) controls of uncontrolled free culverts (adopted from Normann et. al., 1985).

For the inlet control with upstream unsubmerged, flow is treated as the flow through a weir as the flow becomes critical at the inlet. The flow becomes like a weir flow in other words the discharge is proportional to the $HW^{3/2}$. On the other hand, for inlet controlled flow with upstream submerged, flow becomes like an orifice i.e. discharge is proportional to $HW^{1/2}$. For the outlet control the flow is calculated on the basis of the energy balance equations and again the discharge is proportional to $HW^{1/2}$.

Equations (1.1) to (1.3) are used in inlet control culverts with equation (1.3) specifically used for the submerged inlet condition.

$$\frac{HW_i}{D} = \frac{H_c}{D} + c[\frac{Q}{AD^{0.5}}]^2 + Y - 0.5S \quad (1.1)$$

$$\frac{HW_i}{D} = K[\frac{Q}{AD^{0.5}}]^M \quad (1.2)$$

$$\frac{HW_i}{D} = c[\frac{Q}{AD^{0.5}}]^2 + Y - 0.5S \quad (1.3)$$

where

D : interior height of the culvert barrel,ft
H_c : specific head at critical depth
Q : discharge through the culvert
A : full cross-sectional area of the culvert
S : culvert barrel slope
K, M, c, Y: constants dependent on the shape and entrance.

$$Z_3 + Y_3 + \frac{\alpha_3 V_3^2}{2g} = Z_2 + Y_2 + \frac{\alpha_2 V_2^2}{2g} + H_L \quad (1.4)$$

where

Z_3 : Upstream invert elevation of the culvert
Y_3 : The depth of water above the upstream culvert inlet
V_3 : The average velocity upstream of the culvert
α_3 : The velocity weighting coefficient at the upstream of culvert
g : gravitational acceleration
Z_2 : Upstream invert elevation of the culvert
Y_2 : The depth of water above the upstream culvert inlet
V_2 : The average velocity upstream of the culvert
α_2 : The velocity weighting coefficient at the upstream of culvert
H_L : Total energy loss through the culvert

Examples using these relations between headwater and discharge are calculated and performance curves are plotted in Figure 2. These curves are widely used in the design of the culverts. For both upstream control and downstream control culvert flow computations employ empirical coefficients i.e. the use of *K, M, c, Y* in the upstream control culvert flow and use of Manning's empirical coefficients in the computation of H_L. For the gated culverts as we shall see there are empirical coefficients that vary with

the shape and entrance of the culverts in order to accurately calculate the head loss. This raises the question about the reliability and robustness of the existing performance curve equations, especially when more stringent design criterions are expected to be met due to environmental concerns.

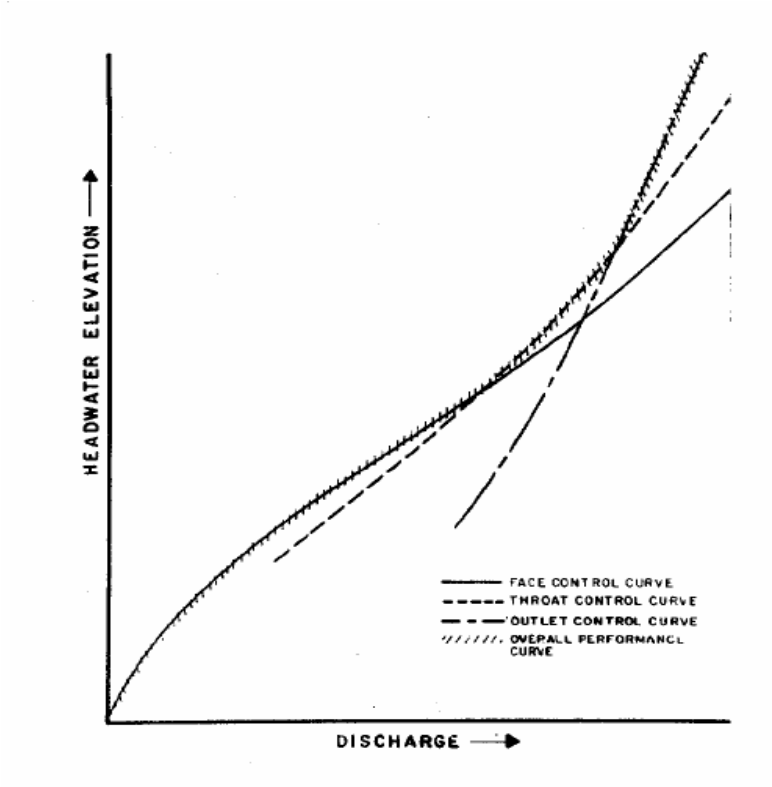

Figure 2 Culvert performance curve without overtopping (adopted from Normann et al. 1985).

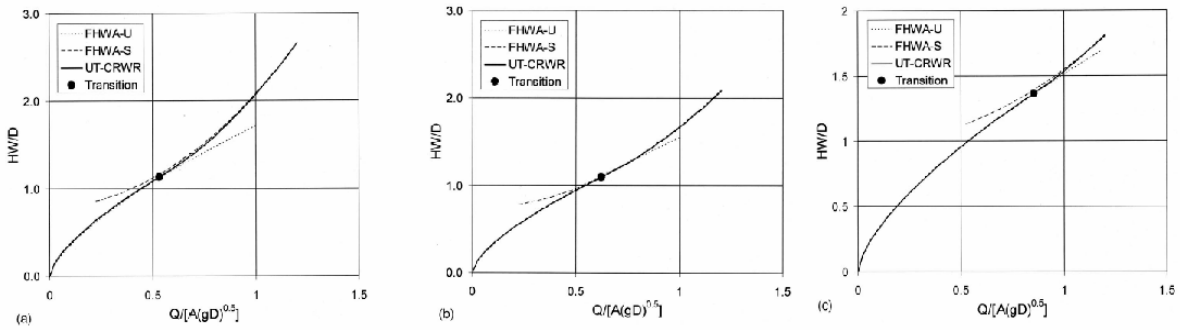

Figure 3 Reevaluation of the performance curve by Charbeneau et al. (2006).

There are studies attempt to reduce the number of empirical coefficients. In Charbeneau et al. (2006), the number of empirical coefficients is reduced from four to two, including the contraction coefficient and the soffit contraction coefficient. The HW relation from culvert performance and discharge is equalized and solved for HW. Also the singular point at the transition between the submerged and unsubmerged inlet control flow is eliminated as the derivatives of both relations are found to be equal from the aforementioned relation, giving a more flexible tool for design purposes.

Rating algorithms for *gated* culverts are scarce in the literature. One can determine the flow by simplifying the flow a 1-D basic fluid flow. Gonzalez (2005) presented the pressurized fluid flow through two types of gated culverts (Figure 4). In the first type (Figure 4A), the flow is governed by the gate; while in the second type (Figure 4B) the flow is controlled by the weir erected at the upstream of the gate. In the first type, the discharge coefficient is represented in terms of loss coefficients and ratio of the consecutive cross sectional area ratios as well as the frictional losses throughout the culvert pipe which is obtained as a result of Manning's formula proposed by Yen (1992). In the second type the discharge coefficient, due to hardships in monitoring the flow throughout the flow the estimation is obtained based on the weir flow equation. In other words, the discharge coefficient is expressed in terms of the difference between HW and weir elevation at the upstream, weir crest length in the transverse direction.

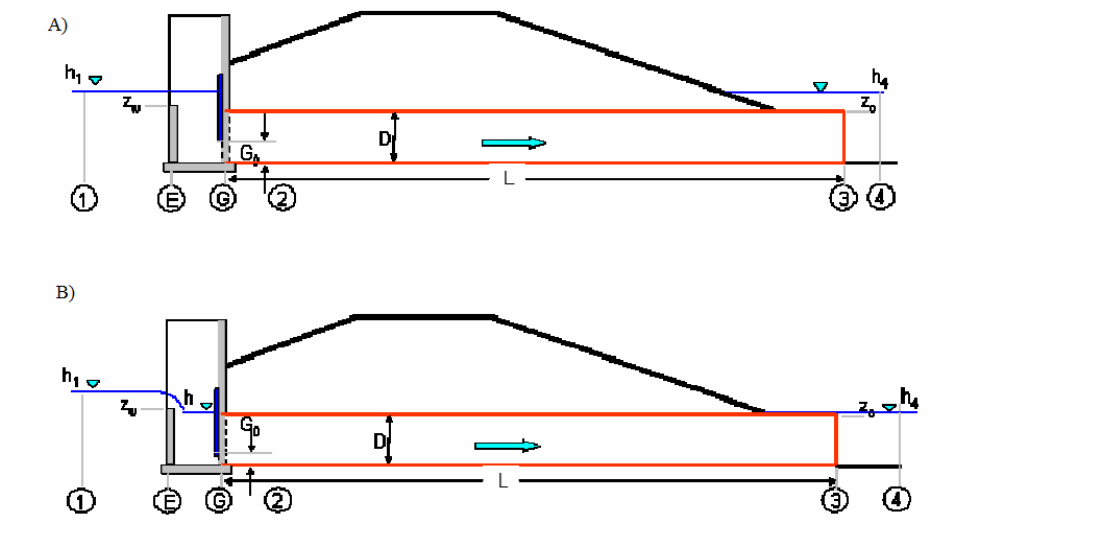

Figure 4 Two flow configurations for pressurized gated culvert flow (adopted from Gonzalez, 2005)

The studies so far, which are primarily based on simplified 1-D equations and field studies, are primarily led by the hydraulics design considerations. The main objective is to find simple relations to make the design time minimal and keeping the results reasonable. However as previously mentioned, any error in the culvert flow may propagate in larger scale and for environmental concern, one requires more stringent

level of accuracies in the culvert designs. The contribution potential from 3-D flow analysis has not been assessed for culvert flow in order to minimize and evaluate the error introduced by these simplified equations. In addition, the likelihood of scour, which is a common problem around culverts, can be determined by 3-D turbulent characteristics of the flow and the resulting bed shear stress. Very little has been done to determine the detailed turbulent flow characteristics of culvert flow. Day (1997) investigated flow turbulence at the inlet of a pipe culvert by laboratory experiments. The flow field was measured by means of electromagnetic current meter. Averaged flow field and the turbulent intensity were evaluated near the inlet.

Gonzalez (2005) reports results based on field experiments of flow through culverts structures. The flow is measured by monostatic acoustic Doppler flow meters (ADFMs). Its contrivance is based on two pairs of transducers one to estimate the flow depth and the other to estimate the flow velocities. As its name implies the flow velocity is estimated by the shift in the signals created by the transducer. Afterwards, this study combines the flow data with the depth data and utilizes the no slip boundary condition at the wall.

3.CFD Applications

More accurate and physical-based approaches for developing rating curves require detailed analysis that directly resolves the 3D flow field in the culvert structure. Comprehensive 3D flow analysis can be accomplished by detailed flow measurements and/or utilizing Computational Fluid Dynamics (CFD) as a tool. While detailed flow measurements are essential but often time-consuming and expensive, flow analysis based on CFD has been becoming an effective and economical design tool in various industrial and engineering applications. In this study, we believe it is possible to use CFD analysis to resolve 3D fluid flow and the dissipation around culverts and hence improves upon the rating algorithms based on simple 1D flow equations. The turbulence created at the upstream of the culvert combined with the irregularities of in the flow field has a unique effect in the performance of a culvert. Although in the classical evaluation, irregularities are included in the discharge equations through empirical coefficients, their robustness and accuracy are of question. Therefore it is the authors' belief that it is highly potent that CFD analysis can improve the accuracy and reliability of the discharge coefficient in the rating curves.

Nearly all environmental flows are turbulent flows. Therefore, errors resulted from CFD modeling/simulation for environmental flow are due to the combination of 1) modeling errors, 2) discretization errors, 3) iteration errors and 4) programming and user errors. These aspects are discussed in the following sections.

3.1.Modeling Errors

Turbulent flow is difficult to model because of its random, stochastic and unsteady nature. The most accurate solution of turbulent flow is the direct numerical simulation (DNS) as it solves all the scales of turbulent motion. The use of DNS will not yield any modeling error and hence it is often utilized to calibrate and validate other turbulence modeling approaches (e.g., RANS, or LES approaches). The practical use of DNS is limited due to its requirement of high spatial and temporal resolution and hence CPU time. The spatial resolution should be smaller than the Kolmogorov length scale to resolve the smallest eddy scale. In a three-dimensional space this implies computational requirement that scales with $Re^{9/4}$ (e.g., Pope 2000). In addition, one often needs to compute DNS for significant length of time in order to obtain meaningful turbulence statistics. Hence, currently the use of DNS is limited to lower Reynolds number flow (Bhagangar et al. 2002).

For hydraulics application, the most popular approach is based on solving Reynolds-Averaged Naviers-Stokes (RANS) equations with turbulence closures. The RANS approach is efficient. However, the fundamental assumption of RANS approach implies parameterizations on all the scales of turbulence and hence the inherited turbulence closure problems require careful consideration. Recently, the improved computer power allows using Large-Eddy Simulation (LES) approach for some hydraulic and fluvial applications (e.g., Keylock et al. 2005). Comparing with the RANS approach,

LES is more accurate in turbulence closure because most of the anisotropic energy containing turbulent eddies are directly resolved and the sub-grid closure scheme is only required for small scales, which is easier to parameterize. Despite the computational requirements in LES remains significant for high Reynolds number hydraulics flow, it is possible to utilize LES to conduct few detailed simulations to provide flow databases in order to calibrate the turbulence closure scheme in the RANS approach (e.g., Rodi et al. 1997). In this report, we primarily focus on RANS approach and its turbulence closures for engineering applications. However, we will also pursue evaluating the RANS approach using LES and small-scale laboratory experimental data.

The eddy viscosity closure is the most popular scheme for solving the Reynolds Averaged Navier-Stokes equations. In the RANS approach, the instantaneous, intermittent turbulence is averaged out. Although this causes loss of information in the instantaneous flow field, it gives the overall statistical quantities of turbulence which is in fact is the more useful information for most practical engineering applications. Utilizing the eddy-viscosity hypothesis, the most popular model for second order closure scheme is the k-ε model. Turbulent kinetic energy k and its dissipation rate, ε, are the model parameters to calculate the eddy viscosity and the preceding parameters are closed by means of the prognostic equations given as follow:

$$\frac{\partial}{\partial t}(\rho k)+\frac{\partial}{\partial x_i}(\rho k u_i)=\frac{\partial}{\partial x_j}[(\mu+\frac{\mu_t}{\sigma_k})\frac{\partial k}{\partial x_j}]+G_k+G_b-\rho\varepsilon-Y_M+S_k \tag{2.1}$$

$$\frac{\partial}{\partial t}(\rho \varepsilon)+\frac{\partial}{\partial x_i}(\rho \varepsilon u_i)=\frac{\partial}{\partial x_j}[(\mu+\frac{\mu_t}{\sigma_\varepsilon})\frac{\partial \varepsilon}{\partial x_j}]+C_{1\varepsilon}\frac{\varepsilon}{k}(G_k+C_{3\varepsilon}G_b)-C_{2\varepsilon}\rho\frac{\varepsilon^2}{k}+S_\varepsilon \tag{2.2}$$

In these equations, G_k represents the generation of turbulence kinetic energy due to the mean velocity gradients. G_b is the generation or damping of turbulence kinetic energy due to buoyancy, Y_M represents the contribution of the fluctuating dilatation in compressible turbulence to the overall dissipation rate, $C_{1\varepsilon}$, $C_{2\varepsilon}$, and $C_{3\varepsilon}$ are constants, σ_k and σ_ε are the turbulent Prandtl numbers for k and ε, respectively. S_k and S_ε are the source terms.

The drawbacks of this model can be stated as follows: 1) The eddy viscosity hypothesis itself, which assumes complete analogous to Newtonian viscous fluid, is questionable. Empirical damping function is often used in calculating eddy viscosity. 2) The transport equation of ε is proposed according to several additional assumptions, including high Reynolds number flow. 3) There exist additional source terms in the prognostic equations of both ε and k, 4) Appropriate boundary condition for ε is not always obvious.

Damping functions used in k-ε model is used to mimic the effect of the molecular viscosity such as in the case of near wall low Reynolds number flow. In most applications, the near wall regime is not resolved, instead the model is forced by

parameterized wall-functions. Although it might seem disadvantageous for the reliability of the solution, the review by Patel et al (1985) demonstrate that careful use of the so-call low Reynolds number modifications to k-ε model renders results that agrees reasonably well with the measured data (or LES results). Recently, Goncalves and Houdeville (2001) present the robustness of the wall functions over computational grids ranging from coarse to refined ones.

For different types of flows, the model coefficients in the k-ε model are not necessarily unique. One reason is the existence of uncertainties in the experimental data to obtain these coefficients, which are usually conducted in highly simplified and idealized conditions. Another reason is, complementary to the first reasoning, the dependence of these coefficients to each other in complex flow. The first reasoning is explained in more detail as the following. Each parameter in the equations controls specific transport mechanism and can be obtained by simplified flow conditions that isolate the desired mechanism. For example, $C_{\varepsilon 2}$ can be obtained from the decaying homogeneous turbulent flow. In practice, this is approximated as grid generated turbulence as the other terms vanish in the prognostic equation of the dissipation. However the result of the experimental data is not unique but falls onto a range of values. Although after several experiments and trials for different type of flows, $C_{\varepsilon 2}$ is found to be 1.83, on the physical basis it is not possible to assign a unique value. Another coefficient, $C_{\varepsilon 1}$ is the coefficient responsible for the dispersion of the free shear layers. The growth rate for homogeneous flows is found to be a function of $C_{\varepsilon 2}$- $C_{\varepsilon 1}$ which shows the dependency of both parameters. If the values of $C_{\varepsilon 2}$ and $C_{\varepsilon 1}$ have uncertainties, subsequent calibrations on other parameters are also inevitably uncertain. The experiment of $C_{\varepsilon 1}$ is found to fall onto a range with an upper limit 1.51. However 1.44 gives reasonable results (Durbin and Reif, 2000). Also in the case of high Re, C_{μ} is not calculated correctly although it does not change the mean flow field as the log-layer eddy viscosity is calculated correctly (Durbin and Reif, 2000).

The k-ω model is similar to the k-ε model and ω is the ratio of the dissipation rate to the TKE of turbulence, which has a dimension of inverse of time. Although very similar at glance, the difference between these two parameters becomes obvious in the log layer of the wall for wall bounded flows. For non-homogeneous flows a diffusion term should exist in addition to the homogeneous condition. However, the addition of diffusion term to the homogeneous solution fails as it results in a negative diffusion of time in the log layer. The use of a (inversed) timescale for the second parameter in the two-equation closure might be an alternative to resolve this problem. For this, the use of ω becomes a plausible alternative because ω represents the inverse of a timescale. In fact, one can re-exam this issue by deriving the ε-equation from the ω-equation. The resulting ε-equation has an extra cross-diffusion term as compared to the original ε-equation (e.g., Wilcox 1993).

Despite the time-scale concept used of k-ω may be more meaningful, the k-ω model is not free of errors. Its major drawbacks are 1) it over predicts the shear stress in adverse pressure gradient boundary layer (Menter, 1994) 2) it produces unreliable results in free shear layer flows hence not sensitive to free-stream conditions. Menter (1994)

argued that basic shortcomings of the k-ω can be partly avoided by using two layer approach i.e. use k-ω model in near wall region and k-ε model elsewhere which is also known as SST k-ω model.

RNG based k-ε model is first proposed by Yakhot and Orszag (1986).This model is based on the assumption that the length scales for small eddies are approximated by the Kolmogorov energy spectrum. In the aforementioned model turbulence is created by the assumed random force between two points and any fluctuating variable can be obtained in this manner. However $C_{\varepsilon 1}$ is obtained as 1.063 which yields high TKE growth rate in shear flows compared to physical and numerical experiments (Speziale et. al., 1989). Therefore the model is then modified by cutting the random force for small wave numbers. The equations are then reformulated and the coefficients are reevaluated. As a result the $C_{\varepsilon 1}$ and $C_{\varepsilon 2}$ changed while the remaining stayed the same (Yokhat et. al., 1992).

Nonlinear Reynold's stress model (RSM) is different from eddy viscosity models as additional non-linear terms are added to the eddy viscosity model. In scalar eddy viscosity approach, direction of the mean strain rate and the Reynolds stress are forced to be aligned which is true for pure strain but the flow with mean vorticity. In RSM models in the literature, anisotropy of the turbulent flow has been tried to be modeled. Basically this has been done in two basic approaches. In the first one nonlinear Reynolds stress model is to be developed by employing tensorial viscosity and in the second one the prognostic equations are developed for each Reynolds stress. The former approach has been modeled in three major ways: 1) modeling anisotropic turbulence similar to laminar non-Newtonian flow (Spaziale, 1987) 2) use of statistical approaches (Nisizima and Yoshizawa, 1987) 3) use of RNG theory (Rubinstein and Barton, 1990). In the first one the modeling of non-Newtonian flow is analogous to modeling of Reynold's stress as stress-strain relation is nonlinear and the stresses depend on the mean flow quadratically. In the second case, turbulence is regarded as a phenomenon with universal and non-universal behavior which is the result of either geometry or boundary condition. Therefore the affect of universal behavior on the non-universal one is calculated statistically. This approach yield satisfactory results in square duct flow. In the third case the flow use of RNG yields the Reynolds stresses as power series of a parameter. While the first order simply yields the eddy viscosity model, the second order yields a quadratic nonlinear model. The disadvantage of the first two approaches is that they only contain algebraic equations alone transport effects and in both convection and diffusion. Therefore they can be only applicable to flows where the dissipation and production of TKE is equal.

Though the RSM models heretofore tried to account for the anisotropy of turbulence it fails to predict the return the isotropy after the removal of the strain. To estimate the correct the mentioned deficiency can be overcome by exactly state the nonlinear equation and reinterpret the terms physically and model the terms. The following is the rearranged version of the exact Reynolds stress transport equation;

$$\frac{D\overline{u_i u_j}}{Dt} = (D_{ij}^{t} + \Phi_{ij,p} + D_{ij}^{\upsilon}) + P - \varepsilon_{ij} + (\Phi_{ij,1} + \Phi_{ij,2}) \qquad (2.3)$$

Where D_{ij}^{t} and D_{ij}^{v} are the turbulent and viscous diffusion, respectively, $\Phi_{ij,p}$ is the pressure diffusion, P is the production, ε_{ij} is the dissipation, $\Phi_{ij,1}$ and $\Phi_{ij,2}$ are the is the slow and rapid pressure strain.

In equation (2.3) production term and viscous diffusion need no modeling. Pressure diffusion added to turbulent diffusion, dissipation and pressure strain terms are modeled. These models are given in Tables (1) through (4). Hanjalic and Launder (1972) proposed a model that excludes the pressure diffusion term due to experimental results which shows that pressure diffusion is small compared to turbulent diffusion. Daly and Horlow (1970) proposed a simple gradient diffusion model including pressure diffusion. Chen even proposed a simpler model treating each Reynolds stress term as a fraction of TKE.

Table 1 Modeled Reynolds Stress Equation for diffusion term

	Equation
Daly and Harlow (1970)	$\frac{\partial}{\partial X_k}[C_k \frac{k}{\varepsilon}\overline{u_i u_j}\frac{\partial \overline{u_i u_j}}{\partial X_l}],\ C_k = 0.25$
Hanjalic and Launder (1972)	$\frac{\partial}{\partial X_k}[C_k \frac{k}{\varepsilon}(\overline{u_i u_l}\frac{\partial \overline{u_j u_k}}{\partial X_l}+\overline{u_j u_l}\frac{\partial \overline{u_j u_k}}{\partial X_l}+\overline{u_k u_l}\frac{\partial \overline{u_j u_k}}{\partial X_l})],\ C_k = 0.11$
Chen (1983)	$\frac{\partial}{\partial X_k}[C_k \frac{k^2}{\varepsilon}\frac{\partial \overline{u_i u_j}}{\partial X_l}],\ C_k = 0.09$

Table 2 Modeled Reynolds Stress Equation for dissipation term

Rotta (1951)	$\frac{\overline{u_i u_j}}{k}\varepsilon$
Hanjalic and Launder (1972)	$\frac{2}{3}\delta_{ij}\varepsilon$
Launder (1986)	$\varepsilon_{ij} = \frac{\varepsilon}{k}(\overline{u_i u_j}+\overline{u_i u_j}\,n_k n_j+\overline{u_j u_k}\,n_k n_l+\delta_{ij}\overline{u_k u_l}\,n_k n_l)/(1+\frac{5}{2}\frac{\overline{u_p u_q}}{k}\,n_p n_q)$
Fu et. al. (1987)	$f_\varepsilon \frac{2}{3}\delta_{ij}\varepsilon+(1-f_\varepsilon)\varepsilon_{ij}^{w};\ f_\varepsilon = A^{1/2};\ A=[1-\frac{9}{8}(a_{ij}a_{ij}-a_{ij}a_{jk}a_{ki})];\ a_{ij}=(\frac{u_i u_j}{k}-\frac{2}{3}\delta_{ij})$

Table 3 Modeled Reynolds Stress Equation for slow pressure strain term

Rotta (1951)	$\Phi_{ij,1} = -C_1 \frac{\varepsilon}{k}(\overline{u_i u_j} - \frac{2}{3}\delta_{ij}k)$
Lumley and Khajeh-Nouri (1973)	$\Phi_{ij,1} = -(C_1 + C_1^n a_{ij}a_{ij})\varepsilon a_{ij} - C_1^l \varepsilon(a_{im}a_{jm} - \frac{1}{3}\delta_{ij}a_{ij}a_{ij})$

For the dissipation modeling, at high Re the small scale eddy structures are isotropic and the model proposed by Hanjalic and Launder (1972) can be used without affecting the solution. For the flows of low Re such as near wall Rotta (1951) underestimates the dissipation. Launder (1986) proposed a complex model which adopts the dissipation the same as Hanjalic and Launder (1972) and correct it with pressure-strain correlation. The model proposed by Fu et al. (1987) makes the correction by a function of which parameter is the difference between the isotropic turbulence and anisotropic one.

The model for the slow pressure-strain term there is no agreement in values of the constants. However the highest of two considers the slow pressure-strain term as the contributing term which might be possible for a narrow range of turbulent flows. However there is no acceptable model.

Table 4 Modeled Reynolds Stress Equation for Rapid Pressure Strain Term

Hanjalic and Launder (1972)	$\Phi_{ij,2} = a_{ij}^{ml}(\frac{\partial U_m}{\partial X_l} + \frac{\partial U_l}{\partial X_l})$; $a_{ij}^{ml} = \alpha \overline{u_m u_i}\,\delta_{ij} + \beta(\overline{u_m u_i}\,\delta_{ij} + \overline{u_m u_j}\,\delta_{il} + \overline{u_i u_i}\,\delta_{mj}) + (\gamma\delta_{mi}\delta_{ij} + \sigma[\delta_{mi}\delta_{ij} + \delta_{mj}\delta_{il}])k$; $+C_2(\overline{u_m u_i}\,u_l u_j)\overline{/k} + \nu(\overline{u_m u_j}\,\overline{u_i u_l} + \overline{u_m u_l}\,\overline{u_i u_j})/k$ $\alpha = (10 - 8C_2)/11;\ \beta = -(2 - 6C_2)/11; \nu = -C_2; \gamma = -(4 - 12C_2)/55;$ $\sigma = (6 - 18C_2)/55; C_2 = 0.45$
Launder et. al. (1975)	$\Phi_{ij,2} = -\frac{C_2 + 8}{11}(P_{ij} - \frac{2}{3}\delta_{ij}P) - \frac{30C_2 - 2}{55}k(\frac{\partial U_m}{\partial X_l} + \frac{\partial U_l}{\partial X_l}) - \frac{8C_2 - 2}{11}(D_{ij} - \frac{2}{3}\delta_{ij}P)$ $P_{ij} = (\overline{u_i u_k}\frac{\partial U_j}{\partial X_k} + \overline{u_j u_k}\frac{\partial U_i}{\partial X_k}); P = -\overline{u_i u_j}\frac{\partial U_i}{\partial X_j}; D_{ij} = -(\overline{u_i u_k}\frac{\partial U_k}{\partial X_j} + \overline{u_j u_k}\frac{\partial U_i}{\partial X_i});$ $C_2 = 0.4;$
Gibson and Launder (1978)	$\Phi_{ij,2} = -\xi(P_{ij} - \frac{2}{3}\delta_{ij}P); P_{ij} = (\overline{u_i u_k}\frac{\partial U_j}{\partial X_k} + \overline{u_j u_k}\frac{\partial U_i}{\partial X_k}); P = -\overline{u_i u_j}\frac{\partial U_i}{\partial X_j}; \xi = 0.6$

Fu et. al. (1987)	$\Phi_{ij,2} = 0.6(P_{ij} - \frac{2}{3}\delta_{ij}P) + 0.3\varepsilon a_{ij}(\frac{P}{2\varepsilon}) - 0.2\{\frac{\overline{u_k u_j u_l u_i}}{k}[\frac{\partial U_k}{\partial X_l} + \frac{\partial U_l}{\partial X_k}] -$; $\frac{\overline{u_l u_k}}{k}[\overline{u_i u_k}\frac{\partial U_j}{\partial X_l} + \overline{u_j u_k}\frac{\partial U_i}{\partial X_l}]\} - 0.6[A_2(P_{ij} - D_{ij}) + 3a_{ml}a_{nj}(P_{mn} - D_{mn})]$ $A_2 = a_{ij}a_{ji}\,; a_{ij} = (\frac{\overline{u_i u_j}}{k} - \frac{2}{3}\delta_{ij})$

For the rapid pressure-strain term Hanjalic and Launder (1972) it does not satisfy a kinematic boundary condition and give a wide range of results if there exists a complex strain field. The model proposed by Gibson and Launder (1978) does not predict the effects of swirl on the spreading rate of and axisymetric jet (Launder and Morse, 1979). Generally speaking, return to isotropy is slower with these models, although they might work under different flows (Jaw and Chen, 1997).

Finally, we would like to comment on the Large-eddy simulation (LES) approach. From the computational point of view, LES is somewhat the compromise between DNS and RANS models. It is computationally less expensive than DNS but more costly than RANS, on the other hand history of the flow is preserved. As the large scale motions are more energetic they carry most of the energy and transport of the conserved properties. Likewise LES resolves the energetic structures in the flow and model small ones. The large scale components are obtained by filtering like box filtering, Gaussian filtering, cut-off filter in which above certain value of wave numbers are discarded. The filter length is denoted as Δ. After rewriting the Navier-Stokes equations and subtracting from the RANS equations the result yields us the sub-grid scale Reynold's stress;

$$\tau_{ij}^{s} = -\rho(\overline{u_i u_j} - \overline{u}_i \overline{u}_j) \tag{2.4}$$

This term is modeled by different sub-grid scale models. Smagorinsky models, dynamic models and deconvolution models. Smagorinsky model can be stated as follows;

$$\tau_{ij}{}^{s} - \frac{1}{3}\tau_{kk}{}^{s}\delta_{ij} = \mu_t(\frac{\partial \overline{u}_i}{\partial \overline{x}_j} + \frac{\partial \overline{u}_j}{\partial \overline{x}_i}) = 2\mu_t \overline{S_{ij}} \tag{2.5}$$

$$\mu_t = C_S{}^2 \rho \Delta^2 |\overline{S}| \tag{2.6}$$

Model parameter C_s is usually found from the experiments to be around 0.2. On the other hand for different flow types this value is different as it is a function Re and other non-dimensional flow parameters (such as in stratified flows Richardson or Froude numbers). In shear flows and near the wall the change of this parameter is necessary. To overcome the near wall problem possible recipes are 1) using VanDriest damping

function, 2) reduce the eddy viscosity when sub-grid Re is small (Mac-Millan and Ferziger, 1980) 3) use of RNG theory (Yakhot and Orszag, 1986).

In the dynamic models it is assumed that the largest subgrid scale motions can be modeled by smallest resolved scale motion. Broader filter is used to get a very large scale field and an effective subgrid scale is obtained. Reynold's stress is therefore estimated by this procedure for every point at every time. Consequently the model parameter is produced in a consistent manner and the problems like near wall and anisotropy removed. However model parameter is a rapidly varying function of spatial coordinates and time which leads to high values of model parameter in both signs. If this recurs for a considerable time over a considerable range this causes numerical instability.

Deconvolution method tries to find the sub-grid scale velocities by the filtered ones. Unfiltered velocities are represented by Taylor series expansion. If the series cut off at most up to second order the differential equation for the unfiltered velocity is obtained in terms of filtered ones.

3.2.Discretization Errors

Most of the time governing equations in the fluid flow cannot be solved exactly. The algebraic set of equations to be solved, are obtained as a result of approximations. Evaluation of volume and surface integrals in finite volume and numerical calculation of derivatives are basically obtained after approximations. The details of the numericals will not be given here, however an overview will be given.

Upwind difference scheme (UDS), central difference scheme (CDS), quadratic upwind interpolation for convective kinematics (QUICK) are the existing schemes in most of the commercial CFD codes (for details refer to any textbook regarding this subject). Therefore careful employment of these schemes is crucial for accuracy, simplicity and efficiency. According to the findings of Ferziger and Peric (2001) higher order schemes converge to an accurate result although oscillating on the coarse grids. First order UDS should be avoided as it introduces error function as a diffusion equation which smears out the error especially in 3-D simulations. CDS gives the best compromise regarding efficiency, simplicity and accuracy. Apart from these it is also worth to note that the discretization error introduced on non-uniform grid is proportional to stretching ratio (r) minus unity and it is amplified where there is a strong variation in the flow.

3.3.Iteration Errors

After the discretization there occurs a set of non-linear equations which usually further linearized. The direct solution of these equations is costly and usually they are solved by numerical methods. There is no way that the exact solution can be obtained as a result of these equations hence the solutions are stopped based on the convergence criterions. The criterions are generally set to one order less than the discretization error.

Therefore these types of errors have the least effect on the solution. The details of these can be found in any book related to CFD.

3.4.Programming and User Errors

The most important of all is the boundary condition errors and errors due to poor quality input grid. The flow should essentially reflect the actual conditions of real flow. Most of the time, it is not possible to implement the exact flow boundary conditions and geometrical configuration of the flow field. This may stem either from the solver program or the approximations which has to be made in the flow field. Any error made in boundary conditions propagates –the speed of which depends on the computational scheme employed- in the flow field and undermines the reliability of the solution. This holds true also for the input grid. One should intuitively determine the flow field and reckon the fields where there is high resolution required for the grid generation. Apart from the resolution determination, the topology of computational cells is important in the sense that the accuracy of the central difference scheme is more accurate in quadrilateral and hexahedral cells than the ones in the triangular and tetrahedral elements. Any grid with any topology should satisfy quality constraints which are based on geometric properties of the computational cell such as skewness, stretching ratio (r) of adjacent cells and aspect ratio. The circumcenter of highly skewed elements lies outside the boundaries of the computational cell. Since the pressure and any scalar are stored at the circumcenter, inaccurate results would be obtained for pressure gradients in highly skewed elements. If the aspect ratio of the computational cell is higher than there occur problems in the approximation in the diffusive fluxes which is a major concern in the near wall (Ferziger and Peric (2001)). The use of non-uniform grid is nearly unavoidable in complex flows. Therefore the discretization error, as it has been mentioned in section 3.2 is proportional to r-1. Hence the use of grids with r greater than 2 especially in the regions with high velocity gradients amplifies the discretization error. It should be also mentioned that the grid generation depends on the turbulence model used i.e LES requires higher resolution than RANS models but less than direct numerical simulation (DNS). In LES, one often needs to check the model results for resolved energy field or the calculated energy spectrum to ensure that appropriate grid resolution is adopted.

4. Recommendations

Although currently there is no detailed field data available, it is the authors' belief that CFD is a potential tool to understand the physics of the flow field. As stated in the previous section, the RANS approach is less expensive compared to LES and DNS. Despite several existing criticisms on the limitation of eddy-viscosity-based two-equation approach for complex flows, the use of more appropriate closure model (less restrictive assumptions) such as RSM and RNG models shall yield more accurate results. Also in RANS approach, the grid generation will require less time as compared to the LES grid generation.

Because the limited field data and the scale involved in the prototype culvert structure, the feasibility of using LES for CFD computation cannot be assessed with confidence at this point. In addition, the high quality input grid (geometry of the culvert structure) should be assured. This restriction may sometimes cause the application of LES nearly impossible to implement, such as the geometry of draft tube in the hydropower structures. Even if detailed geometry is available, it often takes a great amount of time to make the sensitivity analysis of the input grid. Therefore the applicability of LES should be investigated with the actual geometric data and the flow conditions. On the other hand, the payback of the LES employment is large because it theoretically gives more accurate results. Especially in the lack of field and laboratory data, LES results can be used as the computational experiment tool in complex field configuration (in which DNS cannot be used, See Constantinescu et. al., 2006). Consequently if accurate LES results can be obtained, one can conduct useful inter-comparison among the turbulence models and the optimum one among them could be evaluated in terms of computational expense and accuracy and eventually used as design tool. With the exiting computational power in the water resource group at University of Florida, we shall be able to employ few LES parallel computations using the new 20-processor cluster system. These few LES results can provide as valuable database to evaluate various RANS approaches.

As it is previously mentioned, the accuracy of CFD simulations depends on the quality of the input grid and the boundary conditions. The flow characteristic of a culvert flow is unique as the upstream boundary conditions differ with the topography of the flow field. This is because any perturbation to the flow field upstream will be conveyed to downstream which also affects the flow through the culvert. However the degree of uniqueness of the flow can be evaluated for the same structure at different locations. This necessitates apart from the structural details of the culvert data, the actual topographic and flow data at different culvert locations (can you re-phrase, I am not getting it). In addition if the real time flow field data is available, the turbulence closure models should be directly tested.

The study of Gonzalez (2005) shows that for the gated-culvert flow, there are various empirical loss coefficients exist to parameterize energy dissipation at different component of a culvert system. Due to the high complexity of these energy dissipation mechanisms, Gonzales (2005) employed lumped approach in which the details of these

coefficients were not evaluated while an bulk discharge coefficient is defined in terms of dimensionless numbers. These bulk coefficients are then evaluated by fitting a best-fit curve with respect to the ratio of the cross sectional areas of gate opening to the cross sectional area of the culvert barrel. The lumped approach employed by Gonzalez (2005) is plausible because there is no available loss coefficient data for each component in the culverts in the literature and it is not easy to directly measure the flow in these kinds of structures. We believe that with the use of CFD, it it possible to evaluate each of these loss coefficients carefully. In addition to these empirical parameters, the momentum correction factor, α_1, used in the inlet weir controlled structure, should also be evaluated numerically with CFD, which will also include the 3-D affect. All the CFD results along with available field data may then be used to re-formulate the rating curves which shall improve upon the existing one based on lumped approach.

References

Bhagangar, K., Rempfer,D., and Lumley,J.L., 2002, Direct numerical simulation of spatial transition to turbulence using fourth-order vertical velocity second-order vertical vorticity formulation, *J. Comp.Phys*.180:200-228.

Charbeneau R. J, A. D. Henderson, and L. C. Sherman (2006), Hydraulic Performance Curves for Highway Culverts, J. Hyd. Engrg., ASCE 132(5), 474-481.

Constantinescu, S.G., W.F. Krajewski, C. E. Ozdemir, T. E. Tokyay (2006), Simulation of Airflow around rain gauges: Comparison of LES with RANS models, Advances in Water Resources (in press).

Daly, B. J., and Horlow, I. H. (1970), Transport Equations in turbulence, Phys. Of Fluids, 13, 2634-2649.

Day R. A.(1997), Preliminary Observations of Turbulent Flow at Culvert Inlets, J. Hyd. Engrg., ASCE 123(2), 116-124.

Durbin, P.A.,B.A.P. Reif, Statistical Theory and modeling for Turbulent Flows, Wiley, Stanford, C.A.,2000.

Ferziger, J. H., M. Perić, Computational Methods for Fluid Dynamics, 3rd Edition, Springer, Berlin, 2002.

Fu, S, Launder, B. E., and Tselepidakis, D. P. (1987). "Accommodating the effects high strain rates in modeling the pressure-strain correlation, Rep TFD/87/5, UMIST, Manchester, Dept. Mech. Engrg.

Gibson, M. M. , and Launder , B. E.(1978), Ground Effects on pressure Fluctuations in the Atmospheric Boundary Layers, J. Fluid Mech. , 86, 491-551.

Goncalves E. and R. Houdeville (2001), Reassesment of the Wall Function Approach for RANS Computations, Aerosp. Sci. Technol 5, 1-14.

Gonzalez, J. A. (2005), Ratings for the Pressurized Flow in Gated Culverts with Weir Box Inlet G304A-J and G306A-J,Technical Publication SHDM Report # 2005-02.

Hanjalic, K. , Launder, B. E. (1972) , A Reynold's Stress Model of Turbulence and its Applications to thin shear. Part 4, J. Fluid Mech., 86, 491-551.

Jaw, S.Y, and C. H. Chen (1998), Present Status of Second Order Closure Turbulence Models. I:Overview, J. Engrg. Mech 124(5), 485-501.

Keylock, C. J., Hardy, R. J., Parsons, D. R., Ferguson, R. I., Lane, S. N. and Richards, K. S., 2005. The theoretical foundation and potential for large-eddy simulation (LES) in fluvial geomorphic and sedimentological research, *Earth-Science Reviews.,* 71, 271-304.

Launder, B. E. (1976) , Low Reynol's Number Turbulence turbulence near walls, Rep. TFD/86/4, UMIST, Manchester, Dept. Mech. Engrg.

Launder, B. E. , Morse, A.P. (1979), Numerical Prediction of axi-symmetric free shear flows with a Reynold's Stress Closure, turbulence Shear Flows, Springer , Heidelberg, Germany, 274-295.

MacWilliams, M.L., R. L. Street, and P. K. Kitanidis , Modeling Floodplain Flow on Lower Deer Creek, CA., River Flow 2004: Proceedings of the Second International Conference on Fluvial Hydraulics, Greco, Carravetta, & Della Morte (eds.), Vol. 2, 1429-1439, Balkema, 2004.

McMillan, O. J. , Ferziger, J. H. (1980), Tests of New Subgrid scale Models in Strained Turbulence. AIAA J. 80, 1339.

Menter, F. R., Two Equation Eddy Viscosity Turbulence Modelsfor Engineering Applications, AIAA J.32, 1598-1605.

Nisizima, S. ,and Yoshizawa, A (1987), Turbulent Channel and Couette Flows using an anisotropic k-ε model, AIAA J., 25(3), 414-420.

Normann, J. M., Houghtalen, R. J., and Johnson, W. J. (1985), Hydraulic design of highway culverts. *Hydraulic Design Series No. 5*, 2nd Ed., Federal Highway Administration, Washington, D.C.

Patel V.C, W Rodi and, G Scheuerer (1985) turbulence models for near wall and low Reynold's Number Flows- A review, AIAA J.23 (9): 1308-1319.

Pope, S. B., 2000. Turbulent Flows, Cambridge University Press.

Rodi, W., Ferziger, J. H., Breuer, M., Pourquie, M., 1997. Status of large eddy simulation: reulsts of a workshop, ASME*, J. Fluids. Eng*., 119, 248-262.

Rotta, J. (1951), Sattistical Theory of non-homogeneous Turbulence, Rep. TWF/TN/38, TWF/TN/39, Imperial Coll., London.

Speziale, C. G. , Gatski T. B., and Mac Giolla Mhuiris, N. (1989), A Critical Comparison of Turbulence models for Homogeneous Shear Flows in a Rotating Frame. Proc., 7th Symp Turb. Shear Flows, Standford, Calif., 227.3.1-27.3.6.

Wilcox, D. C., 1988. Turbulence modeling for CFD, DCW Industries

Yakhot, V., and Orszag, S.A. (1986), Renormalization Group Analysis of Turbulence. I. Basic Theory, J. Scientific Computing 1(1), 3-51.

Yen, B.C. (1992). Dimensionally Homogeneous Manning's Formula, *J. Hydr. Eng. Div.*, ASCE, 118(9), 1326–133.

Development and documentation of upconing and drawdown models for regulatory use

Basic Information

Title:	Development and documentation of upconing and drawdown models for regulatory use
Project Number:	2006FL147B
Start Date:	3/1/2006
End Date:	2/28/2007
Funding Source:	104B
Congressional District:	6
Research Category:	Ground-water Flow and Transport
Focus Category:	Models, Groundwater, Water Supply
Descriptors:	
Principal Investigators:	Louis H. Motz

Publication

1. Motz, L. H., and Acar, Ozlem. 2006. Evaluation and Documentation of SJRWMD Groundwater Models for Use by Permit Applicants, Draft Final Report, St. Johns River Water Management District, Palatka, Florida, 84 pp.

PROJECT STATUS

EVALUATION AND DOCUMENTATION OF SJRWMD GROUNDWATER MODELS FOR USE BY PERMIT APPLICANTS

by

Louis H. Motz and Ozlem Acar

Department of Civil and Coastal Engineering

University of Florida

1.1 Background and Objectives

In groundwater permit applications to the St. Johns River Water Management District (District), applicants may be required to address pumping impacts in terms of saltwater upconing and drawdown impacts. Extensive hydrogeological investigations that include numerical modeling may be required in some cases to address these issues. However, in other cases, analytical modeling techniques may be sufficient to assess impacts. In particular, analytical modeling techniques are useful in screening for impacts and/or conducting preliminary investigations that may indicate the need for more detailed investigations. The District currently utilizes several analytical groundwater models for these purposes, including a saltwater upconing model and a pumping impact model that are based on solutions by Motz (1992) and Denis and Motz (1998). For these two District models, there is a need to improve their utilization and prepare model documentation in a manner that will make these models more accessible to permit applicants and others through the District's web site. To meet this need, the University of Florida (University) has evaluated the two existing models and modified the computer codes to enhance their capabilities and accessibility to permit applicants. In addition, the University has documented the improvements in the model codes so that the executable codes and documentation can be posted on the District's web site.

1.2 Scope of Work

The investigation described in this report consisted of four tasks:

- Enhancement of the saltwater upconing model;
- Enhancement of the two-layer drawdown model;
- Preparation of a draft final project report (user's manual); and
- Preparation of a final project report (user's manual).

In the first task, documentation was developed for the model that calculates vertical upconing of the saltwater-freshwater interface beneath a single pumping well and beneath multiple pumping wells in a wellfield. Pumping beneath a single well is simulated using the single-well steady-state solution for a leaky aquifer (Motz 1992). The pumping effects of

multiple wells are simulated using the steady-state solution for multiple wells pumping from a leaky aquifer (Motz 1994). Benchmark testing of the saltwater upconing solution was performed, and the FORTRAN source code SWUP (Saltwater Upconing Program for single and multiple wells) and executable files for single- and multiple-well applications were submitted to the District for review. In the second task, documentation was developed for the model that is used to calculate pumping impacts on groundwater levels in a two-layer aquifer system. This model, based on Denis and Motz (1998), is used to calculate steady-state and transient drawdowns due to pumping from one or more wells that can be located in either or both layers and can be designated as either pumping or recharge wells. Similar to the saltwater upconing model, benchmark testing of the two-layer drawdown model was performed, and the FORTRAN source code COUAQ (Coupled Aquifer Program for single and multiple wells) and executable files for single- and multiple-well applications were submitted to the District for review. In the third task, a draft report was prepared as a user's manual that included a description of the problem, the solutions used, listings of the source codes, the results of the benchmark testing, and example problems to illustrate how to use the enhanced models. The fourth task consisted of submitting this final project report that incorporates the review comments and suggested revisions resulting from the District's review of the draft report. Along with the final report, electronic copies of the source codes, executable files, and input and output files for the benchmark and example problems will be submitted to the District. In addition, a one-day training session will be provided to District staff.

Complete details of this project are available in the Final Project Report:

Motz, L. H., and Acar, Ozlem. 2006. Evaluation and Documentation of SJRWMD Groundwater Models for Use by Permit Applicants, Draft Final Report, St. Johns River Water Management District, Palatka, Florida, 84 pp.

Information Transfer Program

During FY 2006, the Florida WRRC actively supported the transfer of water resources research findings and results to the scientific and technical community that addresses Florida's water resource problems. Specific activities that were part of this task included maintaining a center website which is used to provide timely information about research proposal deadlines, conference announcements and calls for papers. The Center webpage provides information regarding ongoing research supported by the WRRC, lists research reports and publications that are available, and provides links to other water-resource organizations and agencies, including the five water management districts in Florida and the USGS. The Center maintains a library of technical reports that have been published as a result of past research efforts. Hard copies of the reports can be checked out and electronic copies are distributed free of charge based upon request through the website. The Center also provided support for publication of research results in refereed scientific and technical journals and conference proceedings.

Information Transfer

Basic Information

Title:	Information Transfer
Project Number:	2006FL148B
Start Date:	3/1/2006
End Date:	2/28/2007
Funding Source:	104B
Congressional District:	6
Research Category:	Not Applicable
Focus Category:	None, None, None
Descriptors:	None
Principal Investigators:	Kirk Hatfield, Mark Newman

Publication

1. Yamout, G., K. Hatfield, and E. Romeijn. 2007. Comparison of new conditional value-at-risk-based risk management models for optimal allocation of uncertain water supplies. Water Resources Research, (In Press).
2. Cho, J., M.D. Annable, J.W. Jawitz, and K. Hatfield. 2007. Passive fluxmeter measurement of water and nutrient flux in porous media. Journal of Environmental Quality, (In Press).
3. Lee, J., P.S.C. Rao, I.C. Poyer, R.M. Toole, M.D. Annable, and K. Hatfield. 2007. Oxyanion flux characterization using passive flux meters: Development of field testing of surfactant-modified sorbents. Journal of Contaminant Hydrology, (In Press).
4. Klammler, H., M. Newman, E. Szilagyi, J. Padowski, K. Hatfield, J. Jawitz, and M. Annable. 2007. The passive surface water fluxmeter to measure cumulative water and solute fluxes. Environmental Science and Technology, 41 (7), 2485 -2490.
5. Klammler, H., K. Hatfield, and M. Annable. 2007. Concepts for measuring horizontal groundwater flow directions using the passive flux meters. Advances in Water Resources (In Press).
6. Klammler, H., K. Hatfield, M. D. Annable, E. Agyei, B. Parker, J. Cherry, and P.S.C. Rao. 2007. General analytical treatment of the flow field relevant to the interpretation of passive fluxmeter measurements. Water Resour. Res., 43, W04407, doi:10.1029/2005WR004718.
7. Bhat, S., K. Hatfield, J. M. Jacobs, and W. D. Graham. 2007. Relationships between military land use and storm-based indices of hydrologic variability. Ecological Indicators, 7, 553-564.
8. Perminova, I.V., L.A. Karpiouk, N.S. Shcherbina, S.A. Ponomarenko, St.N. Kalmykov, and K. Hatfield. 2007. Synthesis and use of humic derivatives covalently bound to silica gel for Np(V) sequestration. Journal of Alloys and Compounds (In Press).
9. Campbell, T. J., K. Hatfield, H. Klammler, M. D. Annable, and P.S.C. Rao. 2006. Magnitude and directional measures of water and Cr(VI) fluxes by passive flux meter. Environmental Science and Technology 40(20), 6392-6397.
10. Newman, M., K. Hatfield, J. Hayworth, P.S.C. Rao, and T. Stauffer. 2006. Inverse characterization of NAPL source zones. Environmental Science and Technology, 40(19), 6044-6050.
11. Sedighi, A., H. Klammler, C. Brown, and K. Hatfield, 2006. A semi-analytical model for predicting water quality from an aquifer storage recovery system. Journal of Hydrology, 329, 403-412.
12. Mohamed, M.M.A. and K. Hatfield, and A.E. Hassan. 2006. Monte Carlo evaluation of contaminant biodegradation in heterogeneous aquifers. Advances in Water Resources, 29(8), 1123-1139.
13. Basu, N., P.S.C. Rao, I.C. Poyer, M.D. Annable, and K. Hatfield, 2006. Flux-based assessment at a manufacturing site contaminate with trichloroethylene. Journal of Contaminant Hydrology, 86 (1-2), 105-127.
14. Agyei, E., and K. Hatfield. 2006. Enhancing gradient-based parameter estimation with an evolutionary approach. Journal of Hydrology, 316(1-4), 266-280.
15. Bhat, S., J. M. Jacobs, K. Hatfield, and J. Prenger. 2006. Relationships between water chemistry and land use in military affected watersheds in Fort Benning, Georgia. Ecological Indicators, 6(2), 458-466.
16. Brown, C.J., K. Hatfield, M. Newman. 2006. Lessons Learned fom a Review of 50 ASR Project from the United States, England, Australia, India, and Africa. Proceedings UCOWR/NIWR Annual Conference, July 18-20, Santa Fe, New Mexico.

Student Support

Student Support					
Category	**Section 104 Base Grant**	**Section 104 NCGP Award**	**NIWR-USGS Internship**	**Supplemental Awards**	**Total**
Undergraduate	0	0	0	0	0
Masters	3	0	0	0	3
Ph.D.	13	0	0	0	13
Post-Doc.	2	0	0	0	2
Total	18	0	0	0	18

Notable Awards and Achievements

The Center facilitated development of research at both the state and national level and produced 23 peer reviewed publications some of which received national and international recognition:

1. (Best Technology Paper published in ES&T, 2006)

2. ESTCP/SERDP, Project of the Year Award, 2006

Publications from Prior Projects

1. 2004FL57B ("Sensitivity of the Hydroperiod of Forested Wetlands to Alterations in Topographic Attributes and Land Use") - Articles in Refereed Scientific Journals - Nachabe, M. H. 2006. Equivalence Between Topmodel and the NRCS Curve Number Method in Predicting Variable Runoff Source Areas. Journal of the American Water Resources Association. Volume 42, Number 1, February 2006, pages 225-235.
2. 2004FL57B ("Sensitivity of the Hydroperiod of Forested Wetlands to Alterations in Topographic Attributes and Land Use") - Articles in Refereed Scientific Journals - Nachabe, M. H., N. Shah, M. Ross, and J. Vomacka. 2005 . Evapotranspiration of Two Vegetation Covers in Humid Shallow Water Table Environment. Soil Science Society of America Journal, 69:492-499.
3. 2004FL57B ("Sensitivity of the Hydroperiod of Forested Wetlands to Alterations in Topographic Attributes and Land Use") - Articles in Refereed Scientific Journals - Said, A., M. Nachabe, M. Ross, and J. Vomacka. Methodology for Estimating Specific Yield in Shallow Water Environment Using Continuous Soil Moisture Data. 2005. J. Irrig. and Drain. Engrg., Volume 131, Issue 6, pp. 533-538.
4. 2004FL57B ("Sensitivity of the Hydroperiod of Forested Wetlands to Alterations in Topographic Attributes and Land Use") - Articles in Refereed Scientific Journals - DeSilva, M., M. H. Nachabe, J. Simunek, and R. Carnahan 2005. Simulating Root Water Uptake from a Heterogeneous Vegetation Cover using Finite Element Modeling. In press, ASCE, Journal of Irrigation and Drainage Engineering.
5. 2004FL57B ("Sensitivity of the Hydroperiod of Forested Wetlands to Alterations in Topographic

Attributes and Land Use") - Articles in Refereed Scientific Journals - DeSilva, M. and M. H. Nachabe 2006. Influences of Land Use Change and Topographic Attributes on Hydrology of Shallow Water Table Environments. In review, Ecological Modelling.

6. 2004FL59B ("Ground Water Vulnerability Delineation Using Integrated GIS and Neuro-Fuzzy Methods") - Conference Proceedings - Kim, S.Q.,Wdowinski, S., F. Amelung, T. Dixon. C-band interferometric SAR measurements of water level change in the wetlands: examples from florida and Louisiana. Geoscience and Remote Sensing Symposium, 2005. IGARSS '05. Proceedings. 2005 IEEE International. July 25-29. 2005, Volume: 4, pp. 2708- 2710.